Marine Ecosystem Structure and Function from the Late Cretaceous to the Pliocene: Investigating the Origins of Modern Marine Communities

Lydia Helen Woods

Submitted in accordance with the requirements for the degree of Doctor of Philosophy

The University of Leeds,

School of Earth and Environment

November 2025

The candidate confirms that the work submitted is her own except where work which has formed part of jointly authored publications has been included. The contribution of the candidate and other authors to this work has been explicitly indicated below. The candidate confirms that appropriate credit has been given within the thesis where reference has been made to the work of others.

I acknowledge the use of ChatGPT-5 (Open AI, https://chat.openai.com/) to debug code and proofread some sentences.

Acknowledgements

Firstly, a very big massive thank you to Alex Dunhill for helping every step of the way. Thank you also to James Witts, Rowan Whittle, Jenny Dunhill, Andrew Beckerman, Tracy Aze, Maria Beger, Chris Hassall, Jack Shaw, Gawain Antell, Tanya Strydom, Laura Mulvey, Bethany Allen and Lorna Kearns. Thanks to Amy S, Annabel, Lauren, Baran, Amy McG, Kate, Georgia, Khushboo, Lena & Leon, Bob, Meghan & Charles, Chiara, Lila, Ali, Ailsa, Cesca, Charles W, Emily, Andy, Richard Rigby and CEMAC, and staff in SEE. Big thank you to Graham Huggan, Stefan Skrimshire and the Extinction DTP. Thank you to my friends and family and both cats. Thanks also to Aphex Twin for making the best music to write to.

Abstract

The origins of modern marine community structure and function remain incompletely understood. Major mass extinction events, particularly the Cretaceous-Palaeogene (K-Pg, ~66 Ma), profoundly reshaped the composition and taxonomic identities of marine ecosystems. The following Cenozoic Era experienced pronounced climatic variability, from hyperthermal to hypothermal episodes and a long-term cooling trend from the Oligocene onward. These climatic transitions coincided with faunal turnover and the diversification of modern clades, along with shifts in community composition, biogeographic patterns, and benthic dominance, all of which contributed to the establishment of modern marine ecosystems. However, it remains unclear how the K-Pg extinction and Cenozoic climate extremes influenced the development of modern marine community structure and function, whether this 'modernisation' occurred gradually or through punctuated events, as well if and how a functional diversity gradient (LFDG) emerged in relation to the well-documented latitudinal species diversity gradient (LDG).

This thesis addresses these gaps through two studies with three overarching aims: (1) to assess changes in trophic structure across the K-Pg extinction and subsequent recovery interval; (2) to investigate global patterns of marine invertebrate functional diversity from the Late Cretaceous to the Pliocene; and (3) to examine the development of a latitudinal functional diversity gradient over this interval, all to identify the origins of modern marine community organisation.

The findings demonstrate that Antarctic trophic meta-webs experienced only short-term disruption at the K-Pg boundary, with no lasting structural or functional reorganisation. Likewise, global marine invertebrate functional diversity exhibited no directional trend from the Late Cretaceous to the Pliocene and did not decline in association with the K-Pg extinction event. Functional diversity was persistently highest in palaeotemperate regions, and remained decoupled from taxonomic diversity, which shifted from a palaeotemperate peak in the Cretaceous to a tropical maximum by the Late Pliocene. Together, these results indicate the functional structure of marine ecosystems has been comparatively stable over the last 70 Myr, and that the establishment of the modern latitudinal taxonomic diversity gradient apparently occurred independently of changes in functional diversity.

Table of Contents

List of Figures

List of Tables

Abbreviations

EECO Early-Eocene Climatic Optimum

EOT Eocene-Oligocene Transition Event

FD Functional Diversity

GD Generic Diversity

GOBE Great Ordovician Biodiversification Event

K-Pg Cretaceous Paleogene Mass Extinction

LDBF The Lopez de Bertodano Formation, Seymour Island, Antarctica

LDG The Latitudinal [Species] Diversity Gradient

LFDG The Latitudinal Functional Diversity Gradient

LIP Large Igneous Province Region

LTME Late Triassic Mass Extinction

MECO Mid-Eocene Climatic Optimum

MMCT Middle Miocene Climate Transition

MMR – Mesozoic Marine Revolution

MSC Messinian Salinity Crisis

PETM Paleocene-Eocene Thermal Maximum

PTME Permian Triassic Mass Extinction

RFD Raw Functional Diversity

RGD Raw Generic Diversity

SFD Standardised Functional Diversity

SGD Standardised Generic Diversity

SQS Shareholder Quorum Subsampling

SSFD Spatially-subsampled Functional Diversity

SSGD Spatially-subsampled Generic Diversity

Chapter 1 – Introduction

1.1. Marine Ecosystem Structure over Deep Time:

1.1.1. Major mass extinctions have shaped global ecosystems

Major mass extinctions are arguably the most influential events for having shaped biodiversity and ecosystems over the Phanerozoic (Fig. 1). Fossil record analyses, including Sepkoski (1981), has revealed five major mass extinctions: the end-Ordovician Extinction (~445 Ma); Late Devonian Extinction (~375-359 Ma); Permian-Triassic Extinction (PTME, ~252 Ma); Late Triassic Mass Extinction (LTME, ~201 Ma), and the Cretaceous-Paleogene Mass Extinction (K-Pg, ~66 Ma), along with multiple lesser extinctions (Vermeij 1977; Raup & Sepkoski 1982; Sepkoski 1984; 1997; Bambach et al. 2004). These biotic crises incited widespread disruption to ecosystems and fundamentally altered global biodiversity patterns (Alvarez et al. 1980; Hallam & Wignall 1997). Although major radiations and ecological transition events such as the Cambrian Explosion (~541-530 Ma), the Great Ordovician Biodiversification Event, GOBE (~485-443 Ma) and the Mesozoic Marine Revolution, MMR (~200-66 Ma) also likely restructured marine communities (Vermeij 1977; Conway-Morris 1993; Buatois et al. 2016a), the repeated and severe biodiversity loss associated with mass extinctions had a striking impact on ecological communities across macroevolutionary timescales. Yet, despite extensive documentation of global and regional diversity effects (e.g. Alvarez et al. 1980; Hallam & Wignall 1997; Webby et al. 2004; Bond & Grasby 2017), the consequences of mass extinctions on global and community-level structure and function remain underexplored (Foster & Twitchett 2014; Hull 2015; Dunhill et al. 2018).

1.1.2. The K-Pg mass extinction - an ecological turning point?

The K-Pg mass extinction (~66 Ma) had the potential to restructure communities and stands as a candidate for the origin of modern trophic organisation (Dunne et al. 2014). Along with causing a shift in benthic dominance from sessile bivalves to motile gastropods (Crame et al. 2014), the K-Pg is thought to have altered the taxonomic identity and composition of marine communities (Alroy et al. 2008). The top ocean predators in the Late Cretaceous were the large marine reptiles (i.e. mosasaurs and plesiosaurs) and the non-acanthomorph fishes. Following the K-Pg, these groups were replaced by marine mammals and acanthomorph fishes, respectively (Friedman 2010; Uhen 2010; Hull & Darroch 2013; Hull 2015). As well as this, the loss of the ammonites, belemnites, rudist reef-building bivalves and other groups paved way for the proliferation of other modern taxa (Bambach 2006; Hernández 2011; Crame 2014; Hull 2015; Witts et al. 2016).

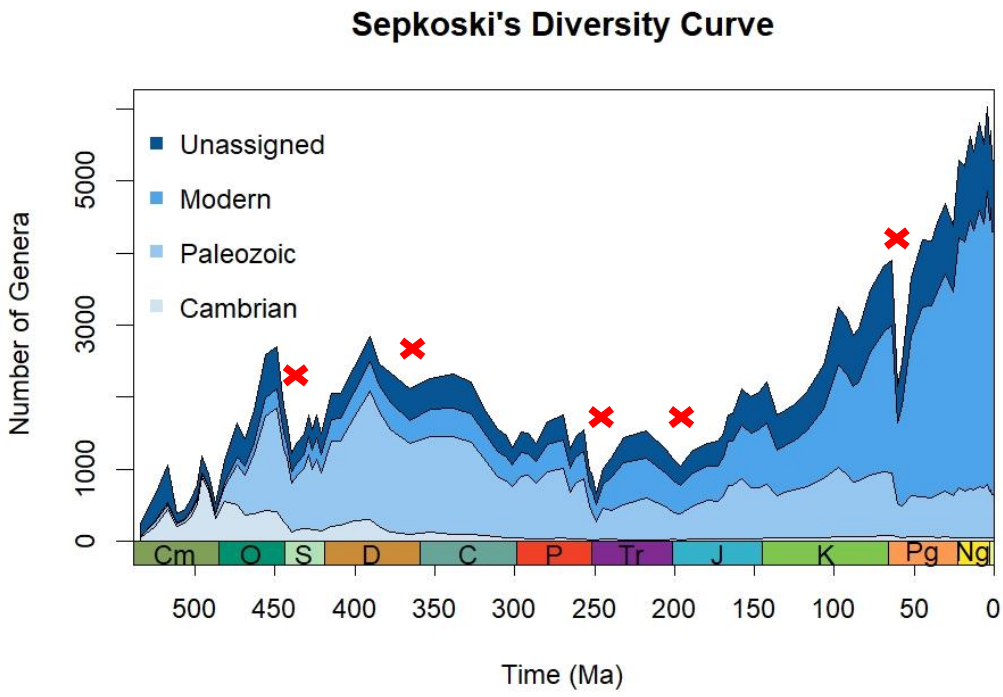

Figure 1. Sepkoski's [invertebrate] diversity curve, as per Sepkoski (1981), with Cambrian (palest blue), Paleozoic (baby blue), Modern (blue) and Unassigned (dark blue) genera. The five red Xs mark the positions of the five major mass extinctions; in chronological order; the Ordovician-Silurian, Late Devonian, Permian-Triassic, Triassic-Jurassic and Cretaceous-Paleogene mass extinctions. This curve was created using *Palaeoverse* package *Sepkoski_curve()* (Jones et al. 2023) in R version 4.4.1.

The greenhouse Early-Cenozoic saw major radiations of modern midwater fish, including lanternfish and anglerfish (Near et al. 2012), and diversifications of planktonic foraminiferal communities (Coxall et al. 2007, Norris et al 2013). Additionally, multiple modern clades of coral reef fish evolved during the greenhouse interval ~ 42-57 Ma, (Near et al. 2012; Norris et al 2013; Price et al. 2014). This leads Norris et al. (2013) to suggest the extensively flooded Early-Cenozoic continental shelves facilitated the evolution of modern coral reef ecosystems. As well as this, Hull (2017) points out that the rise in predation and defence that defines the Mesozoic Marine Revolution likely continued into the Cenozoic Era. Thus, the K-Pg extinction and the taxonomic and biogeographic shifts in its wake, could well have permanently altered community structure and function, perhaps producing more modern characteristics than previously (Dunne et al. 2014).

1.1.3. Marine communities are an ideal case study

Marine communities possess one of most robust macrofossil records available, particularly marine invertebrates (Valentine et al. 2006; Alroy et al. 2008; Tyler &

Kowalewski 2025). Marine communities perform a multitude of roles that are critical to maintaining ecosystem functioning, for example infaunal processes such as bioturbation influence nutrient cycling and sediment oxygen concentrations (Mermillod-Blondin 2011). Because of this, previous studies of fossil community structure and function have often included rates of standing diversity of marine invertebrates across deep time and mass extinctions (Raup & Sepkoski 1982; Sepkoski 1986). The diverse functions marine communities perform have allowed the impact of certain mass extinctions to be examined previously (Foster & Twitchett 2014; Dunhill et al. 2018; Whittle et al. 2019). Thus, marine ecosystems represent an ideal case study for understanding community structure and function over deep time, climate extremes and mass extinctions.

1.2. Patterns in marine community structure and function

1.2.1. What is marine ecosystem/community structure and function?

Marine ecosystem structure defines the organisation of the physical, chemical and biological components of a marine ecosystem (Carvalho & Barros 2017). Marine community structure defines only the organisation of the biotic components of a marine ecosystem (McIntosh 2004). Analysing marine community structure, e.g. trophic structure, provides an understanding of the natural processes that influence marine systems, the mechanisms behind observed patterns and identifies key ecological interactions (Yu et al. 2010). Ecosystem function refers to the natural processes that maintain the strength and stability of an ecological system (Patterson et al. 2013). In marine systems, functions include nutrient cycling, energy flow, habitat modification and the regulation of faunal populations (Aller 2001; Dolbeth et al. 2015). Understanding ecosystem function is crucial to assessing resilience to environmental perturbation under past, present and future climate change. Yet, our understanding of community-level structure or function across the Phanerozoic (~541-0 Ma) and how these responded to macroecological events remains poorly resolved.

1.2.2. Functional diversity in the fossil record

Functional diversity (FD) is defined as the diversity of organismal life habits and ecological traits in a community or population (Tilman 2001; Petchey & Gaston 2006; Mouillot et al. 2013). Functional diversity (FD) indices are commonly used to assess ecosystem response to perturbation, on both a global (Pimiento et al. 2020; Trindade-Santos et al. 2024) and regional scale (Mouillot et al. 2013; Dolbeth et al. 2015; Gusmao et al. 2016). Quantifying marine FD can identify which components of a

community are affected by environmental disturbance and to what extent (Villamor & Becerro, 2012; Rincón-Díaz et al. 2018; McQuatters-Gollop et al. 2019). Functional redundancy itself may increase resilience and robustness against ecological degradation (Raymundo et al. 2009), something that has been hypothesised to have influenced community response to extreme climates in the past. For example, Roopnarine & Angielczyk (2015) showed that stability across the PTME depended critically on functional diversity and patterns of guild interaction, regardless of species diversity. Foster & Twitchett (2014) and Dunhill et al. (2018) cite high pre-extinction functional redundancy as the leading mechanism behind the little to no loss of guilds during the PETM and LTME, respectively.

Functional diversity indices can be applied to fossil datasets to investigate community function across deep time (Hull & Darroch 2013). One concept is that 'ecospace occupancy', which considers marine invertebrate resource use, substrate interaction and life habit (Bambach et al. 2007; Novack-Gottshall 2007), has increased across the Phanerozoic, particularly across the Paleozoic Era, with the Great Ordovician Biodiversification Event (GOBE) accounting for the most marked rise (Bambach et al. 2007; Bush et al. 2007; Villéger et al. 2011). The Bambach Ecospace Cube method (Bambach et al. 2007) assigns marine invertebrate taxa a mode of life (MoL) code of three digits based on their tiering position, motility level and feeding mode, as is displayed in Fig. 2, below.

Methods such as the Ecospace Cube (Bambach et al. 2007) have facilitated investigation into community function across major mass extinctions (Foster & Twitchett 2014; Dunhill et al. 2018). These have revealed that global marine invertebrate FD was likely unaffected by the Permian-Triassic Mass Extinction (PTME, ~252 Ma) or the Late Triassic Mass Extinction, (LTME, ~201 Ma) despite massive taxonomic losses (Foster & Twitchett 2014; Dunhill et al. 2018). Following the loss of 62-74% of genera, only one global mode of life was lost across the PTME, and only one new mode of life was gained during the recovery interval (Foster & Twitchett 2014). Similarly, no modes of life were lost across the LTME despite a loss of 73% of species, but the species richness *within* each mode of life shifted (Dunhill et al. 2018). It is thought that modes of life were retained during extinction due to the 'skeleton crew hypothesis' (Foster & Twitchett 2014; Dunhill et al. 2018).

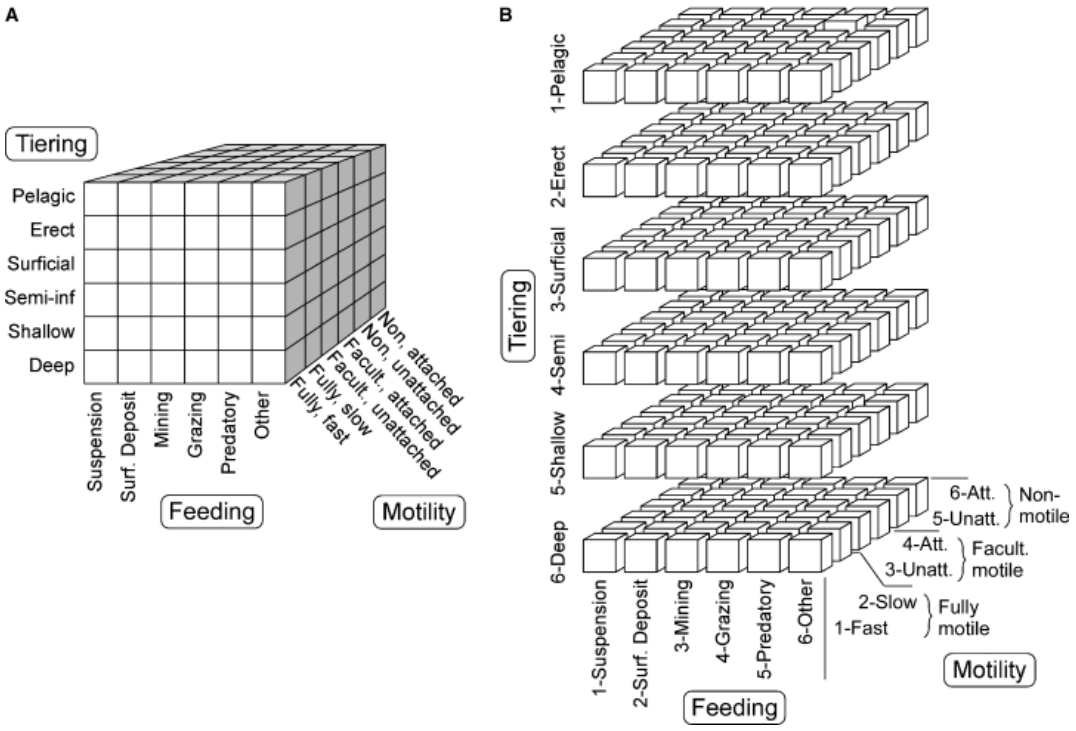

Figure 2 The Bambach Ecospace Cube, from Bambach et al. (2007). Ecospace is defined by the three axes of tiering, motility level and feeding strategy. A, the ecospace cube with categories on each axis labelled. B, the ecospace cube 'exploded', showing 216 modes of life specified by the combination of the categories on each ecospace axis (Bambach et al. 2007).

The 'skeleton crew' hypothesis posits that a high level of functional redundancy may afford the loss of most taxa without losing a significant level of function (Foster & Twitchett 2014). It is hypothesised that worsening environmental conditions push taxa with broadly overlapping niches into closer competition as resources and suitable habitat dwindle, which drives high levels of extinction within guilds yet allows the majority of guilds to persist with low species richness, i.e. a skeleton crew (Foster & Twitchett 2014; Dunhill et al. 2018). Given evidence that global marine FD was resilient to major mass extinction, with regional evidence for this across the K-Pg as well (Whittle et al. 2019), it is likely that global FD also remained stable across the K-Pg extinction. This stability may have persisted through subsequent Cenozoic climate events and the greenhouse-icehouse regime shift. However, with significant losses in FD in the tropics during the LTME (Dunhill et al. 2018), there may have been shifts in community function on a spatial scale across the K-Pg and Cenozoic Era, which also requires investigation.

The climate events of the Cenozoic (e.g. the Paleocene-Eocene Thermal Maximum, PETM) may provide insights into the consequences of ocean acidification, warming and habitat retraction on community function (Inglis et al. 2020). Models

based on Eocene events suggest that modern climate change could cause comparable conditions, over shorter timescales due to the unprecedented pace of anthropogenic greenhouse gas emissions (Tierney et al. 2020). Understanding how marine community structure and function fared during events such as the PETM and other Early Eocene hyperthermals, can inform predictions of the future of marine ecosystems and fate of the services they provide (Westlund et al. 2017; Lopez-Rivas & Cardenas 2024).

1.2.3. Marine trophic structures

Trophic ecology represents community structure using hierarchical trophic organisation; primary producers sit at the bottom of a trophic network, apex predators in the top trophic level and 'intermediate consumers' make up all the nodes in between (Lindeman 1942; Cook 1977; Cattin et al. 2004; Petchey et al. 2008). Organising faunal assemblages into trophic networks allows the quantification of structural metrics and functional motifs, see Table 1 (Dunne et al. 2002; McGill et al. 2006; Allesina et al. 2008; Allesina & Levine 2011; Dunhill et al. 2024). These calculations often require web size, *S*, i.e. the total number of taxa and *L*, the total number of feeding links (Dunne et al. 2004). For example, as Table 1 denotes, connectance, *C*, is the number of realised links out of the total possible links and is a measure of the complexity of a network often calculated to understand wholesale structure (Dunne et al. 2004). Additional normalised metrics include mean chain length, mean and maximum trophic level, in-degree (generality), and out-degree (vulnerability) (Maia et al. 2019; Shaw et al. 2021a). As well as this, normalised motifs such as apparent and direct competition, omnivory and linearity reveal the prevalence of these functions within the marine community, Table 1 (Shaw et al. 2021a; Dunhill et al. 2024).

Modern trophic structure appears to be independent of species identity, abundance or evenness, and is largely consistent across global oceans (Vasconcellos et al.1997; Yeakel & Dunne 2015; Kortsch et al. 2019). The structure of trophic interactions between primary producers, intermediate species and apex predators produces consistent metrics in vastly different marine habitats (Dunne et al. 2004). This implies there are fundamental forces governing the trophic organisation of marine communities that transcend other elements of community structure, e.g. species composition (Yeakel & Dunne 2015). However, it is unknown if this has been the case since the earliest food webs, i.e. the Cambrian Explosion ~541-530 Ma (Dunne et al. 2008), or if this modern structure developed at some point in the Phanerozoic, perhaps following a mass extinction event (Yeakel & Dunne 2015).

Table 1. Common trophic network metrics calculated in literature and in this study, along with their symbols, definitions and references for the definitions.

Metric	Symbol/Alternative name	Definition	References
Size / Diversity	*S*	The number of different taxa (nodes) in a trophic network	Dunne et al. 2004
Number of links	*L*	The number of feeding interactions (links) between nodes in a network	Dunne et al. 2004
Links per species	*L / S*	The number of links divided by the number of nodes in a network	Dunne et al. 2004
Connectance	*C*	The number of realised feeding interactions (L/S^2) in a network	Dunne et al. 2004
Normalised in-degree	*Generality*	The number of prey consumed by each predator in a food web normalised by network size	Dunhill et al. 2024
Normalised out-degree	*Vulnerability*	The number of predators consuming each prey in a network normalised by network size	Dunhill et al. 2024
Maximum trophic level	*Max TL*	The maximum trophic level within a trophic network	Dunne et al. 2004
Mean trophic level	*Mean TL*	The mean trophic level within a trophic network	Dunne et al. 2004
Normalised number of linear chains	*Linearity*	The number of chains linking three nodes in a network, normalised by network size	Dunhill et al. 2024
Normalised number of omnivory motifs	*Omnivory*	The number of occurrences of consumers feeding across multiple trophic levels, normalised by network size.	Dunhill et al. 2024
Normalised number of apparent competition motifs	*Apparent competition*	The number of occurrences of apparent competition: sharing a common predator with another node, normalised by network size	Dunhill et al. 2024
Normalised number of direct competition motifs	*Direct competition*	The number of occurrences of direct competition: sharing a common resource with another node, normalised by network size.	Dunhill et al. 2024

Marine trophic networks have previously been reconstructed across the Early Toarcian Hyperthermal Event (ETEE, ~183 Ma), and it appears trophic structure and function did not permanently change - only temporary perturbations were reported across the event (Dunhill et al. 2024). The authors hypothesise this to be an example of the skeleton crew hypothesis, whereby the functional redundancy was high prior to extinction to afford the loss of most taxa but no net loss of guild or function (Dunhill et

al. 2024). The K-Pg mass extinction had the potential to permanently alter the trophic structure of marine systems, by inciting an impact-driven primary productivity crisis and secondary cascades affecting consumers all the way to the large marine reptiles (Hull et al. 2011; Lowery et al. 2020). Reconstructing trophic networks across the K-Pg mass extinction could shed light on the impact of the extinction at a community-level in the marine realm and if the event represents an ecological turning point in community structure and function. Such investigation could determine if the K-Pg indeed represents the origin of modern marine trophic structure (Dunne et al. 2014).

1.2.4 Latitudinal diversity gradients

Today's marine communities show disparity between the highly species diverse equatorial regions and low diversity polar regions (Jablonski et al. 2006). This is known as the Latitudinal [species] Diversity Gradient (LDG) and is thought to be strongly correlated with both temperature and seasonality (Roy et al. 2000; Jablonski et al. 2006; Mannion et al. 2014; Saupe et al. 2019a; 2019b; Saupe 2023). However, it remains unclear if there exists a modern Latitudinal *Functional* Diversity Gradient (LFDG). The few times an LFDG has been tested alongside the LDG, species diversity did not reliably estimate functional diversity (Stevens et al. 2003; Lamanna et al. 2014; Schumm et al. 2019; Diamond & Roy 2023; Erdős et al. 2023). The few investigations into FD across latitude have been limited to single-clade studies in both modern and ancient oceans (Becker et al. 2021; Grossman et al. 2022; Tang et al. 2022), and there remains a gap in literature for a multi-clade global deep time study of a potential functional gradient using the Ecospace Cube method (Bambach et al. 2007).

The exact nature and timing of the formation of the species LDG remains unknown (Hillebrand 2004; Mannion et al. 2014; Crame 2020; Brodie & Mannion 2023; Fenton et al. 2023). The origin of any potential LFDG also remains unknown at this point, and it is unknown if this could be correlated with temperature and seasonality as is the LDG. The contemporary LDG is indicative of an icehouse climate and consistent seasonality (Jablonski et al. 2006; Mannion et al. 2014). An early Cenozoic radiation, including many modern marine invertebrate species, was most intense in the tropics and is cited as a contributing factor to forming the LDG (Crame 2014; 2020), and perhaps doing the same for functional richness. Meanwhile, consistent cooling from the Eocene-Oligocene boundary (~34 Ma) is another possible driver, forcing warm-water species into lower latitudes, (Zachos et al. 2001; 2008; Mannion et al. 2014; Crame 2020), while shifting the latitude of the zone of peak

species origination (Jablonski et al. 2006).There is microfossil evidence that the modern LDG can be identified from the Langhian (~15 Ma) onwards (Fenton et al. 2023). Investigating the formation of the diversity gradients observed today would pinpoint the formation of modern distribution of ecological diversity on the planet.

1.2.5. Challenges faced when reconstructing fossil communities

The fossil record is biased in what becomes preserved (preservational bias) and what is subsequently recovered (sampling bias) (Shaw et al. 2021a; Raja et al. 2022). Reconstructions of ancient communities face unique challenges compared to modern studies (Shaw et al. 2021a; 2021b). For example, it is hard to be certain of the range of life habits and traits of extinct organisms from body fossils only (Roopnarine 2010). It is also impossible to observe feeding interactions of extinct species, to reconstruct ancient food webs (Pillar et al. 1992; Roopnarine 2010 Sperling et al. 2013). Moreover, Shaw et al. (2021a; 2021b), find authors often fail to account for key differences between modern and ancient ecological datasets, noticeably the missing soft-bodied taxa from fossiliferous sequences. However, it seems soft-bodied organisms (cephalopods, jellyfish, and most annelids) are omitted by the fossil record in a predictable manner, allowing for comparison between datasets and potential *post hoc* additions of soft-bodied taxa (Shaw et al. 2021b). Additionally, time-averaging risks grouping species together that may not have existed at the same time in reconstructed meta-communities (Fürsich & Aberhan 1990; Kidwell 2013). To account for uncertainty, analyses are often deliberately restricted to the exceptional preservation of Lagerstätten (Dunne et al. 2008). From Lagerstätten, functional morphology, gut contents, coprolite, damage patterns, mouth parts and body size restraints have all been used to deduce ancient feeding interactions (Dunne et al. 2008; 2014; Roopnarine & Angielczyk 2015; Roopnarine et al. 2017).

1.3. The Cretaceous-Paleogene (K-Pg) Boundary:

1.3.1. The K-Pg extinction – a bottom-up extinction cascade?

As mentioned earlier, the K-Pg mass extinction (~66 Ma) is the last major mass extinction in the fossil record (Raup & Sepkoski 1982). It is thought the K-Pg extinction caused ~60% of marine species to go extinct (Alroy 2008). It is widely accepted that the K-Pg was caused by the Chicxulub meteorite impact, into what is now the Yucatán Peninsula, Mexico (Alvarez et al. 1980; Hildebrand et al. 1991; Schulte et al. 2010). Impact particulates were likely ejected into the stratosphere, blocking solar irradiation to Earth's surface and severely impeding global primary productivity (Jablonski 1994).

As well as this, impact-induced greenhouse gas emission and sulphuric acid rain led to ocean acidification which catalysed extinction selectivity towards calcareous nanoplankton and further impeded primary productivity (Henehan et al. 2016; 2019; Lowery et al. 2020).

The large-scale loss of primary productivity is thought to have led to bottom-up extinction, through secondary extinction cascades (Hull et al. 2011; Lowery et al. 2020). Primary consumers suffered with dwindling plankton resources and in turn secondary consumers suffered from a loss of prey and so forth, until extinction reached the highest trophic levels, where it had profound impact (Jablonksi 1994; D'Hondt 2005). The apex predators of the Late Cretaceous, the large marine reptiles (mosasaurs and plesiosaurs) became extinct during the K-Pg due to their large energy requirements (Jablonksi 1994; D'Hondt 2005). The K-Pg also led to a breakdown in water column stratification which further affected benthic communities and sparked further secondary extinction cascades (Hull et al. 2011). The complex nature of the extinction, particularly targeting the bottom of trophic networks directly and the top of them indirectly through secondary extinction cascades makes it possible that the structure of marine ecosystems was permanently altered by this event. Following the major loss of marine taxa, there was a shift in benthic dominance from sessile filter-feeding bivalves to motile grazing or predatory gastropods (Crame et al. 2014), altering the primary feeding strategies in the benthos. As well as this, with Early-Cenozoic radiations of modern midwater fish, including lanternfish and anglerfish (Near et al. 2012), and multiple modern clades of coral reef fish (Near et al. 2012; Price et al. 2014), the K-Pg could represent a turning point that forged modern trophic structure (Dunne et al. 2014).

Furthermore, despite the Chicxulub impact being the widely-accepted cause of the K-Pg extinction, it is still debated whether the Deccan Traps Large Igneous Province Region (LIP) degraded ecosystems in the latest Cretaceous, prior to impact (Keller et al. 2008; Sakamoto et al. 2016; Hull et al. 2020). Multiple previous mass extinctions were likely induced by intense LIP volcanism, for example the PTME is thought to have been caused by the Siberian Traps (Reichow et al. 2009; Burgess et al. 2017), and the LTME coincides with the Central Atlantic Magmatic Province eruptions (Davies et al. 2017). There is debate over whether terrestrial dinosaur communities were in decline due to Deccan volcanism prior to the K-Pg boundary (Sakamoto et al. 2016; Allen et al. 2024). There is no published evidence of ecological decline within the marine realm prior to the K-Pg, with plentiful evidence of an abrupt extinction indicative of a meteorite impact extinction driver (Witts et al. 2015; 2016;

Whittle et al. 2019). Detailed study across the boundary is necessary to unpick the effects of the mass extinction on marine trophic organisation. Investigation would also determine if the Deccan Traps LIP led to decline in marine trophic structure prior to the Chicxulub impact.

1.3.2. Recovery from the K-Pg and the emergence of new ecological strategies

Both taxonomic and functional diversity is thought to have recovered rapidly from the K-Pg mass extinction (Lowery et al. 2018). Geographic heterogeneity in biotic recovery from the K-Pg arose from factors including global biogeochemical cycling (D'Hondt et al. 1998; Hull et al. 2011; Hull 2015). Tethys Sea carbon export, for example, indicates a return to a Late Cretaceous level around 300 kyr after the extinction boundary (Henehan et al. 2019; Lowery et al. 2020). This coincides with global biogeochemical cycle and primary productivity recovery, at around 300-500 kyr post K-Pg (Jiang et al. 2010; Witts et al. 2018; Birch et al. 2021). Antarctic benthic molluscs saw three new species appear directly above the extinction horizon, in the earliest Paleogene (Whittle et al. 2019) i.e. less than 500 kyr from impact, indicating a rapid recovery here.

As mentioned, many modern marine taxa have their evolutionary roots in the early-Cenozoic radiation following the K-Pg event (Uhen 2010; Meredith et al. 2011; Crame et al. 2014; Price et al. 2014; Schwarzhans et al. 2024). For example, the K-Pg resulted in the 'broad framework' of modern reef fish assemblages, through 10 Myr of reef colonisation following the extinction (Price et al. 2014). The K-Pg also led to a shift in benthic communities, from being dominated by suspension-feeding bivalves to grazing/predatory gastropods (Witts et al. 2018). In particular, the significant radiation of many modern groups, including the Neogastropoda points to the possibility of modern marine trophic structure arising out of the K-Pg extinction with potential structural changes in Cenozoic systems that set them apart from their Late Cretaceous counterparts as definitively more modern (Crame et al. 2014; Dunne et al. 2014).

1.3.3. Did modern marine ecosystems originate during the K-Pg, or emerge through the Cenozoic?

The exact origins of modern marine community structure and function remain unknown. It is unclear if 'modernisation' occurred after the K-Pg extinction (Dunne et al. 2014) or incrementally over the last 66 Myr of the Cenozoic Era. Many modern taxa proliferated in the wake of the K-Pg mass extinction and into the early Cenozoic (Renne et al. 2013; Crame et al. 2014; Hull 2015). The K-Pg also likely influenced marine community structure and function. For example, there was a shift in benthic

dominance across the boundary, from suspension-feeding bivalves to motile gastropods, a dominance that remains today (Tracey et al. 1993; Hull et al. 2011; Crame et al. 2014). However, several events across the Cenozoic also led to modern marine taxa proliferating. For example, global cooling and glaciation at the Eocene-Oligocene Transition likely explained a major turnover in marine microfossils and an increase in cold-water taxa at the poles, as is characteristic of modern assemblages (Williams et al. 2007; Bordiga, 2015; Trejos et al. 2024). Therefore, detailed investigation across both the K-Pg boundary and the following Cenozoic Era, may shed further insight into how marine communities gained modern characteristics of trophic structure and function.

1.4. Current Knowledge gaps:

1.4.1. The origins of modern community structure and function and the resilience of the last 66 Myr

It remains unknown if modern marine community structure and function originated out of the K-Pg mass extinction or incrementally during the following Cenozoic Era. The K-Pg is also the last major mass extinction event, after which no further mass extinction has been identified in the fossil record (Sepkoski 1981). Some suggest ecosystems gained a robustness across the Phanerozoic from repeated exposure to extinction (Erwin 2008). Roopnarine, (2006), proposed evolving community structures explain deep-time trends of declining Phanerozoic background extinction. Whereas others (e.g. Dunne et al. 2014; Hull 2015) believe the K-Pg extinction itself forged modern marine trophic structure from protracted environmental and biotic change during and after the extinction, which led to a greater resilience and robustness to perturbation.

Despite no major mass extinction, Earth experienced extreme climate events during the Cenozoic Era (Westerhold et al. 2020), with both hyperthermal events (e.g. the Paleocene-Eocene Thermal Maximum) and hypothermal events (e.g. the Eocene-Oligocene Transition) (Speijer et al. 2012; Hutchinson et al. 2021). The effects of such events on marine ecosystems at a community-level remain largely unexplored. As mentioned, Cenozoic events may have led to marine communities gaining a modern structure, both globally and regionally - for example the strengthening of the LDG and turnover of marine taxa.

1.4.2. Trophic structure and community function across extinctions

Published literature is also lacking in investigations of the trophic structure of marine communities across mass extinctions and their following recovery intervals (Roopnarine & Angielczyk 2015; et al. 2017; Dunhill et al. 2024). Roopnarine & Angielczyk (2015) found that paleocommunities exhibited significantly greater local stability across the Permian-Triassic Mass Extinction (PTME), depending on their functional rather than species diversity. Similarly, the Karoo Basin ecosystem appears to have resisted structural breakdown despite a significant reduction in species across the PTME (Roopnarine et al. 2017). Such studies are crucial to understand and evaluate the impacts of mass extinction and their role in the development of modern marine communities. Yet, neither trophic networks nor global and regional community function have been reconstructed across the mass extinction that occurred closest in time to modern communities, i.e. the K-Pg (~66 Ma).

1.4.3. Functional diversity gradients and the timing of the LDG

As mentioned, it remains unknown if there exists a modern Latitudinal Functional Diversity Gradient (LFDG) akin to the modern LDG. The nature and timing of the formation of the modern LDG also remains undetermined. Debate remains as to if the LDG existed in the early Cenozoic, i.e. pre-Oligocene (Crame et al. 2018) or if this developed later in the Cenozoic, i.e. post-Oligocene (Fenton et al. 2023). If an LFDG exists in the modern oceans, it remains unknown how and when this may have formed and if its formation is coupled with that of the species diversity gradient.

1.5. Thesis Aims and Hypotheses:

Thesis Aim: To evaluate whether modern marine community structure and function originated in the aftermath of the K-Pg mass extinction and following Cenozoic Era.

Study 1 Aim: To examine trophic structural shifts across the K-Pg extinction and recovery interval.

Study 1 Hypothesis: The K-Pg extinction collapsed trophic networks, but recovery phases saw the origin of new trophic network structures resembling modern ones.

Study 2 Aim 1: To investigate global functional diversity across the Cenozoic Era

Study 2 Hypothesis 1: Global marine invertebrate functional diversity will shift significantly across the K-Pg boundary but not across the following Cenozoic events.

Study 2 Aim 2: To investigate global functional diversity across the Cenozoic Era

Study 2 Hypothesis 2: A latitudinal functional diversity gradient (LFDG) emerged during the Cenozoic, paralleling or diverging from taxonomic patterns – i.e. bimodal subtropical or temperate peaks during greenhouse Early-Cenozoic and a shift towards a single equatorial peak in the later Cenozoic as the climate cooled to icehouse conditions (Mannion et al. 2014).

1.6. Chapter Summaries:

1.6.1. Chapter 2 Summary (Study 1):

This study reconstructed four trophic meta-webs using the fossil-specific PFIM model (Shaw et al. 2023), spanning the K-Pg boundary (Late Cretaceous to Mid-Eocene) from well-preserved assemblages on Seymour Island, Antarctica. By comparing structural and functional network properties, this study found no significant or permanent shifts in marine community architecture across the extinction interval. The results indicated ecological stability and functional resilience within this marine ecosystem through the K-Pg crisis. Moreover, there was no detectable evidence that the Deccan Traps Large Igneous Province (LIP) caused widespread ecological degradation prior to the boundary, supporting the interpretation that the Chicxulub impact alone was the principal driver of extinction.

1.6.2. Chapter 3 Summary (Study 2)

Part A: The first half of this study reconstructed the functional diversity (FD) of global marine invertebrates at stage level between the Campanian and the Piacenzian, inclusive. Using the Ecospace Cube method (Bambach et al. 2007) and a PBDB data download, the Mode of Life (MoL) diversity of all major marine invertebrate phyla was investigated. Analyses indicated some stage-to-stage variation but no directional trend in FD across the K-Pg boundary to the Pliocene. However, there were sustained rises in FD across the Eocene, and Miocene, coinciding with both global heating (Eocene) and cooling (Miocene) events and long-term trends. Additionally, the proportion of global genera within each MoL was altered across the K-Pg boundary, with a decline in cephalopod-associated MoLs and reef-builders and a large increase in proportion of gastropod-associated MoLs for the rest of the interval. The Bray Curtis

Dissimilarity Index (Bray & Curtis 1957) also indicated a substantial shift in taxonomic composition across the K-Pg. However, at no point was functional composition significantly dissimilar between stages, indicating no substantial functional shifts likely occurred during the interval, on a global scale.

Part B: The second half of this study reconstructed the same global invertebrate communities as above but split them into palaeolatitude bands of 10˚ width, between 60˚N/S, at both stage level and epoch level (for a larger sample size) between the Campanian and Piacenzian. Consistent temperate peaks in marine invertebrate functional and taxonomic diversity occurred in almost every stage and epoch. The latest stages of the interval (Zanclean and Piacenzian) saw the beginnings of a tropical peak in taxonomic diversity, however functional diversity remained at its highest in the temperate North during this time. These results conclude that latitudinal functional diversity has remained remarkably stable across latitude from the Late Cretaceous to the Pliocene, i.e. across the K-Pg and Cenozoic climate events. This may be an artefact of sampling bias or perhaps suggests the existence of an LFDG that decoupled from the taxonomic diversity distribution across latitude (LDG) in the later Cenozoic.

Chapter 2 – Marine trophic structure across the Cretaceous-Paleogene (K-Pg) mass extinction

Abstract

The Cretaceous–Paleogene (K-Pg) mass extinction eradicated ~60% of marine species and reshaped global biodiversity. While post-extinction radiations established many modern lineages, it remains unclear whether this event fundamentally altered marine community structure and function. It has been proposed that the K-Pg marked the emergence of modern marine ecosystems, yet this has not been empirically tested. Four trophic meta-webs were reconstructed using the fossil-specific PFIM model, spanning the K-Pg boundary (Late Cretaceous–Eocene) from well-preserved assemblages on Seymour Island, Antarctica. By comparing structural and functional network properties, this study finds no significant or permanent shifts in marine community architecture across the extinction interval. These results indicate ecological stability and functional resilience within this marine ecosystem through the K-Pg crisis. These findings refute the hypotheses that the K-Pg event permanently altered and marked the origin of modern marine community structure and function. Moreover, there is no detectable evidence that the Deccan Traps Large Igneous Province (LIP) caused widespread ecological degradation prior to the boundary, supporting the interpretation that the Chicxulub impact alone was the principal driver of extinction.

The candidate (LHW) downloaded and reviewed the dataset, contributed additional entries, conducted statistical analyses and drafted the manuscript. All authors (LHW and supervisors) contributed to project direction, data interpretation and editing the manuscript. The data and code used in this chapter are available via the link: LHW_Supplementary_Material

The work in Chapter 2 will appear in the manuscript: Woods, L.H. Whittle, R.J. Witts, J.D. Shaw, J.O. Beckerman, A.P. Dunhill, A.M. 2025. The K-Pg Mass Extinction did not permanently restructure a marine food web. *In prep*

2.1 Introduction

Major mass extinctions have repeatedly triggered vast losses of species in the deep past and brought extensive ecological turnover on relatively short time scales (Raup 1986). Causing considerable taxonomic shifts, mass extinctions potentially restructured ecosystems and modified ecological functioning at times across the Phanerozoic (Erwin 2008; Price et al. 2014; Dunne et al. 2014; Hull 2015; Crame 2020). Investigation into the potential for extinctions to restructure marine communities provides a deep-time understanding of marine macroevolution and clues to how modern systems may fare under ever-increasing anthropogenic stressors.

The Cretaceous-Paleogene mass extinction (K-Pg), ~66 Ma, represents a strong candidate for a major structural shift in marine communities. The most recent mass extinction in Earth's history, the K-Pg caused a global loss of ~60% of marine species (Alroy 2008). Due to its timing and magnitude, not only does the K-Pg extinction represent a potential turning point in the structure of marine communities, but could also be the point of origin of 'modern [marine] trophic organisation' or modern marine community structure (Dunne et al. 2014). However, this is yet to be quantitatively investigated.

It is widely accepted that the K-Pg mass extinction was a result of the Chicxulub meteorite impact in the Yucatán peninsula (Chiarenza et al. 2020), which likely ejected particulates into the stratosphere, blocking solar irradiation to the surface and inhibiting primary productivity (D'Hondt et al. 1998; Schulte et al. 2010; Kaiho 2016). Impact-induced ocean acidification, triggered by greenhouse gas release as well as sulphuric acid to rain into the oceans likely catalysed extinction selectivity towards calcareous nanoplankton in particular, with over 90% species extinction - a near total loss of the clade (Henehan et al. 2016; 2019; Lowery et al. 2020). The K-Pg also led to a breakdown in water column stratification which further affected benthic communities, sparking secondary extinction cascades as well as those caused by the depletion of primary production alone (Hull et al. 2011). As a result, pelagic apex predators were seriously affected due to their large energy requirements, whereby bottom-up extinction cascades led to the large marine reptiles becoming extinct in particular (Bardet 1994; Gallagher 2005). The K-Pg was a complex extinction, particularly targeting the bottom of trophic networks directly and the top of them indirectly through secondary extinction cascades. Thus, it is entirely possible that the structure of marine ecosystems was permanently altered by this event; a turning point that may have forged modern marine ecosystem structure (Dunne et al. 2014).

Both taxonomic and functional diversity recovered rapidly from the K-Pg extinction, with factors including Earth-system succession (e.g. global biogeochemical cycling) contributing to geographic heterogeneity in biotic recovery (D'Hondt et al. 1998; Hull et al. 2011; Hull 2015; Lowery et al. 2018). For example, Tethys Sea carbon export indicates a return to a Late Cretaceous level of productivity ~300 Kyr after the Chicxulub impact (Henehan et al. 2019; Lowery et al. 2020), coinciding with global biogeochemical cycle and primary productivity recovery (Jiang et al. 2010; Witts et al. 2018; Birch et al. 2021). Many modern marine taxa have their evolutionary roots in the early-Cenozoic radiation following the K-Pg event (Uhen 2010; Meredith et al. 2011; Crame et al. 2014; Price et al. 2014; Schwarzhans et al. 2024). Ecological turnover following the K-Pg extinction included a shift in marine benthic communities, from suspension-feeding bivalve domination to grazing/predatory gastropod domination (Witts et al. 2018). In particular, the arrival of the Neogastropoda in the Danian points to the possibility of modern trophic organisation arising out of the K-Pg extinction with potential structural changes to Cenozoic systems that set them apart from their Late Cretaceous counterparts (Crame et al. 2014; Dunne et al. 2014).

Furthermore, despite the majority consensus that the K-Pg extinction was indeed caused by the Chicxulub meteorite, ~66 Ma (Schulte et al. 2010; Chiarenza et al. 2020), debate remains as to whether the Deccan Traps Large Igneous Province Region (LIP, ~66.4-65.5 Ma) instigated ecological decline in communities prior to impact, as has been postulated for terrestrial dinosaur communities (Keller et al. 2009; Keller et al. 2011; Sakamoto et al. 2016; Schoene et al. 2019). In the marine realm, taxonomic and functional diversity appear to display a single sharp decline, more consistent with a bolide impact alone and no discernible input from Deccan Traps volcanism has been found (Witts et al. 2015; 2016). However, calcium isotopes have shown a 'wasp-waist' scenario, indicating that large marine reptiles had fewer prey items in the latest Cretaceous stages than in earlier ones, which perhaps catalysed their extinction at the K-Pg boundary (Martin et al. 2017).

The Late Cretaceous to Paleogene sequence of Seymour Island, Antarctica, represents one of the most expansive K-Pg boundary-crossing sedimentary successions in the world (Sadler 1988). This succession is ideal for examining community change over the K-Pg boundary because it has extensive preservation, from the Maastrichtian to the Eocene ~70-33.9 Ma, and displays remarkable lithological homogeneity despite the environmental changes associated with the mass extinction (Witts et al. 2018; Montes et al. 2019). Both the onset of the main phase of Deccan volcanism and the Chicxulub meteorite impact are recorded in the Lopez de

Bertodano Formation (LDBF), permitting detailed study with little change in preservation conditions (Montes et al. 2019). The initial recovery is found in the Danian of the LDBF as well as the Sobral Formation and, after an unconformity in the succession, the recovered system dates to the Early to Mid-Eocene, Cross Valley and La Meseta formations.

Here, I examine marine ecosystem structure across the K-Pg extinction event at Seymour Island, by modelling trophic meta-networks for four broad time intervals from the Late Cretaceous to the Eocene, using fossil occurrences and ecospace traits. The four intervals analysed were the pre-Deccan (Early to Mid-Maastrichtian); Late Maastrichtian; Recovery (Danian); Recovered (Eocene). I used the Palaeo Food Web Inference Model (PFIM) (Shaw et al. 2023), a novel trait-based inference model, to assess the probability of encounter and consumption between every pair of species in a list of occurrences. The PFIM uses rules defined by optimal foraging theory and Bambach ecospace traits, i.e. body size, motility level, tiering position and feeding mode to build a meta-web of likely feeding interactions; a proxy of community structure (Bambach et al. 2007; Shaw et al. 2023). I then compare key network metrics across the four reconstructed meta-webs to answer the following questions: (i) How did the K-Pg mass extinction affect marine meta-community structure?; (ii) Were any changes in meta-community structure permanent and did the K-Pg mass extinction represent the origin of modern marine community structure?; and (iii) Did the Deccan Traps Large Igneous Province main phase of eruptions negatively impact community structure prior to the bolide impact at the K-Pg boundary?

2.2. Materials and Methods

2.2.1. Dataset

Fossil occurrence data was obtained from variety of published and unpublished datasets (Witts et al. 2016; Whittle et al. 2019; Witts & Whittle, unpublished data, 2006; 2009). The study interval extends from the Late Cretaceous to the Eocene of Seymour Island, Antarctica, and consists of the Snow Hill Island Formation, the Lopez de Bertodano Formation (LDBF), the Sobral Formation, the Cross Valley Formation and the La Meseta Formation; Eocene (Sadler, 1988; Montes et al. 2019).

The dataset consists of 358 fossil taxa (categorised mostly to species level but some occurrences are at genus level or higher wherever species-level data were unavailable). The majority of occurrences used in this study were derived from Witts et al. (2016), Whittle et al. (2019) or (Witts and Whittle, unpublished data, 2006; 2009)

supplemented with an extensive literature search (Supplementary file named '*LHW_Supplementary_Refs.xls'*). The data were split into four time intervals across the K-Pg boundary to compare the marine meta-communities across the extinction. The first meta-community, the '*Pre-Deccan'*, dates from the Early to Mid/Late Maastrichtian, ~70–67 Ma. This includes fossils from the Snow Hill Island Formation and the Lopez de Bertodano Formation Units 1 to 8, inclusive. These organisms lived prior to both the onset of the main phase of the Deccan Traps eruptions and to the Chicxulub bolide impact. The next interval is the '*Late Maastrichtian'*, ~67-66 Ma, which includes fossils found in LDBF Unit 9 only. This interval included the onset of the main phase of eruptions of the Deccan Traps ~ 66.4 Ma but was still prior to the K-Pg boundary. The third community, '*Recovery*', dates to the Danian (early Paleocene), ~66-61.6 Ma, and includes fossils found in LDBF Unit 10 and the Sobral Formation, in the aftermath of the K-Pg extinction. Finally, due to an unconformity between the Danian and Eocene, the '*Recovered*' meta-community dates to the Eocene, ~56-45 Ma, and includes fossils from the Cross Valley or the La Meseta formations (Maranessi et al. 2002).

2.2.2. Defining ecological traits of fossil organisms

Four ecological traits were used to reconstruct and quantify the structure of each of the four meta-communities across the K-Pg extinction boundary, using the PFIM model (Shaw et al. 2023). Three of the four traits were the diet, motility, and substrate tiering position of the organisms, as defined by the Bambach Ecospace Cube (Bambach et al. 2007). The fourth trait was body size, an important component of contemporary trophic models, facilitating the use of optimal foraging theory (Petchey et al. 2008).

For each occurrence, ecological traits were obtained from the Palaeobiology Database (PBDB 2022), wider published literature and/or alternative databases (MarLIN; Mindat.org; FishBase 2022). The diet categories were defined as the unique combination of taxa eaten by consumers from the list of other occurring species within each interval. The feeding categories are as listed: Primary; Gastropod_herb; Gastropod_pred; Gastropod_omni; Bivalve; Coral; Brachiopod; Crinoid; Ammonoid; Belemnites; Decapod, Echinoid; Nautiloid; Polychaete; Scaphopod; Fish_duro; Omni_duro; Fish1; Fish2; Fish_plankt; Fish_pisc; Fish_pelag; Hake_cuskeel; Shark1; Shark2; Otodontid; Cow_shark; Carcharinidae; Basilosaur; Plesiosaur; Mosasaur; Penguin; Seabird_herb (see *CH2_Supplementary_Material, S1A* for associated prey items for each). The size categories were defined as the longest axis of the specimen, or using dental allometric formulas (for example, in Chimaeroids, the length of a

palatine plate is approximately 4% of the total body length (Cicimurri et al. 2008) etc. (see *LHW_Supplementary_Refs.xls*). The body size category increased by order of magnitude: 0 – 1 mm; 1 – 10 mm; 10 – 100 mm; 100 – 1000 mm; 1000 – 10 000 mm; and 10 000 – 100 000 mm *(CH2_Supplementary_Material, S1B).*

Tiering categories consisted of: erect; epifaunal; semi_infaunal; shallow_infaunal; boring; deep_infaunal; nektobenthic; nektonic; surface (i.e. near surface waters only – e.g. most sea birds) (*CH2_Supplementary_Material.doc, S1C*). Motility consisted of non-motile; facultatively motile; slow; and fast (*CH2_Supplementary_Material.doc, S1D*). A single node for primary producers was added to the bottom of each web to account for all primary producers and detritus, as per Shaw et al. (2023).

2.2.3. Using the PFIM to reconstruct four communities

The Palaeo Food Web Inference Model (PFIM) (Shaw et al. 2023) was used in R, version 4.3.0 to reconstruct a meta-community food web for each of the four time intervals, utilising body size, diet, tiering and motility (Bambach et al. 2007). The PFIM uses these traits to create an edge list (a list of all occurring species, paired) and then assigns the possibility of encounter and consumption for each pair in the edge list, using rules governed by ecological foraging traits (i.e. diet, motility, tiering and body size) (Shaw et al. 2023). A feeding interaction is realised only when feasible for all four traits, e.g. size category 100–1000 mm could eat category 10-100 mm but not 1000-10,000 mm, and so on with all four traits. The full list of feeding rules created for these analyses is available (*CH2_Supplementary_Material, S2*). Once the fossil communities had been reconstructed into the four most-likely meta-webs, the PFIM produced a graphical 3D representation of each meta-web (Fig. 3). All analyses and visualisations in this chapter were also carried out using R 4.3.0.

2.2.4. Analysing community structure and function:

Structural network metrics were calculated using the PFIM model (code available in the *Supplementary Material, 'LHW_PFIM_Script.R'*). This aimed to compare the structure and function of each of the four communities across the K-Pg boundary. The network metrics and functional motifs calculated are defined in Table 1 and their respective values are displayed in Tables 2 and 3. These consist of web size (i.e. diversity), number of links, number of links per taxa, community connectivity (i.e. connectance), maximum trophic level, mean trophic level, normalised in-degree (i.e. generality), normalised out-degree (i.e. vulnerability) and the prevalence of linearity, omnivory, apparent and direct competition motifs.

2.3. Results and Discussion

The PFIM model (Shaw et al. 2023) was used to reconstruct four meta-community food webs across the K-Pg boundary of Seymour Island, Antarctica. This was to understand the impacts of the K-Pg mass extinction on marine community structure and function using trophic networks, and to ascertain if the Deccan Traps LIP incited decline in marine communities prior to the bolide impact. The results are displayed in Figs. 3 & 4 and Tables 2 & 3 below.

Table 2. The structural network metrics (to 3 d.p.) calculated by the PFIM model for each of the four reconstructed food meta-webs in our study. 'Pre-Deccan' is the Early-Mid Maastrichtian, 'Late Maastrichtian' is the Late Maastrichtian, 'Recovery' is the Danian and 'Recovered' is the Eocene meta-web.

	Pre-Deccan	**Late Maastrichtian**	**Recovery**	**Recovered**
Diversity (no. species)	67	81	27	150
Number of links	808	1176	92	2750
Connectance	0.180	1.179	0.126	0.122
Links per species	12.06	14.519	3.407	18.33
Maximum Trophic Level	4.344	4.779	4.187	4.560
Mean Trophic Level	2.827	3.026	2.266	2.976
Generality	0.180	0.153	0.183	0.119
Vulnerability	0.1461	0.120	0.184	0.124

Table 3. The prevalence of functional motifs (to 4 d.p.) calculated by the PFIM model for each of the four reconstructed food meta-webs in our study, normalised by web size. 'Pre-Deccan' is the Early-Mid Maastrichtian, 'Late Maastrichtian' is the Late Maastrichtian, 'Recovery' is the Danian and 'Recovered' is the Eocene meta-web.

	Pre-Deccan	**Late Maastrichtian**	**Recovery**	**Recovered**
Normalised number of omnivory motifs	0.6832	0.6894	0.1961	0.6107
Normalised number of linear chains	0.5988	1.1969	0.0508	1.0042
Normalised number of apparent competition motifs	0.8621	1.0844	0.2647	1.3650
Normalised number of direct competition motifs	0.6988	0.8520	0.3224	1.4841

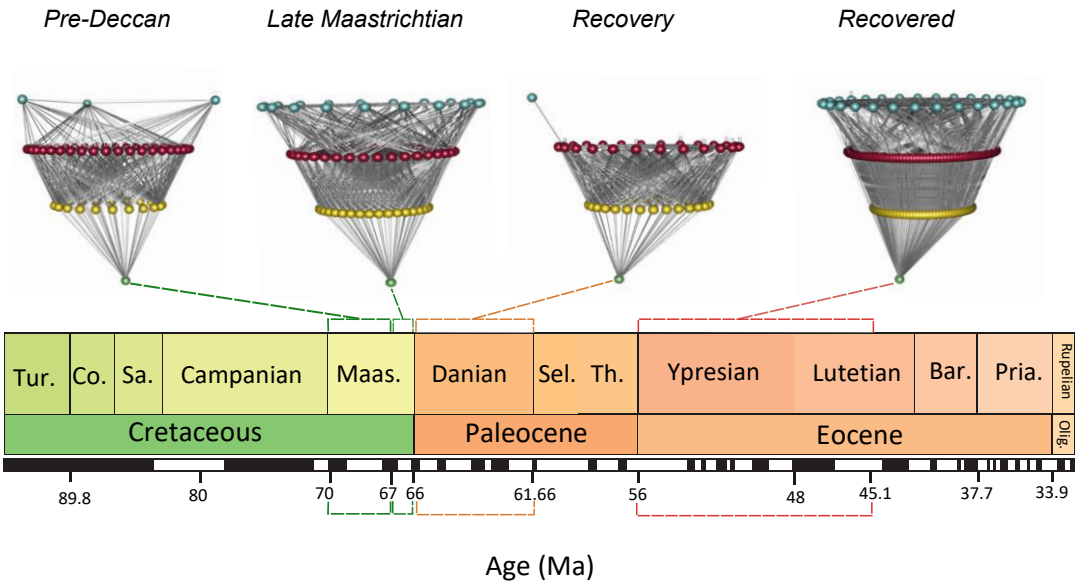

Figure 3. Graphical representations of inferred trophic meta-webs across the K-Pg boundary using fossils from Seymour Island, Antarctica, using the PFIM (Shaw et al. 2023). The associated timescale (colour) is below and the Seymour Island Formation ages below that (black and white). Dashed lines point to associated meta-webs indicating the interval each one was reconstructed from.

2.3.1 How did the K-Pg mass extinction affect marine ecosystem structure?

Both meta-webs from before the K-Pg boundary: the Pre-Deccan and the Late Maastrichtian, report network metrics congruent with contemporary marine food webs - i.e. connectance values of 0.180 and 0.179, for the Pre-Deccan and Late Maastrichtian, respectively; links per species of 12.06 and 14.52, respectively; and mean trophic levels of 2.83 and 3.03, respectively (Table 2). These metrics fall well within the ranges reported in modern marine food webs (Optiz 1996; Yodzis 1998; Dunne et al. 2002; Roopnarine & Hertog, 2013; Filguera & Castro 2011; Kortsch et al. 2015; Navia et al. 2016).

In contrast, across the K-Pg boundary, there is significant taxonomic loss; 86% of diversity and roughly 11.1 links per species are lost (Table 2, Fig. 4). This immense loss of taxa drove turnover in early Paleocene community composition. For example, a shift in benthic dominance from bivalves in the Late Cretaceous to gastropods in the Danian, and the arrival of the Neogastropoda (Crame et al. 2014). The number of modern genera of Neogastropoda rose from 0% in the Maastrichtian to 37% in the Middle Eocene, apparently representing the advent of modern benthic assemblages (Crame et al. 2014; Whittle et al. 2019). Despite these changes, however, the K-Pg

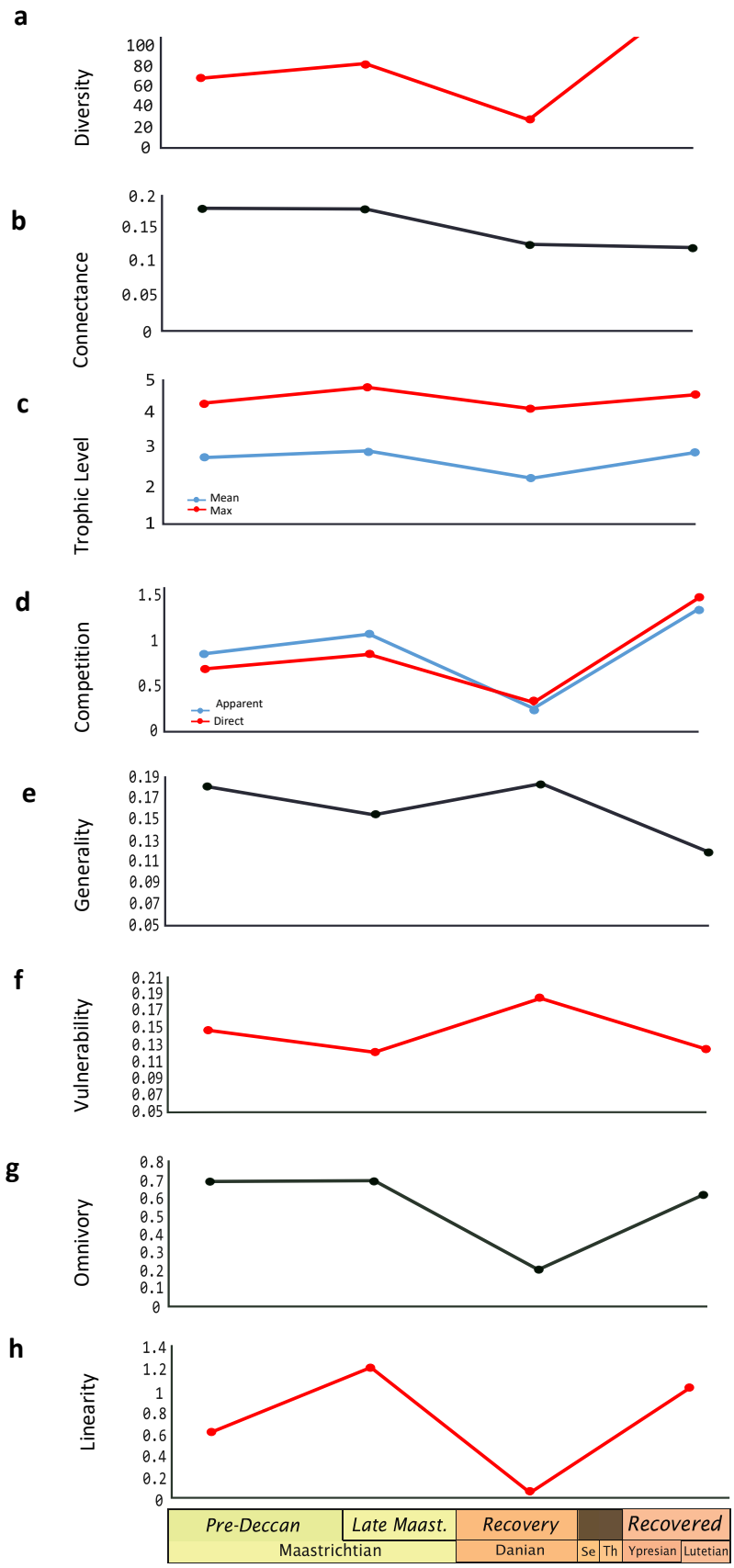

Figure 4. **a** = Network Diversity, **b** = connectance, **c** = trophic level (maximum TL in red, mean TL in blue), **d** = the prevalence of both competition motifs (apparent competition in blue, direct competition in red), **e** = generality (in-degree), **f** = vulnerability (out-degree), **g** = prevalence of the omnivory motif, **h** = prevalence of the linearity motif. See Table 1 for definitions of metrics and motifs. The meta-web name is above each associated point at the top of the plot, and a timeline is below with the meta-web names on above their associated stages.

mass extinction did not drive an observable change in meta-community complexity i.e. network connectance (Fig. 4b). Connectance (Table 1), is a key network metric frequently used to understand wholesale ecosystem structure and function (Dunne et al. 2002; Williams et al. 2002; Leclerc et al. 2023). The lack of substantial change in connectance indicates there were likely no major structural or functional shifts within the Antarctic community out of the K-Pg extinction. This is a novel result for trophic network structure and supports a lack of change in functional diversity (Whittle et al. 2019).

The retention of meta-community function across the K-Pg mass extinction and the resistance to total collapse despite the loss of most taxa is likely an example of the 'skeleton crew' hypothesis (Foster & Twitchett 2014; Dunhill et al. 2018). The skeleton crew hypothesis posits that substantial functional redundancy may permit a marine community to withstand the loss of a numerous species across an extinction event without losing a significant number of ecological niches and/or community function (Foster & Twitchett 2014; Dunhill et al. 2018). The Late Maastrichtian meta-community possesses the highest level of linearity out of all the webs (Fig. 4h), and thus likely held a high level of functional redundancy. Linearity denotes functional redundancy because it is the [normalised] number of chains between three nodes in a network and thus represents the ability to re-wire the web if a node is lost; the ability to maintain energy flow across trophic levels (Rosenfeld 2002; Blanchard 2015). The primary productivity crisis incited by the Chicxulub impact removed a large number of nodes, likely through secondary extinction cascades and subsequently diminished linearity in the Danian recovery community (Fig. 4h), leaving only a 'skeleton crew' to maintain ecosystem function (Krug et al. 2010; Edie et al. 2018). These results support Whittle et al. (2019) who found the number of molluscan modes of life (i.e. functional diversity), remained constant across the K-Pg boundary at Seymour Island, despite significant changes in the richness *within* each mode of life during this period.

While the wholesale structure of the Seymour Island marine community apparently remains intact, there are deviations in network metrics and functional motifs that suggest some perturbation in community function across the K-Pg extinction. For example, both maximum and mean trophic level drop in the Danian recovery meta-web, compared to the Late Cretaceous communities (Fig. 4c), indicating a shorter, less vertically complex trophic network. Maximum trophic level, or trophic height, has been observed to fall with a decrease in biodiversity and linearity (Williams & Martinez 2004; Dobson et al. 2006; Gabara et al. 2021). Similarly, a reduction in linearity from extinction could be due to fewer taxa at higher trophic levels,

providing fewer linear chains up the network. The drop in trophic height and the selectivity against apex predators, i.e. the loss of the mosasaurs and plesiosaurs, could be attributed to bottom-up extinction cascades whereby a probable primary productivity crash led to low energy transfer to the highest trophic levels (Arthur et al. 1987; Ikejiri et al. 2020). As a result, the modelled Danian recovery meta-community exhibits a durophagous cow shark *Notidanodon dentatus* (Cappetta 1975), as an apex predator, in the absence of larger species. Importantly, *N. dentatus* was at least an order of magnitude smaller than the reptilian predators at the top of Cretaceous meta-webs; another sign of energy loss in the system.

Furthermore, the generality (in-degree) and vulnerability (out-degree) both increase across the K-Pg extinction (Table 3, Fig. 4e-f). Generalist feeders are more likely to survive extinctions due to consuming a broader diet than specialist taxa and can adapt to the loss of prey sources by feeding more intensely on those that remain (Dunhill et al. 2024). As a result, so-called ‘disaster taxa’ or those that dominate after an extinction, are most often opportunistic generalist feeders (Rodland & Bottjer 2001) which in the case of the K-Pg, were mid-trophic-level consumers (Vellekoop et al. 2020; Guinot & Condamine 2023). Similarly, vulnerability within the Seymour Island community increases across the K-Pg extinction, due to a vast loss of species from the bottom of the food web (including suspension-feeding bivalves, ammonoids, belemnites and nautiloids). It is likely consumers had fewer viable resources to feed from as a result (Dobson et al. 2006; Dunhill et al. 2024). Finally, the drop in taxonomic diversity likely also drove the observed reduction in omnivory motifs (Fig. 4g) across the K-Pg. Post-extinction there are far fewer species within each niche to feed upon and also fewer consumers capable of feeding across trophic levels, explaining the drop in prevalence of omnivory motifs within the network (Gabara et al. 2021).

Finally, the drop in both apparent and direct competition motifs (Table 3, Fig. 4d) is once again likely due to lower taxonomic diversity (Pascual & Dunne 2006). The loss of the majority of taxa in the system, particularly at the top trophic levels, likely resulted in fewer consumers within each guild to compete for prey items (direct competition), and thus less competition between remaining prey species eaten by the same predator (apparent competition). The drop in competition is another indicator of a loss of functional redundancy across the K-Pg boundary (Fig. 4d). In summary, the reduction of the previously diverse community to a skeleton crew across the K-Pg boundary, suggests that the resulting early Paleocene community had low functional redundancy and would have been vulnerable to further environmental perturbation.

2.3.2. Did the K-Pg cause permanent changes to marine ecosystem structure?

An unconformity in the Seymour Island sequence means the initial recovery phase in the Danian is followed by the Eocene Cross Valley and La Meseta formations (Sadler 1988). The Eocene began 10 million years after the K-Pg extinction and global biodiversity had long recovered by this point (Lowery et al. 2018; Cocozza & Clarke 2020), however calcareous phytoplankton had likely only just returned to Late Cretaceous levels of diversity by the beginning of the Eocene (Arthur et al. 1987; Aberhan et al. 2007). By the Eocene, Seymour Island taxonomic diversity appears to recover to beyond that of either of the Late Cretaceous communities (Fig. 4). Along with taxonomic diversity, connectance does not substantially change from the Danian meta-community (or both Late Cretaceous communities), once again highlighting the lack of change in wholesale ecosystem structure and function across the K-Pg mass extinction.

Furthermore, by the Eocene, the Seymour Island community has undergone a complete recovery in all structural network metrics (Fig. 4). Both generality and vulnerability return to levels similar to those observed in the Late Cretaceous, reflecting the recovery of high degrees of specialism and trophic variety that can only be achieved under stable environmental conditions. To add to this, the maximum and mean trophic levels also recover to Late Cretaceous levels (Fig. 4c), with the origination of the early cetaceans such as Basilosauridae, increasing the trophic height of the community by re-occupying large apex predator niches. Such results are consistent with the recovery of a high level of functional redundancy, reflected in the recovery of linearity, as well as omnivory and both apparent and direct competition (Table 3, Fig. 4). In fact, both competition motifs surpass the levels recorded in the pre-extinction communities which might be evidence to support the idea of increasing robustness of ecological communities into the Cenozoic Era (Roopnarine 2006; Erwin 2008).

Overall, despite drastic taxonomic turnover, there are no detected permanent structural or functional shifts across the K-Pg mass extinction in the Seymour Island marine community. Based upon this evidence, we refute the hypothesis that the K-Pg boundary represents the origin of modern marine community structure, nor the unique structure of Antarctic marine ecosystems today (Convey et al. 2001; Dunne et al. 2014). Moreover, as stated earlier, all four reconstructed marine communities in this study display a ‘modern’ structure, i.e. connectance values between 0.01–0.3, number of links per species between 1.85–16.49, and mean trophic level between 1.35-3.1 (Optiz 1996; Yodzis 1998; Dunne et al. 2002; Roopnarine and Hertog. 2013;

Kortsch et al. 2015). Despite that fact that the immediate post-extinction recovery meta-web does exhibit marginal differences in metrics compared to the other three webs, its structural properties still fall well within modern ranges. These results suggest that if there has been a particular turning-point in the creation of modern marine community structure, it likely occurred prior to the Late Cretaceous.

2.3.3. Did Deccan Traps Volcanism cause ecological decline in marine communities?

The onset of the main phase of the Deccan Traps Large Igneous Province volcanism (~66.4 Ma) sits within the Late Maastrichtian time interval in this study (~67-66 Ma), yet no discernible negative effect on the structure of the Seymour Island community is detected at this resolution. It is not possible to split Unit 9 of the Lopez de Bertodano Formation into occurrences before and after the onset of the Deccan Traps, and therefore the effect of the volcanism may be masked by time averaging across the ~1 Myr interval. However, the results align with Witts et al. (2018) and Whittle et al. (2019) who report no decline in molluscan taxonomic nor functional diversity over the Late Maastrichtian, but rather a single abrupt drop in both at the Cretaceous-Paleogene boundary, 66 Ma. Despite potential masking due to time-averaging, the results are supported by modelled scenarios of Deccan outgassing that fit best with empirical temperature records of the Late Cretaceous (Hull et al. 2020). The most likely scenario for Deccan volcanism was that up to 87% of outgassing occurred and diminished before the Chicxulub impact, in a short impulse (Hull et al. 2020). Thus, the estimated 2˚C of global warming in the Late Maastrichtian likely cooled back to a prior temperature before the K-Pg extinction (Hull et al. 2020), which may be why there is no discernible ecological response to the volcanism at this resolution.

Finally, the Late Maastrichtian meta-community has greater taxonomic diversity compared with the previous interval (Fig. 4a). This, along with negligible changes in connectance and number of links per species, points again to a lack of major change in ecosystem structure, whether advantageous or deleterious. The Late Maastrichtian meta-community shows a slight increase in maximum and mean trophic level, omnivory, and both apparent and direct competition, as compared to the Pre-Deccan meta-community (Table 3, Fig. 4). The level of linearity increases from 0.599 in the Pre-Deccan to 1.197 in the Late Maastrichtian meta-community, which represents an increase in functional redundancy, a metric expected to decrease under significant environmental stress (Dunhill et al. 2024), such as is also reported across the K-Pg boundary. This is further evidence to suggest Deccan Traps volcanism did

not affect Antarctic marine communities. In summary, although limited by temporal resolution, this study confirms that the K-Pg mass extinction was likely primarily caused by the Chicxulub meteorite impact. In turn, this paved the way for the emergence of early Cenozoic communities.

Overall, this study finds the K-Pg mass extinction likely did not cause permanent change to marine trophic structure and is likely not the origin of modern marine trophic structure as previously suggested (Dunne et al. 2014). Despite taxonomic loss and species turnover, the wholesale structure of the Seymour Island marine meta-community did not undergo change across the K-Pg boundary. This is likely due to the skeleton crew hypothesis (Foster & Twitchett 2014; Dunhill et al. 2018) whereby the substantial functional redundancy in the Late Maastrichtian meta-web (as implied by the linearity motif) afforded the loss of most taxa without losing any function in the Recovery meta-web. However, the K-Pg did incite temporary perturbations in meta-community function consistent with a productivity crisis and large-scale diversity loss (i.e. decreased vertical complexity, reduced mean trophic level, increased generality and reduced competition). Furthermore, finds that the sole cause of the K-Pg mass extinction is likely the Chicxulub impact at the K-Pg boundary. Deccan Traps volcanism did not inflict ecological damage to marine communities prior to impact, at this resolution. This being a regional study, global investigation into community structure and function is now needed to support these results.

Chapter 3 - Marine invertebrate functional diversity across time and space in the Cenozoic

Abstract

The Cretaceous-Paleogene (K-Pg) extinction and the subsequent Cenozoic Era were pivotal in shaping modern marine taxonomic diversity and composition. However, functional diversity (FD) remains comparatively understudied across this interval, despite the Cenozoic Era featuring major climatic perturbations, some comparable with worst-case climate change projections such as the Paleocene-Eocene Thermal Maximum (PETM). This study investigates how marine ecosystem functioning changed from the Late Cretaceous to the Pliocene. Part A reconstructed global marine invertebrate FD at stage level from the Campanian to the Piacenzian. Part B examined FD patterns across palaeolatitude bands (10° width, 60°N-60°S) at both stage and epoch levels. Both analyses used the Ecospace Cube method (Bambach et al. 2007) and occurrence data from the Paleobiology Database to quantify Mode of Life (MoL) diversity across major invertebrate phyla, applying raw, standardised (*iNEXT*; Alroy, 2010a), and spatially-standardised (*divvy*; Antell et al. 2024) approaches. Across all methods, Part A revealed considerable stage-to-stage variation in FD but no long-term directional trend from the Late Cretaceous to the Late Pliocene, nor any identifiable K-Pg extinction effect. However, sustained rises in FD occurred in the Eocene and Miocene, coinciding respectively with global warming events and cooling. The relative proportion of gastropod-associated MoLs increased markedly across the K-Pg boundary, while Bray-Curtis dissimilarity analysis indicated no major shifts in functional composition occurred despite significant taxonomic turnover. Part B found a consistently strong temperate (30-40°N/40-50°N) FD and taxonomic diversity peak through most stages and epochs. By the Pliocene, taxonomic diversity began shifting towards the tropics, yet FD remained highest at temperate latitudes. These findings indicate that latitudinal FD has remained remarkably stable from the K-Pg to the Pliocene, suggesting either a persistent latitudinal functional diversity gradient (LFDG) decoupled from taxonomic diversity, or that apparent stability reflects sampling and methodological bias.

The candidate (LHW) downloaded and reviewed the dataset, contributed additional entries, conducted statistical analyses and drafted the manuscript. All authors (LHW and supervisors) contributed to project direction, data interpretation and editing the manuscript. The data and code used in this chapter are available via the link: LHW_Supplementary_Material

The work in Chapter 3 will appear in the manuscript: Woods, L.H. Dunhill, A.M. 2025. Marine Invertebrate Functional Diversity from the Late Cretaceous to the Pliocene. *In prep*.

3.1 Introduction

Functional diversity (FD) is an umbrella term containing multiple metrics, including functional richness, i.e. the range of traits that all species in a community possess (Tilman et al. 2001; Mouillot et al. 2013) and functional evenness, i.e. the relative abundance of species in each functional group (Villéger et al. 2008; Mammola et al. 2021). Marine invertebrates occupy a range of functional groups and are key to ecosystem functioning (Aller 2001; Mermillod-Blondin et al. 2002; Glud 2008). Marine invertebrates also retain a robust fossil record, enabling deep time study of faunal communities (Vermeij 1977; Klug et al. 2015). However, palaeoecological study of macroinvertebrate FD is still less common than that of modern oceans, and there remain significant temporal gaps in our knowledge of both global and regional FD over deep time (Laliberté & Legendre 2010; Tilman et al. 2014).

Marine invertebrate FD is thought to have increased over the Phanerozoic (Bush et al. 2007; Novack-Gottshall 2007). The Cambrian Explosion (541-530 Ma) saw the origins of all modern phyla (Buatois et al. 2016a), but it was during the Great Ordovician Biodiversification Event (GOBE), ~497 Ma, where the most marked rise in the functional diversity of marine fauna occurred (Webby et al. 2004; Bambach et al. 2007; Mondal & Harries 2016). Marine invertebrate functional diversity likely continued to rise incrementally over the remainder of the Phanerozoic (Villéger et al. 2011), although this has not been formally tested for the Cenozoic Era.

Many palaeoecological examinations of marine FD have focused on mass extinction events, providing insight into the resilience of marine communities (Foster & Twitchett 2014; Mondal & Harries 2016; Dunhill et al. 2018; Whittle et al. 2019). In their investigation, Mondal & Harries (2016) postulate that *no* mass extinction has significantly affected bivalve functional diversity despite devastating impacts on taxonomic richness. Evidence to support this is found for the Permian-Triassic Mass Extinction (PTME, ~251 Ma) i.e. Foster & Twitchett (2014), the Late Triassic Mass Extinction (LTME, ~201 Ma), i.e. Dunhill et al. (2018) and regionally for the Cretaceous-Paleogene Mass extinction in the Antarctic (K-Pg, ~66 Ma) (Aberhan & Kiessling 2015; Whittle et al. 2019). These studies reported a net loss of just one (PTME) or no (LTME & K-Pg) modes of life (MoLs) across these major extinctions (Foster & Twitchett 2014; Dunhill et al. 2018; Whittle et al. 2019). Such study has

much aided our understanding of the stability of FD across major extinctions, however, less is known about community structure and function following the K-Pg mass extinction. The Cenozoic Era lacked a major extinction event but did see global climate upheaval and taxonomic shifts towards modern marine assemblages (Hull 2015; Westerhold et al. 2020).

An extensive radiation occurred in the wake of the K-Pg, with the proliferation of many extant clades today. These include the Neogastropoda and numerous foraminifera, decapod, bivalve and echinoid taxa (Benton 1995; Schram & Dixon 2004; Hull & Darroch 2013; Crame et al. 2014). The modern latitudinal species diversity gradient (LDG) is thought to have formed sometime after the K-Pg extinction, although its exact timing is debated (Krug et al. 2009; Brown 2014; Crame 2020; Brodie & Mannion 2023; Fenton et al. 2023). The K-Pg itself has previously been proposed as the origin of modern marine trophic organisation (Dunne et al. 2014). However, this was found not to be the case for trophic structure in Antarctica in the second chapter of this study. Despite this, the K-Pg had 'modernising' effects in other ways, for example, the K-Pg resulted in the 'broad framework' of modern reef fish assemblages through 10 Myr of reef colonisation following the extinction (Price et al. 2014). With these changes and many others, the K-Pg extinction and Cenozoic Era stand as good candidates to investigate the nature and timing of modern invertebrate community function.

The Cenozoic Era (66-0 Ma) likely saw no mass extinction despite several extreme climate events and a long-term cooling trend (Kennett & Scott 1991; Thomas et al. 2002; Lisiecki & Raymo 2005). Earth retained a greenhouse climate throughout the Paleogene (Zachos et al. 2001) and multiple hyperthermal extremes are recorded in the first ~30 Myr of the Cenozoic. This includes the 'Early Eocene hyperthermals', the Paleocene-Eocene Thermal Maximum (PETM, ~55.8-55 Ma), the Early Eocene Climatic Optimum (EECO, ~53-51 Ma) and the Middle Eocene Climatic Optimum event (MECO, ~40 Ma) which likely represent the highest sustained temperatures in the Cenozoic (Bohaty & Zachos 2003; Stokke et al. 2020). For example, the EECO saw ~14°C of global warming, and the MECO is thought to have increased SST by up to 6°C (Smith et al. 2010; Giorgioni et al. 2019; Inglis et al. 2020). Despite these temperature extremes, there is little evidence of extinction or ecological decline in macrofauna during the Early Eocene (Foster et al. 2020). However, microfossils reportedly saw extinctions in deep-sea benthic foraminifera and poleward range shifts in planktic foraminifera, radiolaria and dinoflagellates during these events (Thomas & Shackleton 1996; Foster et al. 2020; Li et al. 2020; Sarkar et al. 2022). Global

macroinvertebrate FD likely remained stable throughout these and other extreme Cenozoic climate events, given the reported stability across major extinctions (i.e. Foster & Twitchett 2014; Dunhill et al. 2018). Alternatively, certain Cenozoic climate events may have affected the structure of invertebrate communities, e.g. the regional distribution of FD and the strengthening of the species diversity gradient (LDG).

The latter half of the Cenozoic Era witnessed cooling as the climate transitioned towards an icehouse regime (Westerhold et al. 2020). The Eocene-Oligocene Transition (EOT, ~34-33.6 Ma), is thought to have caused a significant turnover in benthic foraminifera (Thomas 2007) and a minor macrofaunal extinction in the marine realm (Prothero 1994). Both the Oligocene and following Miocene saw sustained cooling and sea level fall (Halfar & Mutti 2005; von der Heydt & Dijkstra 2006). The Middle Miocene Climate Transition (MMCT, ~14 Ma) caused a wave of extinctions, likely via cooling and falling sea level (Mourik 2010; Pierce et al. 2017; Agustí et al. 2013). It is thought Earth crossed the threshold of an 'icehouse' climate in the Piacenzian, latest Pliocene (Westerhold et al. 2020). A marine megafaunal extinction has been found over the Pliocene-Pleistocene boundary (Pimiento et al. 2017). However, marine invertebrate community function during the Pliocene climate transition remains underexplored.

Previous shows of global-scale stability in FD potentially mask the regional-scale effects of extreme climates. Dunhill et al. (2018) report the effects of the LTME were felt most keenly at lower latitudes, reflected by the collapse of tropical reef systems despite no global net loss of FD. Therefore, although it is likely non-extinction climate events (e.g. PETM, EOT) did not incite a global shift in FD, the potential for a regional signal remains possible. For example, microfossil analyses of the EOT, led Oleinik & Marincovich (2003) to believe cooling was felt most keenly at low latitudes, where warm-water taxa suffered while their cold-water counterparts thrived. Some Cenozoic events, such as the Messinian Salinity Crisis (MSC, 5.97-5.33 Ma) are regional in nature (Roveri et al. 2014). The MSC was a biological crisis in the Mediterranean, whereby restriction of water exchange with the Atlantic Ocean led to increased salinity (Krijgsman et al. 1999; Roveri et al. 2014). The effects of regional crises may be masked at a global resolution and reiterate the use of spatial analyses to understand multiple facets of ancient communities. Due to a lack of evidence of any macroinvertebrate community-level response to most Cenozoic climate extremes, latitudinal variations in response in particular mostly remain unreported.

Furthermore, the latitudinal distribution of taxonomic diversity has likely correlated with the temperature and seasonality of climate regimes throughout the

Phanerozoic (Roy et al. 2000; Mannion et al. 2012; 2014). The modern LDG consists of an equatorial peak in species richness, indicative of an icehouse climate with consistent seasonality (Jablonski et al. 2006: Kiessling et al. 2012). However, few studies have attempted to identify a latitudinal *functional* diversity gradient (LFDG), past or present, which would not only enable us to further understand the geographical distribution of diversity on Earth but would determine if/how FD correlates with climate. The few studies that explore a modern LFDG are single-clade analyses e.g. Berke et al. (2014) noting bivalve FD sharply decreases with increasing latitude. Meanwhile, Copepoda exhibit bimodal FD peaks at subtropical and temperate Pacific latitudes (Becker et al. 2021; Tang et al. 2022). The deep time potential for an LFDG is even less examined (e.g. Grossman et al. 2022) and a gap remains for investigations of multiple invertebrate phyla across latitude over mass extinctions and their recovery periods.

Here, I analyse marine invertebrate FD, from the Late Cretaceous to the end of the Pliocene both globally and across latitude. I use the Paleobiology Database (PBDB 2024) to analyse invertebrate mode of life (MoL) richness, across a total of 19 stages, from the Campanian to the Piacenzian inclusive. I use occurrence data and ecospace traits (Bambach et al. 2007) to answer the following questions: (i). How did global marine invertebrate FD vary from the Campanian to the Piacenzian? (ii). Did any detectable variations in FD coincide with the timing of Cenozoic climate events? (iii). How did invertebrate FD vary with latitude over the Cenozoic Era, in comparison to global analyses? And (iv). Is there evidence for a latitudinal functional diversity gradient (LFDG) in marine invertebrates between the Campanian and the Piacenzian (~83.6-2.58 Ma)?

3.2 Materials and Methods

3.2.1 Dataset

Marine invertebrate occurrence data were downloaded from the Paleobiology Database (PBDB 2024) across the study interval and consisted of the following phyla, from marine settings only: Annelida; Arthropoda; Brachiopoda; Bryozoa; Cnidaria; Echinodermata; Mollusca; Porifera; Sipuncula. The 19 stages of the interval contained the Campanian (~83.6-72.1 Ma); Maastrichtian (~72.1-66 Ma); Danian (~66-61.6 Ma); Selandian (~61.6-59.2 Ma); Thanetian (~59.2-56 Ma); Ypresian (~56-47.8 Ma); Lutetian (~47.8-41.2 Ma); Bartonian (~41.2-37.8 Ma); Priabonian (~37.8-33.9 Ma); Rupelian (~33.9-27.8 Ma); Chattian (~27.8-23 Ma); Aquitanian (~23-20.4 Ma);

Burdigalian (~20.4-16 Ma); Langhian (~16-13.8 Ma); Serravallian (~13.8-11.6Ma); Tortonian (~11.6-7.2 Ma); Messinian (~7.2-5.33 Ma); Zanclean (~5.33-3.6 Ma); and the Piacenzian (~3.6-2.58 Ma). The dataset was then cleaned to exclude any uncertain generic assignments, i.e. aff., cf., ex gr., *sensu lato*, or 'informal', as well as removing form and ichnotaxa. The resulting dataset consisted of 214,653 occurrences within 7,997 genera. Each genus was assigned a mode of life code (MoL) based upon its tiering, motility level and feeding habit, in that order, following the 'Ecospace Cube', as per Bambach et al. (2007). See Table 4 for the MoL assignments. Ecological information was sourced from the PBDB or published literature (see *LHW_Supplementary_Refs.doc)*. Of the 7,997 initial genera, there were 48 that could not be assigned a MoL with certainty, leaving the raw dataset with 213,145 occurrences of 7,949 genera. The *CH3_Supplementary_Material, S4* contains a list of the 49 MoLs observed in this study. All subsequent standardisation techniques, analyses and visualisations in this chapter were carried out using R version 4.4.3 (R Core Team, 2024).

Table 4. Trait categories used to assign genera a mode of life code (MoL) component, using Tiering Habit, Motility Level and Feeding Habit, in that order, as per the 'Ecospace Cube' of Bambach et al. (2007). For example, an erect (2), stationary-attached (6), suspension-feeder (1) would be assigned the MoL, 261.

Tiering Habit	**MoL Component 1**
Nektonic	1
Erect	2
Epifaunal	3
Semi-infaunal	4
Shallow infaunal (<= 5cm below surface)	5
Deep infaunal (>5cm below surface)	6
Motility Level	**MoL Component 2**
Fast-moving	1
Slow-moving	2
Facultatively motile-unattached	3
Facultatively motile-attached	4
Stationary-unattached	5
Stationary-attached	6
Feeding Habit	**MoL Component 3**
Suspension-feeder	1
Surface deposit feeder	2
Miner	3
Grazer	4
Predator	5
Other (parasitic, autotrophic etc.)	6

3.2.2 Global Analyses

A global approach was first used, to create a stage-level time series of both functional (FD) and generic (GD) diversity including direct diversity counts and global functional and generic composition analysis per time interval. Table 5 defines the acronyms used to shorten the names of the values of functional and generic diversity after two different levels of standardisation.

Raw data

The raw data were used to calculate raw functional diversity (RFD, i.e. raw MoL diversity) and raw generic diversity (RGD) to inspect global patterns across deep time and identify potential points of bias. These are displayed in Fig. 5 and were created using the *ggplot2* package (Wickham 2016) as were all plots within this study. To assess spatial bias, the modern geographical distribution of raw occurrences are displayed in the *CH3_Supplementary_Material.doc, S1-S2*, created using *rnaturalearth* (Massicotte & South 2025).

The raw data were analysed for the percentage (%) proportion of global genera within each mode of life, across the 19 stages, as displayed in Fig. 6. This aimed to understand how the raw proportion of taxa within each functional group shifted across the study interval. The Bray-Curtis Dissimilarity Index (Bray & Curtis 1957) was also applied to the raw functional and generic compositions across the study interval, using the *vegan* package (Oksanen et al. 2022). The Bray-Curtis Dissimilarity Index evaluates the difference in the ecological composition of two communities, falling between 0 and 1, with values closer to one indicating a larger degree of dissimilarity between the compositions in question (Bray & Curtis 1957). The Bray-Curtis test was applied between each sequential stage in chronological order to obtain dissimilarity between both the MoL and generic compositions of the stages in the study interval, and applied between the Maastrichtian and every subsequent stage thereafter, to obtain dissimilarity between the latest Cretaceous and Cenozoic communities over increasing temporal distance.

Table 5 The acronyms used in the results and discussion sections for both global and latitudinal analyses.

Acronym	Definition
RFD	Raw functional diversity
RGD	Raw generic diversity
SFD	Functional diversity after coverage-based standardisation
SGD	Generic diversity after coverage-based standardisation
SSFD	Functional diversity after spatial-standardisation
SSGD	Generic diversity after spatial-standardisation

Coverage-based Standardisation

The observed fossil record is an incomplete and/or biased reflection of true diversity due to uneven preservation, exposure and collection of fossils (McGowan & Smith 2011), an effect known as sampling bias (Kidwell & Holland 2002). Coverage-based methods remain an effective approach to mitigate the effects of sampling bias in palaeobiological analyses (Alroy 2010). The *iNEXT* package was used to correct for temporal sampling bias, whereby the raw data were subject to coverage-based rarefaction derived from the equations of Chao and Jost (2012) and extrapolation using the Chao1 estimator in R (Hsieh et al. 2016; 2024), which is analogous to shareholder quorum subsampling, i.e. SQS (Alroy 2010). The quorum levels used were those between 0.1-0.9, by 0.1.

Spatial-Standardisation

In addition to temporal sampling bias, spatial sampling bias in the fossil record arises because intervals are sampled unevenly across geographic regions, so observed shifts in diversity or composition may more reflect disparity between sampling locations rather than true evolutionary patterns over time (Nanglu & Cullen 2023). Accounting for spatial bias by spatial-standardisation or modelling geographic coverage is essential for more reliable palaeoecological inferences (Close et al. 2020). The R package, *divvy*, has been developed to facilitate spatial-standardisation of fossil occurrence data, by reducing bias caused by uneven geographic sampling across time (Antell et al. 2020; 2024). By standardising the number and spacing of fossil localities, *divvy* can facilitate more accurate comparisons of ecological diversity through time. After spatial-standardisation, *divvy* utilises *iNEXT* to perform subsequent coverage-based standardisation (akin to Shareholder Quorum Subsampling, as per Alroy 2010). The *divvy* function, *cookies()* rarefies localities within circular regions of standard area. Spatial-standardisation was performed on the raw data using the *cookies()* function, whereby 300 iterations of a cookie, with a radius of 2,000 km, were seeded and 12 unique localities were randomly selected from within each cookie, for each stage (Antell et al. 2024). A cookie radius of 2,000 km is efficient for occurrences spread across continents, without covering excessive space in a single subsample. Meanwhile, 300 iterations provide sufficient repeats to cover the global distribution of occurrence sites for a more accurate representation of the geographical heterogeneity in functional or generic richness values. Finally, capping the random selection to 12 unique localities, ensures that not only fossil-rich sites are subsampled, and smaller samples (sized between 10 and 20) likely preserve key diversity patterns while minimising spatial bias (Antell et al. 2024). The *sdSumry()*

function then calculated coverage-based rarefaction using *iNEXT* internally on the data at the 12 randomly-selected sites within every cookie taken from each Stage (Antell et al. 2024). The resulting diversity outputs, *'SQSdiv'* provided 300 richness values for each stage in the study interval.

Furthermore, the spatially-standardised data were also analysed for percentage (%) proportion of global genera within each mode of life, across the 19 stages. This was in order to investigate beyond the single metric of functional richness and aimed to understand how the proportion of taxa within each functional group shifted across the study interval, and to compare subsampled patterns with those in the raw data. A Bray-Curtis Dissimilarity Index (Bray & Curtis 1957) was also applied to the spatially-standardised functional and generic compositions across the 19 stages in the study interval. As above, this was applied between each stage in chronological order, to obtain the dissimilarity between stages of the study interval, and also between the Maastrichtian and each stage thereafter, for the dissimilarity between the Late Cretaceous and Cenozoic stages with increasing temporal distance.

3.2.3. Palaeolatitudinal Analyses

The second aim of this study was to investigate palaeolatitudinal patterns in marine invertebrate functional diversity as well as a potential latitudinal functional diversity gradient (LFDG) across the 19 stage intervals. Palaeolatitudinal analyses were carried out at both the stage and epoch level – despite an increased risk of time-averaging, epoch level analyses benefit from a larger sample size and greater spatial coverage. The epochs used were the Late Cretaceous (Campanian and Maastrichtian), the Paleocene (Danian, Selandian, Thanetian), the Eocene (Ypresian, Lutetian, Bartonian, Priabonian), the Oligocene (Rupelian and Chattian), the Miocene (Aquitanian, Burdigalian, Langhian, Serravallian, Tortonian, Messinian) and the Pliocene (Zanclean and Piacenzian).

The raw occurrences were first sorted into their respective discrete palaeolatitude bins of 10°, i.e. 0-10˚N/S; 10-20˚N/S; 20-30˚N/S; 30-40˚N/S; 40-50˚N/S; 50-60˚N/S; 60-70˚N/S; 70-80˚N/S; 80-90˚N/S. This was to inspect the raw pattern across palaeolatitude over the interval, and identify potential bias on a latitudinal scale prior to subsampling. The raw data within each palaeolatitude bin was also subject to both coverage-based (*iNEXT*) and spatial (*divvy*) standardisation. There was insufficient data within many palaeolatitude bins and as such *divvy* spatial-standardisation could only be successfully performed on Northern Hemisphere bins,

from 0˚ to 60˚N at stage level, i.e. the bins, 0-10˚N; 10-20˚N; 20-30˚N; 30-40˚N; 40-50˚N; and 50-60˚N only. At epoch level, however, some Southern Hemisphere values could be calculated for functional and generic diversity, although there were still many gaps across the study interval. Wherever viable, the *divvy* package and the *cookies()* function were used with the same parameters as above, i.e. 300 iterations of cookies with r = 2,000 km and nSite = 12 unique localities to be randomly selected from each cookie (Antell et al. 2024).

3.3 Results

Part A. Global Patterns

3.3.1 Raw patterns of functional diversity at global scale

Firstly, the raw global functional diversity (RFD) and raw global generic diversity (RGD) of marine invertebrates were investigated across the study interval (Fig. 5). In total, 49 modes of life (MoL) are observed from the Campanian to the Piacenzian, using the PBDB (2024) download of major invertebrate phyla occurrences *(*see *CH3_Supplementary Material.doc, S5* for full MoL list). Overall, RFD displays no obvious long-term directional trend over the interval, i.e. relative stability, although there are 'short-term' variations between stages (Fig. 5). Raw GD follows a similar pattern to RFD, with more volatility in the Neogene in particular, and a slight increasing trend from the Miocene onwards, despite variation (Fig. 5).

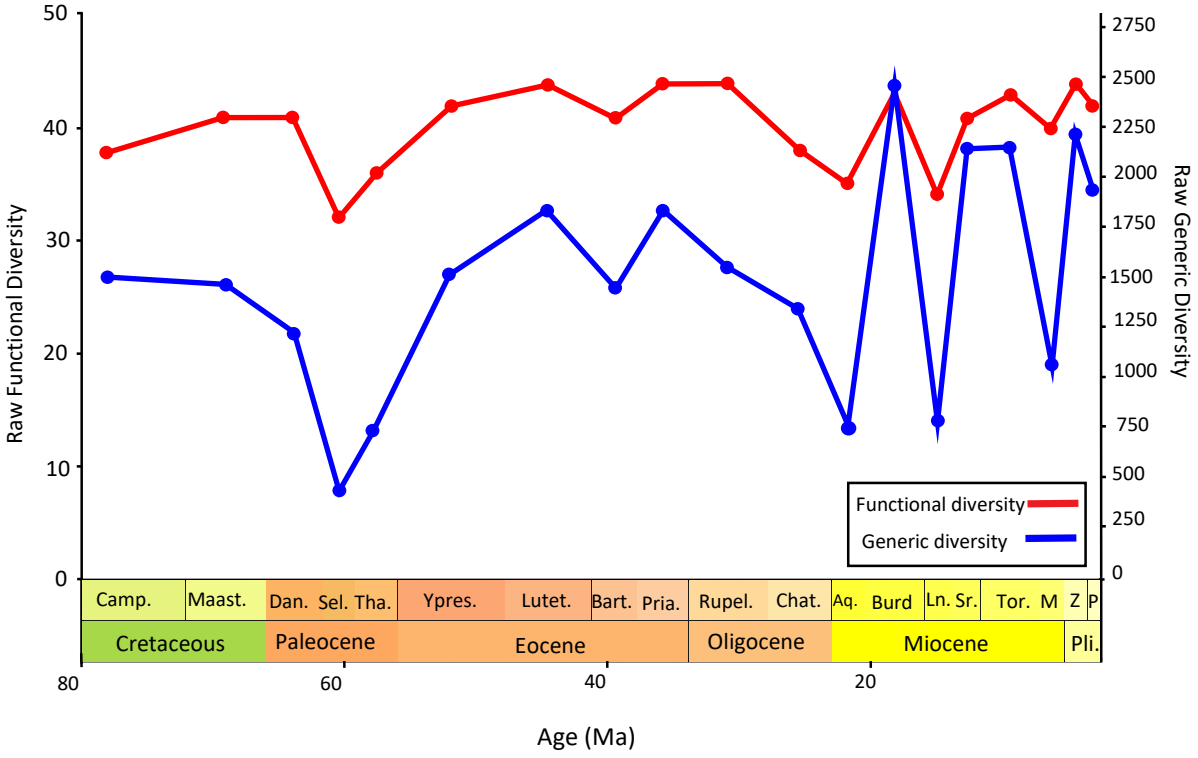

Figure 5. Raw global functional (RFD) and generic diversity (RGD) from the Late Cretaceous to the Pliocene. The left y-axis is associated with the red points and line, displaying RFD for each of the 19 stages. The right y-axis is associated with the blue points and line and represents the global RGD across the 19 stages. Raw functional diversity looks like raw generic diversity over the interval, with no long-term directional trends over time, although RGD appears to present a slight increasing trend from the Miocene onwards.

There is a slight increase in RFD between the Campanian (38 MoLs) and Maastrichtian (41 MoLs), accompanied by a small decrease in RGD; 1511 genera in Campanian and 1473 genera in Maastrichtian (Fig. 5). There exists no obvious signal from the K-Pg mass extinction at this resolution between the Maastrichtian and Danian, with stability in RFD and a minor drop in RGD (Fig. 5). Both RFD and RGD report a sharp decline from the Danian to their lowest value in the Selandian (i.e. Selandian RFD = 32; RGD = 444) (Fig. 5). As well as this, both counts report a sustained increase over the late Paleocene (Thanetian), into and across the Eocene (i.e. Ypresian, Lutetian, Bartonian and Priabonian) (Fig. 5). The highest RFD value is reported in the Lutetian, middle Eocene (i.e. Lutetian RFD = 45), followed by a slight drop in the Bartonian, which is also observed in RGD (Fig. 5). Additionally, RFD remains stable from the Priabonian (44 MoLs) to the Rupelian (44 MoLs) in the early Oligocene but falls to 38 MoLs into the Chattian. Raw GD shows a continuous decline from the Priabonian (1843 genera) to the Chattian (1352 genera). Both RFD and RGD drop further from the Chattian to the Aquitanian (earliest Miocene) but report a peak

in the following Burdigalian, which represents the maximum RGD in the interval (2481 genera). Both RFD and RGD witness several peaks and troughs throughout the Miocene, with RFD remaining more stable than RGD (Fig. 5). Here, both counts observe a peak in the Serravallian (RFD = 41; RGD = 2156), Tortonian (RFD = 43; RGD = 2165) and Zanclean (RFD = 44; RGD = 2229), before slightly decreasing into the Piacenzian (RFD = 43; RGD = 1940), the final stage of the study interval (Fig. 5).

In addition, of the 49 MoLs observed in total, 36 occur continuously across the entire study interval, while 13 do not (See *CH3_Supplementary_Material, S5*). Of these 13 MoLs, two disappear within the study interval, i.e. first appearance date (FAD) prior to the Campanian but last appearance date (LAD) is before the end of the Piacenzian: 115 (nektonic fast-moving predator, LAD = Zanclean) and 525 (shallow-infaunal slow-moving predator, LAD = Rupelian). However, there is plentiful evidence of both MoLs 115 and 525 existing in the marine realm after the end of the Piacenzian (PBDB, 2025). There are also seven MoLs that appear within the study interval, i.e. FAD sometime after the Campanian, and occur for the rest of the study interval. These are: 125 (nektonic slow-moving predator, FAD = Danian); 311 (epifaunal fast-moving suspension feeder, FAD = Maastrichtian); 362 (epifaunal stationary-attached deposit feeder, FAD = Maastrichtian); 365 (epifaunal stationary-attached predator, FAD = Maastrichtian); 441 (FAD = Ypresian); 541 (shallow-infaunal facultatively-motile-attached suspension-feeder, FAD = Lutetian); 566 (shallow-infaunal stationary-attached other, FAD = Aquitanian). However, there is also published evidence for each of these modes of life prior to the early Campanian, within the PBDB (2025) and supplement to Bambach et al. (2007). Finally, there are four MoLs that both first appear (FAD) and last appear (LAD) within the study interval, some with very short temporal ranges. These are 251 (erect stationary-unattached suspension-feeder, Thanetian-Chattian); 326 (epifaunal slow-moving other, Danian-Chattian); 452 (semi-infaunal stationary-unattached deposit-feeder, Maastrichtian-Rupelian); 512 (shallow-infaunal fast-moving deposit-feeder, Tortonian-Messinian). However, once again, evidence for these MoLs can be found both before and after the study interval (PBDB, 2024). Thus, no invertebrate MoLs appear to truly appear or disappear within the study interval.

There are several small-scale shifts in the proportion (%) of raw global genera within each MoL over the study interval (Fig. 6). For example, there is a substantial percentage (~10%) of raw global genera within the MoL 115 (nektonic fast-moving predator, e.g. Cephalopoda), in both the Campanian and Maastrichtian, which is vastly reduced in the Danian and remains low for the remainder of the interval (Fig.

6). As well as this, from the Danian onwards, the largest proportion of raw global genera (~25%) is consistently found within gastropod-associated MoL 325, (epifaunal slow-moving predator) (Fig. 6). It is worth noting that the MoLs 325, as well as MoL 324 (epifaunal slow-moving grazer) are not limited to Gastropoda exclusively although these make up most taxa within these MoLs. Meanwhile, semi-infaunal, shallow-infaunal and deep-infaunal taxa retain roughly the same percentage of raw genera throughout the entire study interval (Fig. 6). Reef-builder-associated MoLs, i.e. 261 (erect stationary-attached suspension-feeder, for example rudist bivalves, some corals and sponges) and 266 (erect stationary-attached other, mostly Scleractinian corals), display variation over time. For example, there is a notable decrease in percentage of raw global genera in MoL 261 from the Campanian to the Paleocene and a general increase in 266 after the Selandian, particularly in the Miocene (Fig. 6).

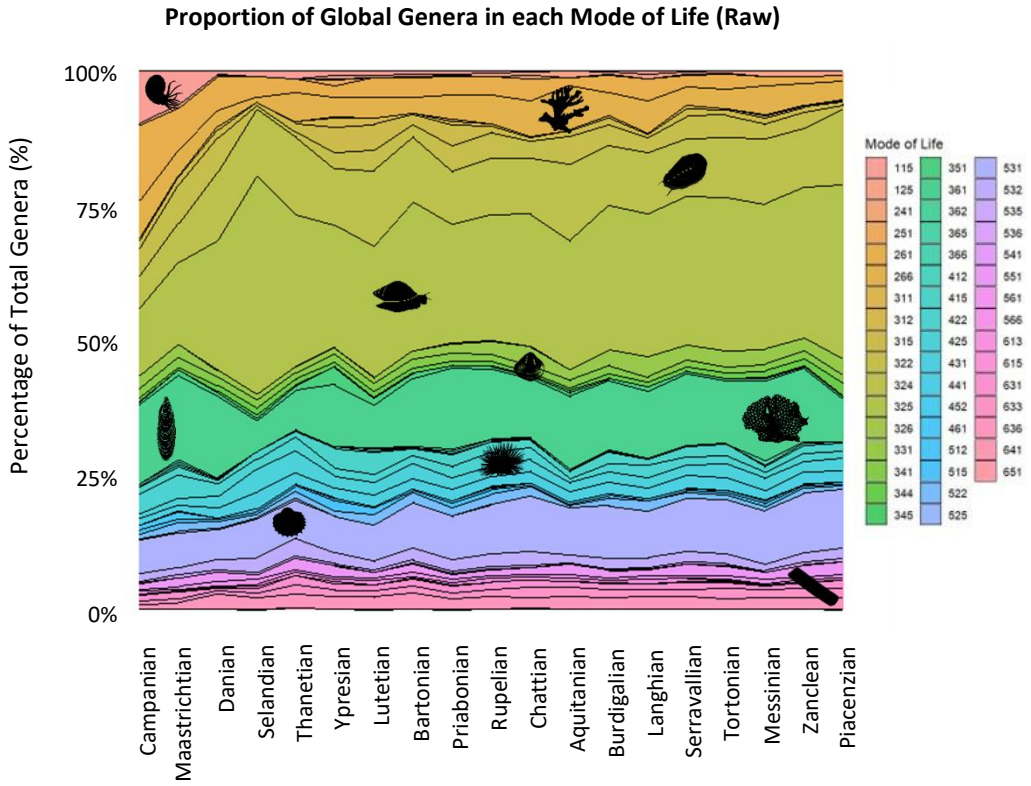

Figure 6. Raw percentage (%) composition of global genera within each mode of life across the 19 stages of the study interval. The data is global. The largest composition of MoL is most commonly 325, typical but not excluded to gastropods, i.e. epifaunal, slow-moving, predators (325), as per Bambach et al. (2007). The silhouettes superimposed give example taxa, and are not the only taxa within that MoL, taken from Phylopic.org (2024).

The raw Bray-Curtis Dissimilarity Index (Bray & Curtis 1957) (Table 6), shows that raw generic composition between stages is more dissimilar than raw MoL

composition in every case. Between each sequential stage, the Bray-Curtis Index for raw MoL composition ranges from between 0.094 (Serravallian-Tortonian) and 0.333 (Danian-Selandian) to 3 decimal places (3 d.p. and thereafter) (Table 6). Meanwhile, raw generic composition ranges between 0.407 (Zanclean-Piacenzian) and 0.750 (Maastrichtian-Danian) in dissimilarity (Table 6). Furthermore, the dissimilarity between the MoL composition of the Maastrichtian (latest Cretaceous) and each stage, thereafter, does not indicate a detectable pattern over the interval, with a range of 0.272 (Maastrichtian-Danian) to 0.450 (Maastrichtian-Selandian), to (Table 6). Raw generic composition between the Maastrichtian and subsequent stages indicates a slight general increase in dissimilarity over time, with a range of 0.750 (Maastrichtian-Danian) to 0.927 (Maastrichtian-Messinian) (Table 6).

Table 6. Raw Bray-Curtis Dissimilarity Index (Bray & Curtis 1957) to 3 d.p. for the interval. The two left-most columns contain the raw dissimilarity of the mode of life and generic compositions, between the labelled stage and the preceding stage. The two right-most columns display the raw dissimilarity between the MoL and generic composition of the labelled stage and that of the Maastrichtian. A value closer to 1 indicates more dissimilarity between the two compositions in question. Raw generic composition is consistently more dissimilar than Raw MoL composition, both between chronological stages and between the Maastrichtian.

	MoL	**Genera**	**Between Maastrichtian (MoL)**	**Between Maastrichtian (Genera)**
Campanian				
Maastrichtian	0.253	0.532		
Danian	0.272	0.750	0.272	0.750
Selandian	0.333	0.589	0.450	0.810
Thanetian	0.255	0.578	0.352	0.806
Ypresian	0.150	0.553	0.364	0.813
Lutetian	0.115	0.438	0.368	0.823
Bartonian	0.164	0.416	0.366	0.827
Priabonian	0.233	0.568	0.294	0.822
Rupelian	0.135	0.557	0.316	0.834
Chattian	0.145	0.531	0.311	0.849
Aquitanian	0.238	0.646	0.361	0.914
Burdigalian	0.227	0.605	0.336	0.849
Langhian	0.078	0.538	0.337	0.870
Serravallian	0.121	0.643	0.309	0.873
Tortonian	0.094	0.512	0.360	0.888
Messinian	0.185	0.573	0.413	0.927
Zanclean	0.143	0.523	0.320	0.883
Piacenzian	0.155	0.407	0.393	0.891

3.3.2 Standardised (coverage-based) functional diversity patterns at global scale

To account for sampling bias, coverage-based interpolation and extrapolation subsampling was performed on the raw data using the *iNEXT* package in R (Alroy 2010; Chao et al. 2014; Hsieh et al. 2016) (Fig. 7). Standardised functional diversity (SFD) (Fig. 7a) appears to display roughly the same pattern as RFD (Fig. 5), albeit with less volatility between certain stages. However, at higher quorum levels (e.g.

0.8), there is a slight decreasing trend in the latter half of the study interval, not observed in the raw data (Fig. 7a).

There is a slight rise in SFD between the Campanian and Maastrichtian of the Late Cretaceous (Fig. 7a). Again, there is little to no signal of the K-Pg mass extinction between the Maastrichtian and the Danian in SFD, with a shallow drop at higher quorum levels (Fig. 7a). The Selandian shows the lowest value of SFD, as observed in the raw dataset (Fig. 7a). The early Eocene shows an increase in SFD, despite a dip in the Bartonian, to reach maximum SFD in the Priabonian (Fig. 7a). From the Priabonian to the Rupelian (early Oligocene), there is a slight decrease in SFD, however SFD remains relatively stable between the Rupelian and Chattian, across the Oligocene. There is a sharp drop in SFD from the Chattian to the Aquitanian, earliest Miocene stage. Standardised functional diversity sees a sustained rise from the Aquitanian for most of the remaining Miocene stages (i.e. Langhian, Serravallian and Tortonian). However, there is a drop in SFD in the Messinian (latest Miocene), before an increase again in the Zanclean of the Pliocene and SFD remains stable across the Piacenzian, the final stage of the interval (Fig. 7a).

Meanwhile, standardised generic diversity (SGD) displays a slight increasing trend across the study interval, with volatility (Fig. 7b). There is a decrease in SGD between the Campanian and Maastrichtian of the Late Cretaceous but an increase in SGD between the Maastrichtian and Danian, i.e. no detectable K-Pg mass extinction signal (Fig. 7b). The Selandian shows the lowest SGD, closely followed by the Thanetian (Fig. 7b). As in RGD, there is a rise in SGD into the Eocene, i.e. over the Ypresian and Lutetian, with a drop in the Bartonian (Middle Eocene) and a peak in the Priabonian (Late Eocene). Standardised GD drops between the Priabonian (Late Eocene) and Rupelian (Early Oligocene) and slightly increases between the Rupelian and Chattian of the Oligocene, before falling again into the Aquitanian (Early Miocene). Across the Miocene, there are several peaks and troughs in SGD, with a steep rise from the Aquitanian to the Burdigalian, a drop in the Langhian and a smaller peak around the Serravallian and Tortonian. The Messinian (latest Miocene) sees a drop in SGD once again, but SGD is at its maximum value in the Zanclean (early Pliocene) and remains relatively stable in the Piacenzian, i.e. the final stage of the interval (Fig. 7b).

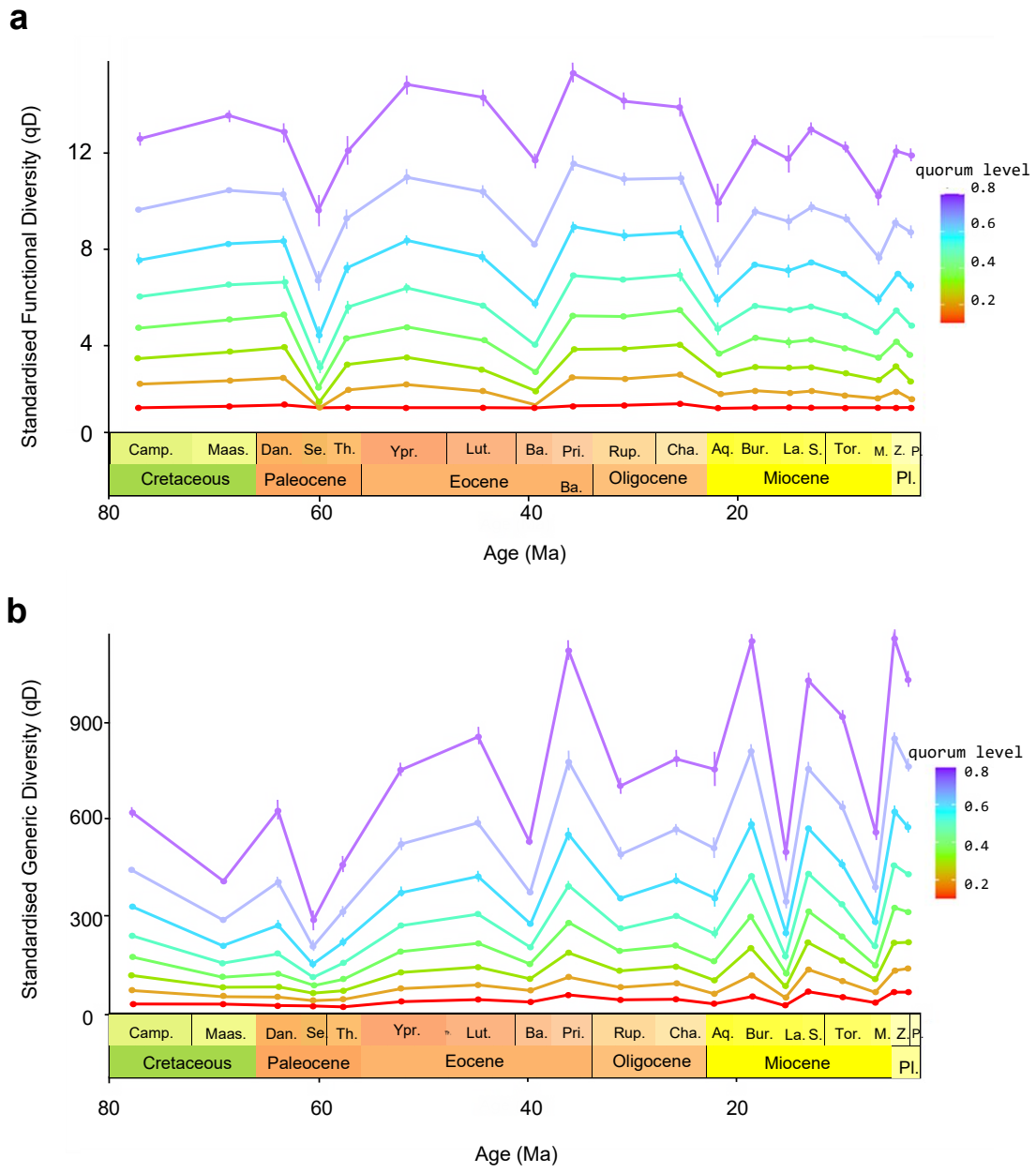

Figure 7. a = Standardised functional diversity (SFD) after coverage-based subsampling, (using the *iNEXT* package in R, Chao et al. 2014; Hsieh et al. 2016) akin to SQS (Alroy 2010) from the Campanian (Late Cretaceous) to the Piacenzian (Late Pliocene). **b =** Standardised generic diversity (SGD) from the Campanian to the Piacenzian. It seems SFD displays no long-term directional trend at lower quorum levels, with a slight decreasing trend at higher quorum levels, meanwhile SGD witnesses an increasing trend at higher quorum levels, despite variation.

3.3.3 Spatially-standardised functional diversity patterns at global scale

To account for spatial bias in the raw data, the *divvy* R package (Antell et al. 2024) was used to perform spatial subsampling (Fig. 8). With 300 repeats for each stage in the interval, the mean global spatially-standardised functional diversity (SSFD) ranges

from 19.01 in the Campanian to 28.58 in the Aquitanian, to 2 decimal places (2 d.p., and thereafter). The pattern in SSFD across the 19 stages is one of relative stability with some variation, like that observed in both RFD and SFD (Fig. 8a). In addition, SSFD mostly but not exclusively follows the pattern observed in spatially-standardised generic diversity, SSGD (Fig. 8b). It is worth noting that the Aquitanian value is likely an anomaly in both SSFD and SSGD (Fig. 8), i.e. Aquitanian mean SSFD = 28.58; mean SSGD =1728.18. This is likely due to the Aquitanian being vastly under-sampled in the PBDB, with 269 collections as opposed to a mean average of 1148 collections per stage in the study interval. The *divvy* parameters used may have been unsuitable for the number and distribution of unique fossil localities for the Aquitanian on the PBDB (see *CH3_Supplementary*, *S2*). This is discussed further in the discussion section below.

Mean SSFD increases over the Late Cretaceous between the Campanian, the lowest mean SSFD in the interval (19.01 MoLs) and the Maastrichtian (21.92 MoLs) (Fig. 8). Whereas mean SSGD remains stable (Fig. 8). Between the Maastrichtian and the Danian there is no major signal of the K-Pg mass extinction, with a relatively minor drop in mean SSFD, i.e. Maastrichtian mean SSFD of 21.92 MoLs and a Danian mean SSFD of 20.02 MoLs. There is an increase in mean SSGD between the Maastrichtian (375.69 genera) and the Danian (564.42 genera). The following Selandian shows the lowest mean SSGD within the interval (309.62 genera), whereas mean SSFD increases from the Danian to the Selandian (22.37 MoLs). The opposite occurs in mean SSFD from the Selandian (22.37 MoLs) to the Thanetian (19.14 MoLs), whereas mean SSGD increases from the Selandian (309.62 genera) and the Thanetian (575.39 genera) (Fig. 8).

Furthermore, there appears to be a sustained rise in SSFD from the Thanetian (latest Paleocene) to the Bartonian, (middle Eocene) (Fig. 8c). Meanwhile, SSGD also increases over the Eocene, but shows a slight drop between the Thanetian and the Ypresian (Fig. 8). The Lutetian represents the highest mean of both SSFD and SSGD, (i.e. mean SSFD = 23.73 MoLs; mean SSGD =739.91 genera), Aquitanian excluded. Furthermore, mean SSFD drops between the Bartonian and Priabonian, but increases into the Oligocene, between the Priabonian and Rupelian (21.40 and 22.42 MoLs, respectively). Mean SSFD decreases across the Oligocene, between the Rupelian and Chattian stages (22.42 and 20.14 MoLs) whereas this is less noticeable in mean SSGD (506.32 and 438.50 genera). The Aquitanian, the first stage Fof the Miocene Epoch, is extremely high for both mean SSFD and SSGD, and lacks any range, i.e. mean SSFD = 28.58; mean SSGD =1728.18. Across the remainder of the

Miocene, mean SSFD remains relatively stable (Fig. 8). The Burdigalian represents the second lowest reported mean SSFD in the study interval, with 19.06 MoLs, followed by a sustained increase to 21.33 MoLs in the Langhian, 21.47 MoLs in the Serravallian and 21.70 MoLs, in the Tortonian. There is a slight decrease into the Messinian (20.02 MoLs), latest Miocene. On the other hand, mean SSGD shows a peak in the Serravallian (middle Miocene), with 667.67 genera, followed by 463.63 in the Messinian. From the Miocene to the Pliocene, there is an increase in both mean SSFD (Messinian = 20.02, and Zanclean = 22.38 MoLs) and SSGD (Messinian = 463.63, and Zanclean = 569.90 genera), more pronounced in SSFD than SSGD. Mean SSFD remains stable into the final stage of the study interval, the Piacenzian (22.11 MoLs), whereas mean SSGD increases across the Pliocene, i.e. Piacenzian mean SSGD = 655.36 genera (Fig. 8).

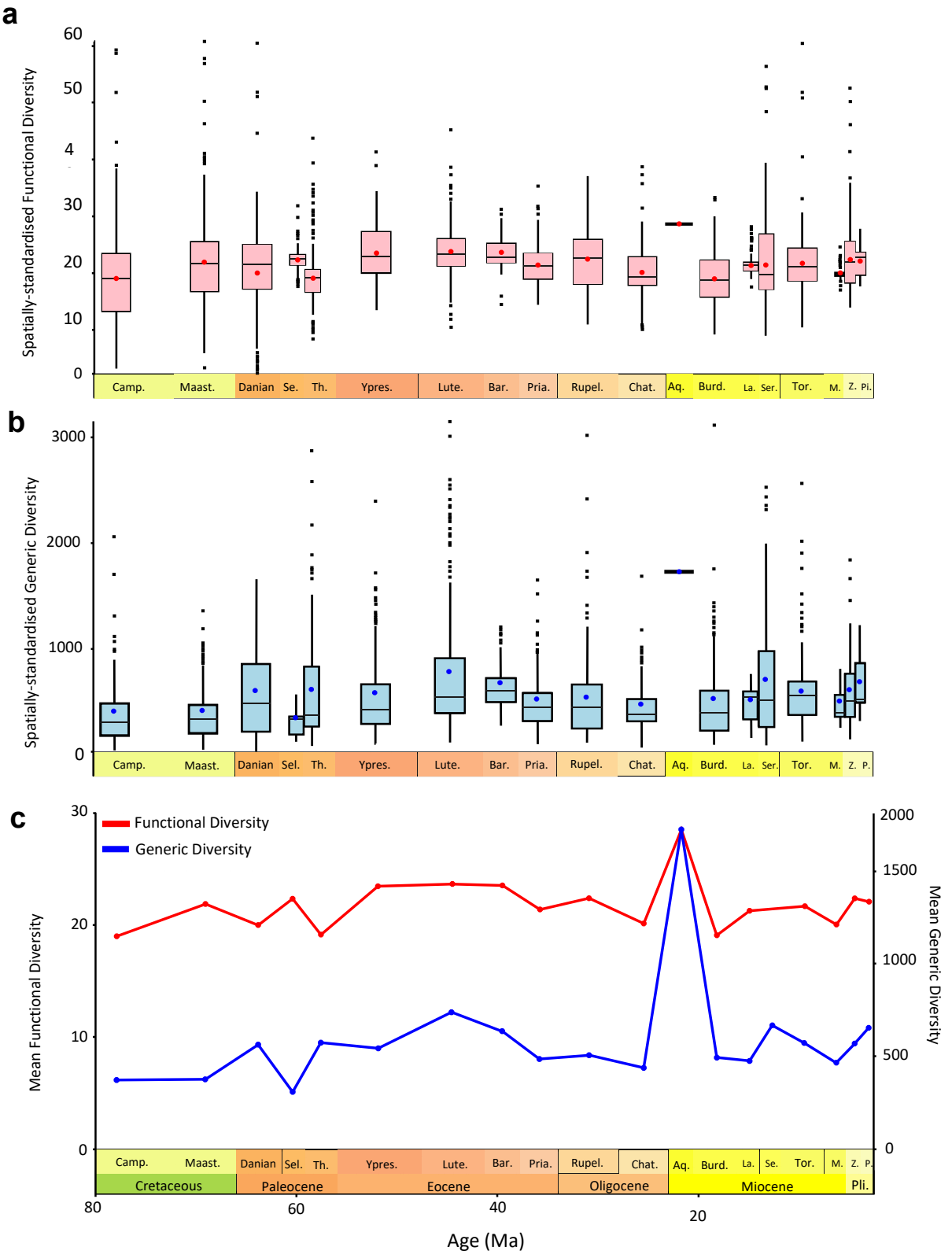

Figure 8. a = Boxplots of spatially-standardised functional diversity (SSFD) across the 19 stages, red points denote mean functional diversity in each stage. **b** = Boxplots of spatially-subsampled generic diversity (SSGD), blue points indicate the mean. NB: The boxplots arbitrarily vary in width and are thinner if their respective stages are shorter and therefore have less space on the page. **c** = the means of panel a (red) and panel b (blue) together. The Aquitanian appears to be an anomalously high result. Mean FD follows a similar pattern to generic richness and both show relative stability, with short-term variation.

Table 7. Bray-Curtis Dissimilarity Index (Bray & Curtis 1957) to 3 d.p. on spatially-standardised analyses. The two left-most columns display the dissimilarities in MoL and generic composition between the labelled stage and that of the preceding stage. The two right-most columns display the dissimilarities between the MoL and generic composition of the labelled stage and that of the Maastrichtian. A value closer to 1 indicates more dissimilarity between the two compositions in question.

	MoL	Genera	Between Maastrichtian (MoL)	Between Maastrichtian (genera)
Campanian				
Maastrichtian	0.372	0.669		
Danian	0.294	0.788	0.294	0.788
Selandian	0.343	0.586	0.481	0.876
Thanetian	0.271	0.595	0.391	0.845
Ypresian	0.175	0.577	0.424	0.854
Lutetian	0.197	0.488	0.390	0.857
Bartonian	0.218	0.486	0.391	0.856
Priabonian	0.267	0.632	0.298	0.843
Rupelian	0.220	0.691	0.400	0.875
Chattian	0.123	0.644	0.332	0.869
Aquitanian	0.325	0.757	0.516	0.909
Burdigalian	0.292	0.722	0.335	0.868
Langhian	0.265	0.708	0.538	0.925
Serravallian	0.377	0.769	0.354	0.893
Tortonian	0.145	0.666	0.382	0.904
Messinian	0.437	0.875	0.423	0.944
Zanclean	0.431	0.870	0.372	0.903
Piacenzian	0.131	0.519	0.384	0.899

The Bray-Curtis Dissimilarity Index (Bray & Curtis 1957) (Table 7) consistently shows that global generic composition is more dissimilar than mode of life composition across each stage boundary sequentially, as well as between the Maastrichtian (Late Cretaceous) and each subsequent stage in the interval. Mode of life dissimilarity is highest Tortonian-Messinian (0.437), closely followed by between the Messinian-Zanclean (0.431). Most dissimilarity values between stages fall between 0.150 and 0.350 for MoL composition, indicating relatively low dissimilarity. Meanwhile, for generic composition, most values are between 0.600 and 0.800, with the two highest reported between the Tortonian-Messinian (0.875) and the Messinian-Zanclean

(0.870), and the third highest value between the Maastrichtian-Danian (0.788), and the lowest dissimilarity being between the Lutetian-Bartonian (0.486). There are no trends over time in the dissimilarity between stages sequentially, but there is a general increase in the dissimilarity of generic composition between the Maastrichtian and each following stage (Table 7). However, no increase is seen in MoL composition between the Maastrichtian and each following stage (Table 7).

Furthermore, after spatial-standardisation, the percentage of global genera within each MoL (Fig. 9) is more volatile than observed in the raw data (Fig. 6). Following the Campanian, the largest percentage proportion of global genera (up to ~35%) are within the gastropod-associated MoL 325 (i.e. epifaunal slow-moving predator), in all but one Cenozoic stage (the Messinian) (Fig. 9). The Messinian shows a sharp reduction of the MoL 325, combined with an expansion of the MoL 351 (epifaunal, stationary-unattached suspension feeders). Meanwhile, the proportion of semi-infaunal and infaunal MoLs remains relatively stable across the interval (Fig. 9). As in the raw data, the MoL most-associated with ammonites and belemnites (MoL 115) reduces in diversity with a drop in the proportion of this MoL between the Campanian and the Maastrichtian and all but disappears after the Maastrichtian (Fig. 9). Reef-builder associated MoLs (261 and 266, i.e. erect stationary attached suspension feeders/other, respectively) report volatility across the interval (Fig. 9). There is a reduction in MoL 261 (most-likely rudist bivalves) across the Cretaceous and K-Pg boundary (Fig. 9). The diversity of MoL 266 (most-likely Scleractinian corals) increases after the Selandian of the Paleocene and into Eocene and Miocene in particular, although there is a distinct low in the Bartonian (middle Eocene) moreso than in the raw data (Fig. 9). The Pliocene sees one of the largest proportions of gastropod-associated MoLs, along with a relatively low proportion of semi-infaunal and reef-builder-associated MoLs.

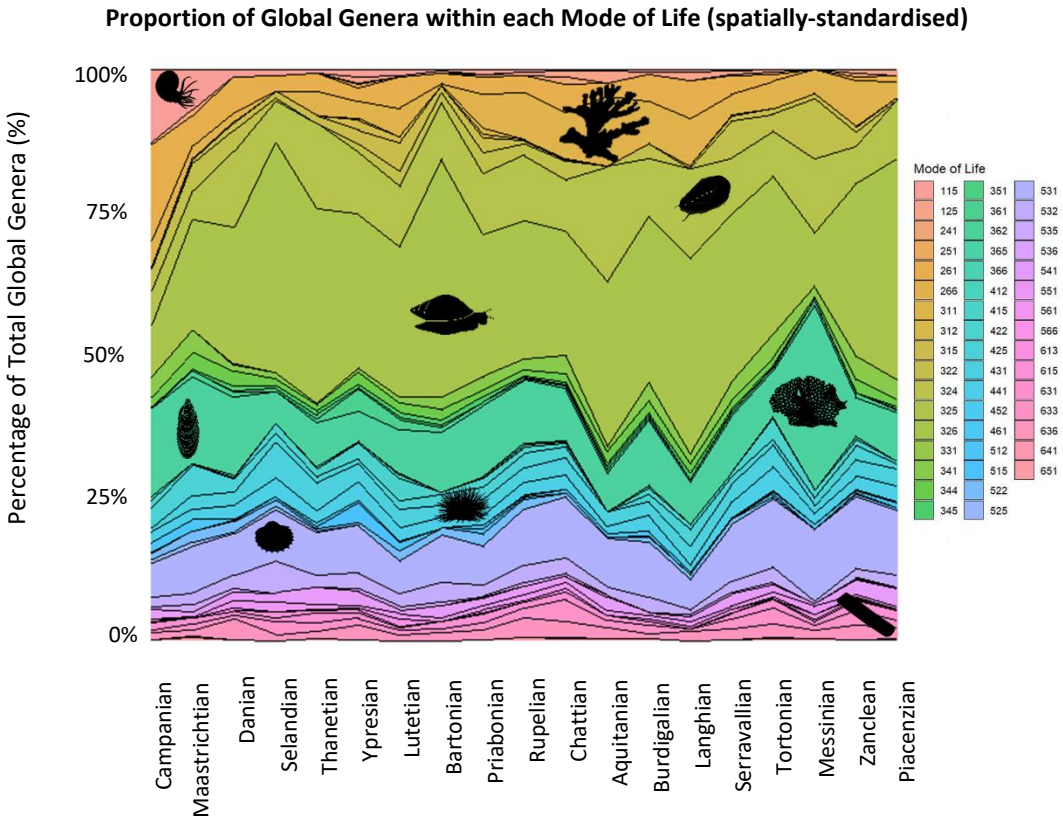

Figure 9. The percentage (%) composition of spatially-standardised global genera within each mode of life across the 19 stages of the interval. The largest proportion of genera are most commonly found within 325, typical but not exclusively associated-with gastropods, i.e. epifaunal, slow-moving, predators (325), as per Bambach et al. (2007). The silhouettes superimposed are to give examples, and are not the only taxa within that MoL, these were taken from Phylopic.org

Part B. Palaeolatitudinal Patterns

3.3.4. Raw patterns in functional diversity across palaeolatitude

The pattern of marine invertebrate raw functional (RFD) and raw generic (RGD) diversity across palaeolatitude bins of 10˚ width, from 0-10˚N/S to 50-60˚N/S over the study interval was inspected (Figs. 10-14).The most striking observation in both RFD and RGD over latitude is consistent mid-latitude peaks (30-40˚N or 40-50˚N, and often 40-50˚S) as well as reduced values in the Southern Hemisphere compared to those reported in the Northern Hemisphere (Figs. 10-14).

The two Late Cretaceous stages, the Campanian and Maastrichtian, report a similar pattern in RFD across palaeolatitude (Fig. 9ai-bi). This includes a Northern Hemisphere mid-latitude peak in RFD, observed in 40-50˚N in the Campanian, closely followed by 30-40˚N, and vice versa in the Maastrichtian (RFD peak at 30-40˚N, closely followed by 40-50˚N) (Fig. 10ai-bi). The highest latitude bin, 50-60˚N, sees a

slight decrease in RFD relative to the 40-50˚N bin in the Campanian and a steeper drop is seen here in the Maastrichtian (Fig. 10ai-bi). Relative to the mid-palaeolatitude peaks, both Late Cretaceous stages witness a steep drop in RFD equatorward to 20-30˚N and a continued gradual decrease through 10-20˚N down to 0-10˚N, which shows the minimum RFD for both stages in the Northern Hemisphere (Fig. 10ai-bi). Additionally, both the Campanian and Maastrichtian report even smaller RFD values in the lowest southern latitudes (0-10˚S, 10-20˚S, 20-30˚S) than northern, dropping to a minimum RFD in the Campanian in 30-40˚S, and Maastrichtian in 20-30˚S (Fig. 10ai-bi). However, RFD increases poleward in both stages, with a peak in the highest Southern Hemisphere latitude bins (40-50˚S, 50-60˚S), although values are smaller here than in analogous bins in the Northern Hemisphere (Fig. 10ai-bi). Late Cretaceous RGD displays almost an identical pattern across palaeolatitude as described in RFD (Fig. 10aii-bii). However, the Campanian peak in RGD is found in 30-40˚N, closely followed by 40-50˚N, i.e. the inverse to RFD, plus there is a steeper drop southward in RGD between 20-30˚N and 10-20˚N than in RFD. Finally, in both stages, RGD shows a shallower drop into the Southern Hemisphere than RFD, along with a shallower rise into the highest southern latitude bins than RFD displays 40-50˚S, 50-60˚S (Fig. 10aii-bii).

Meanwhile, RFD across palaeolatitude bins in the Paleocene, show some disparity from both the Late Cretaceous and between the constituent Paleocene stages i.e. the Danian, Selandian and Thanetian (Figs. 10ci,10di & 11ai). Firstly, the pattern in RFD across palaeolatitude in the Danian is similar to that of the Campanian and Maastrichtian for the most part, except there are additional smaller peaks in RFD in lower northern (10-20˚N and 0-10˚N) and southern (10-20˚S) latitude bins, and a steeper drop into the highest northern latitude bin, 50-60˚N than observed in the Cretaceous (Fig. 10ci). Raw GD in the Danian shares the same latitudinal pattern as is exhibited in the Late Cretaceous (Fig. 10cii). On the other hand, both the Selandian and Thanetian see a secondary peak in lowest southern latitude bin 0-10˚S (most notably in the Selandian), smaller than the 40-50˚N peak, for both RFD and RGD (Figs. 10di-dii & 11ai-aii). Most other palaeolatitude bins in both stages are relatively low, except 50-60˚S in the Thanetian (Fig. 11aii).

All Eocene stages (i.e. Ypresian, Lutetian, Bartonian, and Priabonian) witness peak RFD and RGD at 30-40˚N (Figs. 11bi-12aii), with relatively lower 40-50˚N values than other stages in the interval. There are almost identical patterns in RFD and RGD across palaeolatitude for the Ypresian and Lutetian, with the 30-40˚N peak and southwards drop to 20-30˚N that is maintained until 0-10˚S, and there are smaller

peaks in RFD around 40-50˚S and 50-60˚S (Fig. 11bi-cii). The Bartonian shows peak RFD and RGD at 30-40˚N, which drops in 20-30˚N and rises again to a plateau from 10-20˚N southwards to 0-10˚S (Fig 11di-dii). Bartonian RFD then drops again to another plateau from 10-20˚S to 20-30˚S, before increasing once more to a Southern Hemisphere peak at 40-50˚S (Fig. 11di). The Priabonian (final Eocene stage) presents a similar pattern in RFD and RGD across palaeolatitude as in other Eocene stages; with a midlatitude peak (30-40˚N), a low in the Northern Hemisphere at 20-30˚N, followed by a smaller peak around 0-10˚N and a southward decline to 20-30˚S, with a smaller peak at 40-50˚S (Fig. 12ai-aii).

The Rupelian and Chattian present similar patterns to each other in both RFD and RGD across palaeolatitude (Fig. 12bi-cii). This includes a peak in RFD at 40-50˚N from which there is a general decline to 20-30˚S and 30-40˚S, with a peak again at 40-50˚S (Fig. 12bi & 12ci). Meanwhile, the Aquitanian presents a palaeolatitudinal pattern in RFD similar to that described for the later Paleocene, i.e. the Selandian and Thanetian (Fig. 12di). For example, there is a sharp peak at 40-50˚N, and an equatorward decline to a low at 20-30˚N, but a small lower latitude peak around 10-20˚N and 0-10˚N (Fig. 12). The Southern Hemisphere sees relatively low RFD values in the Aquitanian extending from 0-10˚S until 40-50˚S, where there is a smaller peak than the other two in the Northern Hemisphere (Fig. 12di). To add to this, Aquitanian RGD over palaeolatitude displays the same pattern as described in RFD (Fig. 12dii).

The following stages of the Miocene each present a different pattern in RFD and RGD across palaeolatitude to the Aquitanian and each other (Fig. 13ai-12dii), and all besides the Tortonian report lower 50-60˚N bin values compared to the older stages, i.e. a steeper drop off into the highest latitude bin. The Burdigalian sees the same pattern of a unique number of peaks and troughs in both RFD and RGD, of relatively high FD compared to other stages (Fig. 13ai & 13aii). The largest peak in both RFD and RGD is typical of the other stages, being at 40-50˚N, along with a smaller at 10-20˚N, another smaller still at 0-10˚S and another slightly larger peak at 40-50˚S (Fig. 13ai & 13aii). Meanwhile, the Langhian shows a peak in RFD at 30-40˚N, closely followed by 40-50˚N – which differs from RGD with sees a single peak in 40-50˚N. From 0-10˚N, southward, the Langhian shows consistent low RFD values until a rise at 30-40˚S continued to a smaller peak at 40-50˚S. Meanwhile, Langhian RGD remains low in 30-40˚S until a similar smaller peak at 40-50˚S (Fig. 13bi & 13bii). Furthermore, in the Serravallian, accompanying the 40-50˚N peak, as in most stages, are relatively raised RFD values in lower northern latitude bins, i.e. 20-30˚N, 10-20˚N and 0-10˚N. Once again, the Southern Hemisphere sees the lowest RFD values, with

the minimum at 20-30˚S, but again there exists a Southern Hemisphere peak at 40-50˚S, smaller than that in 40-50˚N (Fig. 13ci). The Tortonian sees a shift in peak RFD and RGD, whereby the larger peak in both is in 10-20˚N, and the smaller peak is 40-50˚N in this instance. This comes as well as a low at 20-30˚S and a smaller peak at 30-40˚S and 40-50˚S in both RFD and RGD (Fig. 13ci-cii).

The final Miocene stage, the Messinian, shows its peak RFD and RGD in 30-40˚N (Fig. 14ai & 14aii). After a southward drop to 20-30˚N, and 10-20˚N there is also a minor peak at 0-10˚N, and the Southern Hemisphere once again sees smaller RFD and RGD values, although small peaks in RFD do occur at 10-20˚S and 40-50˚S (Fig. 14ai-ii). The Zanclean (early Pliocene), sees its maximum RFD at 0-10˚N, and a smaller peak at 30-40˚N, (Fig. 14bi). There is also a Zanclean peak in RFD in the Southern Hemisphere at 10-20˚S, with a smaller peak at 40-50˚S. Zanclean RGD, meanwhile, is largest at 30-40˚N, closely followed by 10-20˚N, with a steep drop to 40-50˚N and similar RFD at 50-60˚N (Fig. 14bii). The Piacenzian, shows maximum RFD and RGD at 10-20˚N, followed by 30-40˚N (Fig. 14). The Piacenzian also shows a steep drop in both RFD and RGD to 40-50˚N and similar at 50-60˚N, which is unique to the Pliocene (Fig. 14ci-ii).

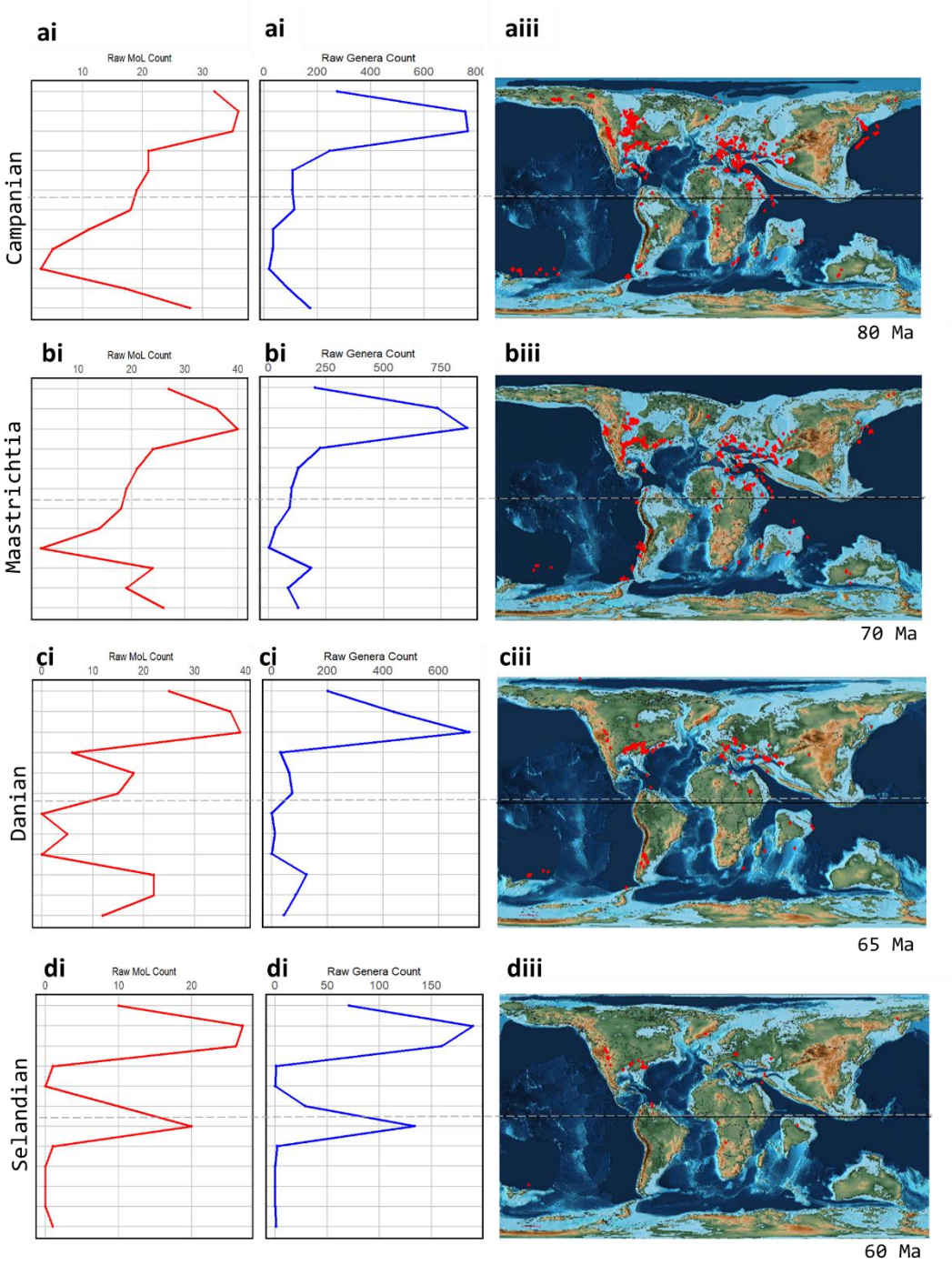

Figure 10. ai to di = Raw invertebrate MoL count (functional diversity) in red and **aii to dii** = raw invertebrate generic diversity (blue) across discrete palaeolatitude bins of 10˚ width, from 50-60˚N to 50-60˚S. This range of palaeolatitude bins is what was viable to perform spatial and SQS subsampling on, albeit with gaps. The four rows represent the first four Stages in the study interval; the Campanian and Maastrichtian (Late Cretaceous) and the Danian and Selandian (Paleocene), **aiii to diii** = a map of the plate reconstructions closest to each stage with palaeolatitude and palaeolongitude of each occurrence used to superimpose the distribution of raw occurrence sites in each stage, made using PALEOMAP, PaleoAtlas, Scotese (2016).

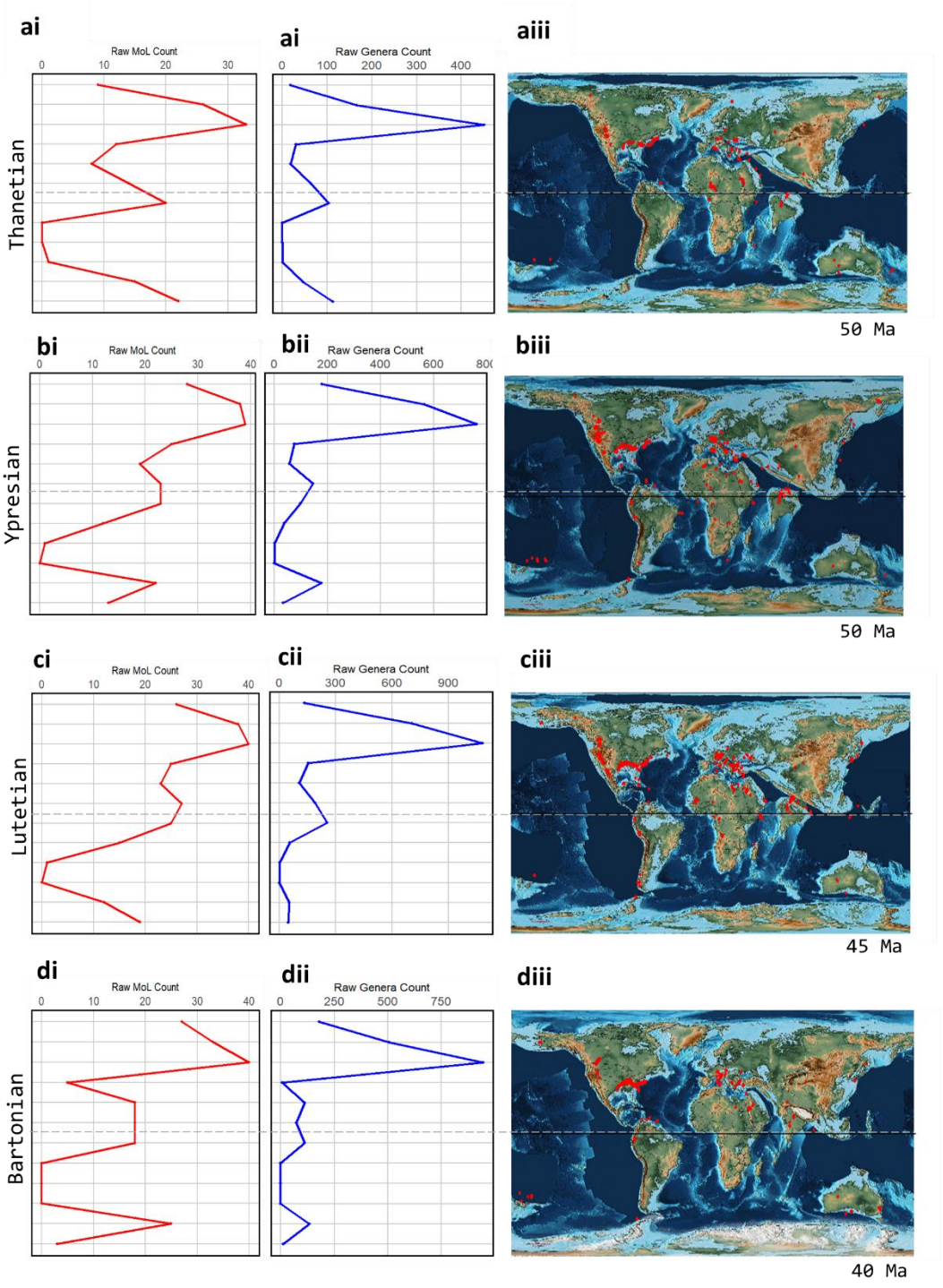

Figure 11. ai to di = Raw invertebrate MoL count (functional diversity) in red and **aii to dii** = raw invertebrate generic diversity (blue) across discrete palaeolatitude bins of 10˚ width, from 50-60˚N to 50-60˚S. This range of palaeolatitude bins is what was viable to perform spatial and SQS subsampling on, albeit with gaps. The four rows represent the first four Stages in the study interval; the Campanian and Maastrichtian (Late Cretaceous) and Ypresian, Lutetian and Bartonian (Eocene); **aiii to diii** = map of the plate reconstructions closest to each stage with palaeolatitude and palaeolongitude of each occurrence used to superimpose the distribution of raw occurrence sites in each stage, made using PALEOMAP, PaleoAtlas Scotese (2016).

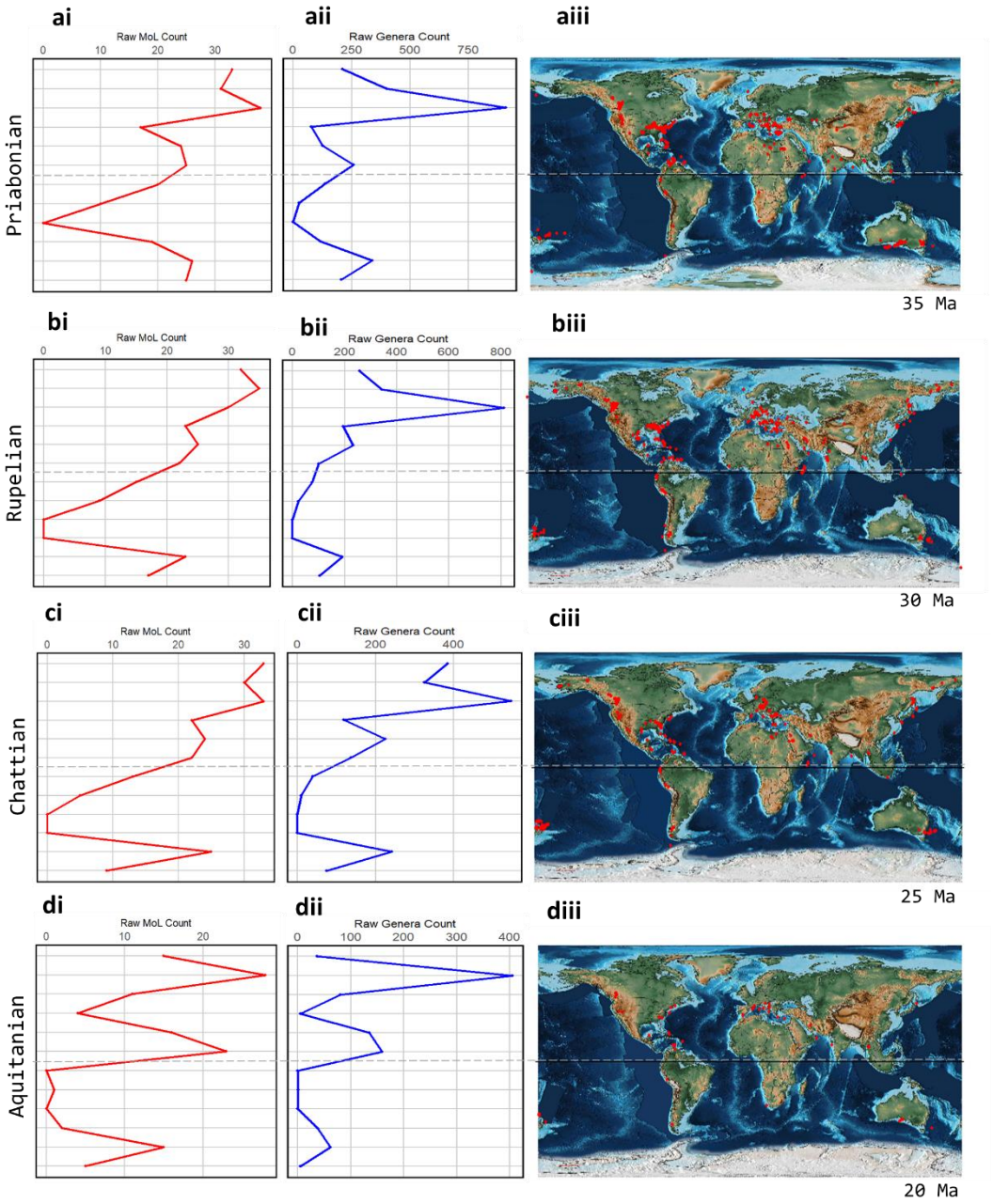

Figure 12. ai to di = Raw invertebrate MoL count (functional diversity) in red and **aii to bii** = raw invertebrate generic diversity (blue) across discrete palaeolatitude bins of 10˚ width, from 50-60˚N to 50-60˚S. This range of palaeolatitude bins is what was viable to perform spatial and SQS subsampling on, albeit with gaps. The four rows represent the Priabonian (Late Eocene), Rupelian and Chattian (Oligocene) and the Aquitanian (Early Miocene); **aiii to biii** = a map of the plate reconstructions closest to each stage with palaeolatitude and palaeolongitude of each occurrence used to superimpose the distribution of raw occurrence sites in each stage, made using PALEOMAP, PaleoAtlas, Scotese (2016).

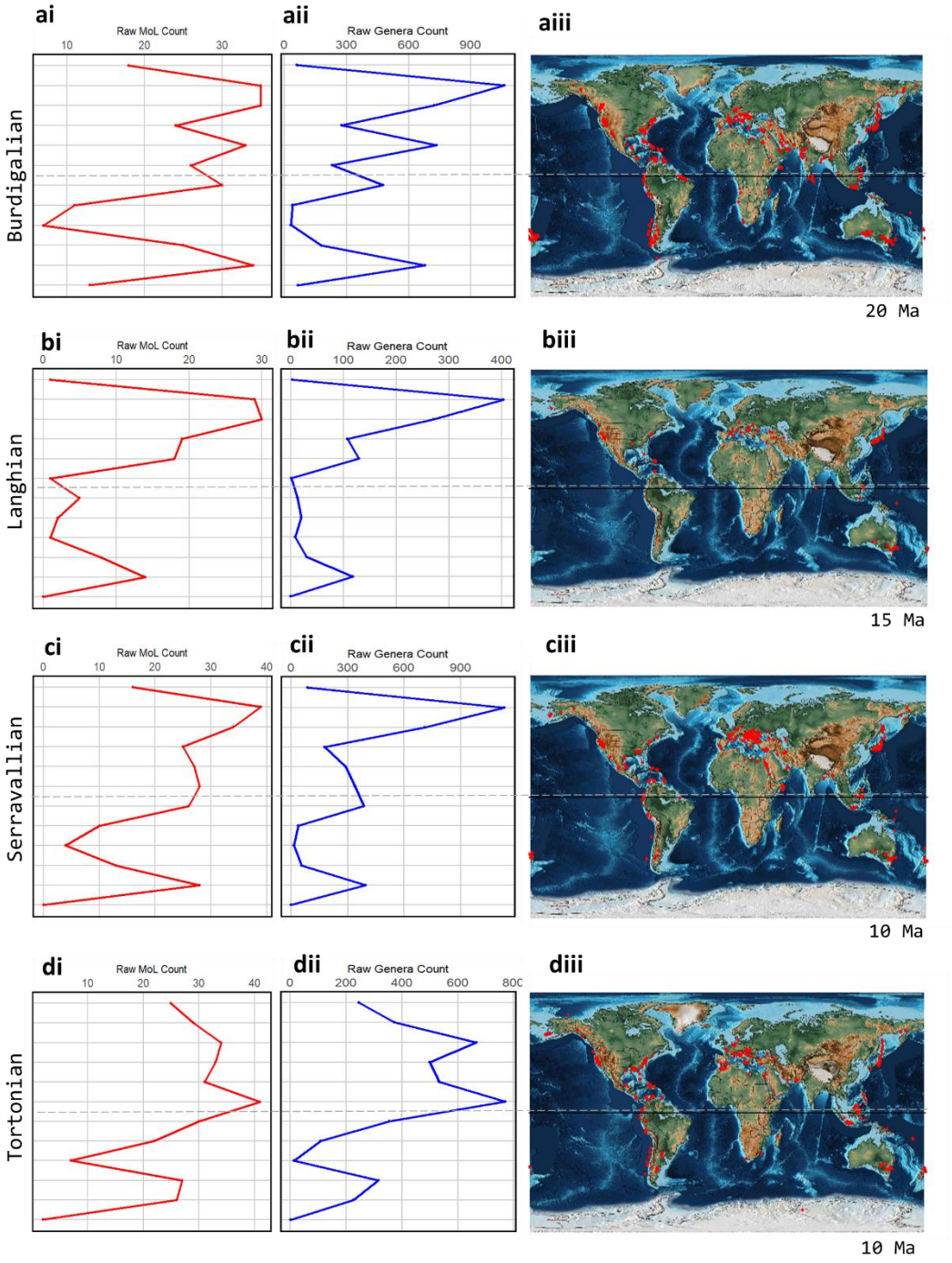

Figure 13. **a** = Raw invertebrate MoL count (functional diversity) in red and **b** = raw invertebrate generic diversity (blue) across discrete palaeolatitude bins of 10˚ width, from 50-60˚N to 50-60˚S. This range of palaeolatitude bins is what was viable to perform spatial and SQS subsampling on, albeit with gaps. The four rows represent the first four Stages in the study interval; the Burdigalian, Langhian, Serravallian and Tortonian (Miocene); **c** = a map of the plate reconstructions closest to each stage with palaeolatitude and palaeolongitude of each occurrence used to superimpose the distribution of raw occurrence sites in each stage, made using PALEOMAP, PaleoAtlas Scotese (2016).

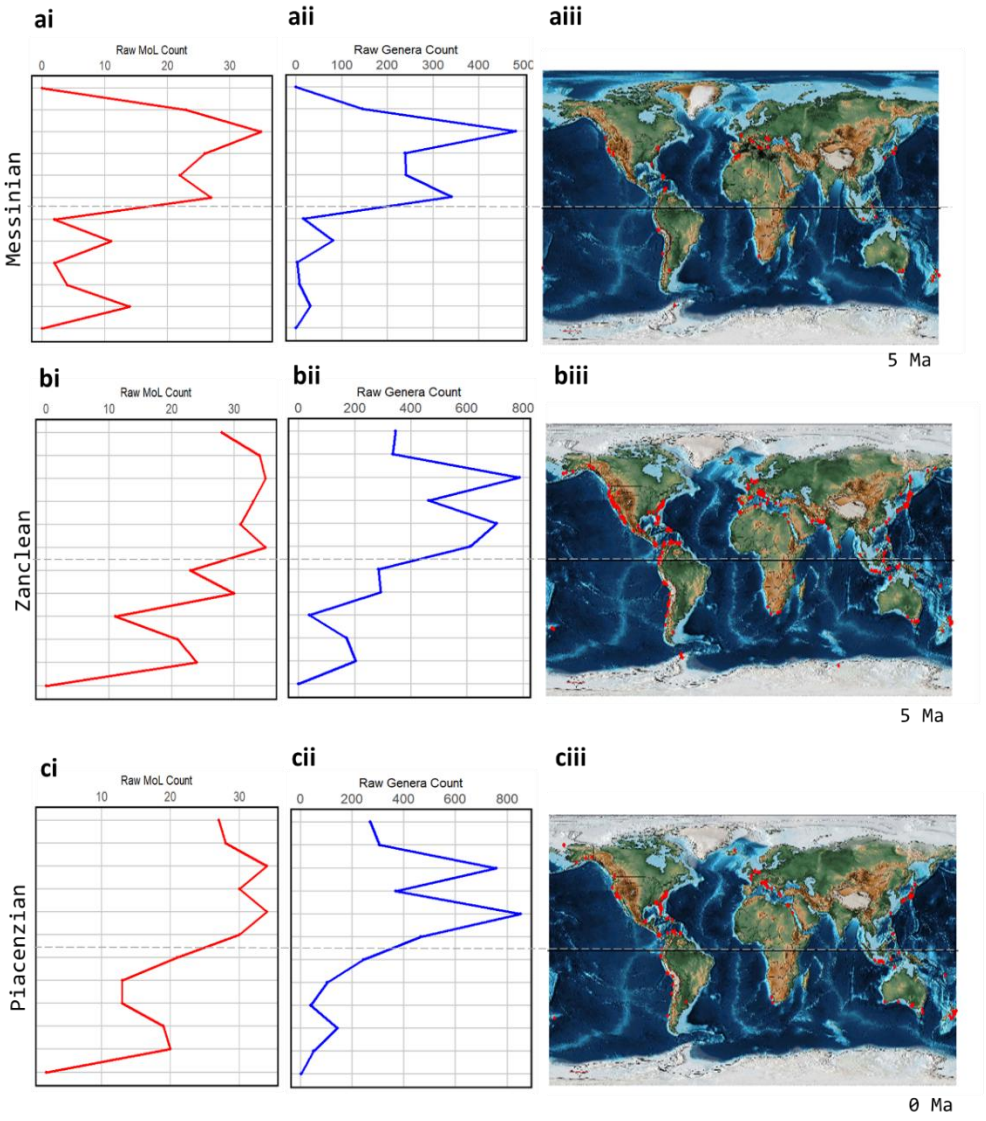

Figure 14. ai to ci = Raw invertebrate MoL count (functional diversity) in red and **aii to cii** = raw invertebrate generic diversity (blue) across discrete palaeolatitude bins of 10˚ width, from 50-60˚N to 50-60˚S. This range of palaeolatitude bins is what was viable to perform spatial and SQS subsampling on, albeit with gaps. The four rows represent the final four Stages of the interval, the Messinian (Late Miocene), Zanclean and Piacenzian (Pliocene); **aiii to ciii** = a map of the plate reconstructions closest to each stage with palaeolatitude and palaeolongitude of each occurrence used to superimpose the distribution of raw occurrence sites in each stage, made using PALEOMAP, PaleoAtlas, Scotese (2016).

3.3.5. Spatially-standardised diversity patterns across palaeolatitude at stage level

Spatial standardisation using *divvy* (Antell et al. 2024) was performed on the raw data within each palaeolatitude bin for each stage in the interval. Figures 15a-i and 16a-i represent the palaeolatitude pattern in SSFD across the Northern Hemisphere (from 0-10˚N to 50-60˚N) for each of the stages in the study period, except the Aquitanian which lacked sufficient data for subsampling in any palaeolatitude bin. Meanwhile, Figures 17a-i and 18a-i represent the SSGD pattern across palaeolatitude for all stages, except the Aquitanian.

Firstly, the Campanian and Maastrichtian (Late Cretaceous) both display a relatively high mean SSFD from 50-60˚N southwards to 30-40˚N, which the Campanian reporting peak SSFD in 40-50˚N and Maastrichtian in 30-40˚N (Fig. 15a & 15b). Both also see a decline equatorward from 30-40˚N, to a low at 20-30˚N for the Campanian and 10-20˚N for the Maastrichtian. Continuing equatorward, the Campanian sees a smaller peak in SSFD in 10-20˚N, remaining relatively stable to 0-10˚N, meanwhile the Maastrichtian sees a smaller peak in 0-10˚N only (Fig. 15a & 15b). The Danian, Selandian and Thanetian of the Paleocene possess insufficient data points to make reliable inference, although the few SSFD values that could be calculated see means comparable to those of the same palaeolatitude bins in other stages (Fig. 15c-15e). The Ypresian (earliest Eocene) displays a similar palaeolatitudinal pattern in SSFD to that observed in the Late Cretaceous, with a peak in mean SSFD at temperate latitude of 40-50˚N, and a drop in the lower palaeolatitude bins (Fig. 15f). This palaeolatitudinal SSFD pattern is also observed through the Lutetian and Bartonian of the middle Eocene, despite gaps (Fig. 15g & 15h). The Priabonian (latest Eocene) witnesses its largest peak in mean SSFD at 40-50˚N, with a steeper drop into 50-60˚N than older stages (Fig. 15i). This is something that cannot be tracked much further into the interval, unfortunately, due to gaps. Priabonian SSFD also declines equatorward from 40-50˚N to a low at 20-30˚N, like most stages. But unlike most stages, the peak in mean SSFD in 10-20˚N is equitable to that seen in 40-50˚N (Fig. 15i).

The Rupelian (earliest Oligocene) shows its maximum mean SSFD in 50-60˚N, distinct to other stages (Fig. 16a). From here, there is an equatorward decline in Rupelian mean SSFD, to a low in 20-30˚N (Fig. 16). Rupelian mean SSFD rises to a smaller peak again into 10-20˚N and remains stable to 0-10˚N (Fig. 16a). Meanwhile, the Chattian (late Oligocene) and Burdigalian (early Miocene, omitting Aquitanian) both report a similar decline in SSFD equatorward from a peak in 40-50˚N, to a low in 20-30˚N, although there are gaps (Fig. 16b & 16c). Despite lacking

sufficient data for reliable inference, the single Langhian mean SSFD, 40-50˚N, is comparable to 40-50˚N of other stages (Fig. 16d).

The apparent common pattern of a maximum peak in mean SSFD in 40-50˚N, an equatorward decline to a minimum at 20-30˚N, and a secondary peak at 10-20˚N is also observed in the Serravallian and later stages (Fig 16e). However, the secondary peak in mean SSFD at 10-20˚N is nearly equal to that of 40-50˚N in the Tortonian and exceeds that of 40-50˚N in the Messinian (Fig. 16f & 16g). The early Pliocene (Zanclean) shows a maximum peak in mean SSFD at 40-50˚N and decline to 20-30˚N with rise in 10-20˚N (Fig. 16h). Finally, the Piacenzian lacks sufficient data for full comparison but does display a peak in SSFD in 40-50˚N (Fig. 16i).

The mean spatially-standardised generic diversity (SSGD) of marine invertebrates across the Northern Hemisphere, broadly mirrors the pattern of functional diversity over the study interval, but is not without its differences (Figs. 17a-i & 18a-i). For example, a peak in mean SSGD is reported at 30-40˚N as often as it is 40-50˚N, whereas mean SSFD maximum is almost exclusively in 40-50˚N. The Campanian and Maastrichtian both display a temperate peak in mean SSGD (40-50˚N in Campanian and 30-40˚N Maastrichtian), and a steeper decline north into the highest palaeolatitude bins than is reported for the Late Cretaceous in SSFD (Figs. 17a & 18b). Both the Campanian and Maastrichtian also witness a steep decline in SSGD southwards from the mid-latitude peak, into the three lowest latitude bins, 20-30˚N, 10-20˚N and 0-10˚N, with a slight rise in Maastrichtian mean SSGD in 0-10˚N (Figs. 17a & 17b). The Paleocene (Danian, Selandian, Thanetian) lacks sufficient data to make reliable inference, but only the Danian sees SSGD values equitable to analogous latitude bins in other stages (Fig. 17c-e). The Ypresian (earliest Eocene) shows a peak in mean SSGD at 30-40˚N, with the mean at 40-50˚N roughly the same as at 0-10˚N (Fig. 17f). There are gaps in the Lutetian and Bartonian, however their maximum SSGD mean is observed at 40-50˚N, as is reported in the Priabonian, which shows a large peak at 40-50˚N, a smaller peak at 0-10˚N and lower values in 20-30˚N and 10-20˚N (Figs. 17g-i).

Furthermore, the Rupelian displays a peak in mean SSGD at 30-40˚N, with declining values north and south from there (Fig. 18a). A peak at 30-40˚N is also seen in the Chattian, where it extends north to 40-50˚N in a plateau, but declines equatorward to 10-20˚N (Fig. 18b). The Burdigalian, (NB the Aquitanian was omitted) also displays a 30-40˚N peak, a low at 20-30˚N and 0-10˚N, with a smaller peak at 10-20˚N (Fig. 18c). The Langhian has only one bin (40-50˚N), and values are comparable to 40-50˚N in the other stages (Fig. 18d). The Serravallian, displays a

relatively steep peak in mean SSGD at 40-50˚N, creating a sharp decline to 30-40˚N and 20-30˚N, but again shows a secondary smaller peak at 10-20˚N (Fig. 18e). Meanwhile the inverse is true for the Tortonian which peaks in mean SSGD diversity at 10-20˚N with a smaller peak at 40-50˚N (Fig. 18f). The final Miocene stage, the Messinian, shows a peak at 40-50˚N, despite gaps (Fig. 18g). The Zanclean, however, shows its maximum mean SSGD at 10-20˚N (like the Tortonian) (Fig. 18h). The Piacenzian retains too many gaps to make viable inference but shows a SSGD peak at 40-50˚N equitable to other stages in the interval (Fig. 18i).

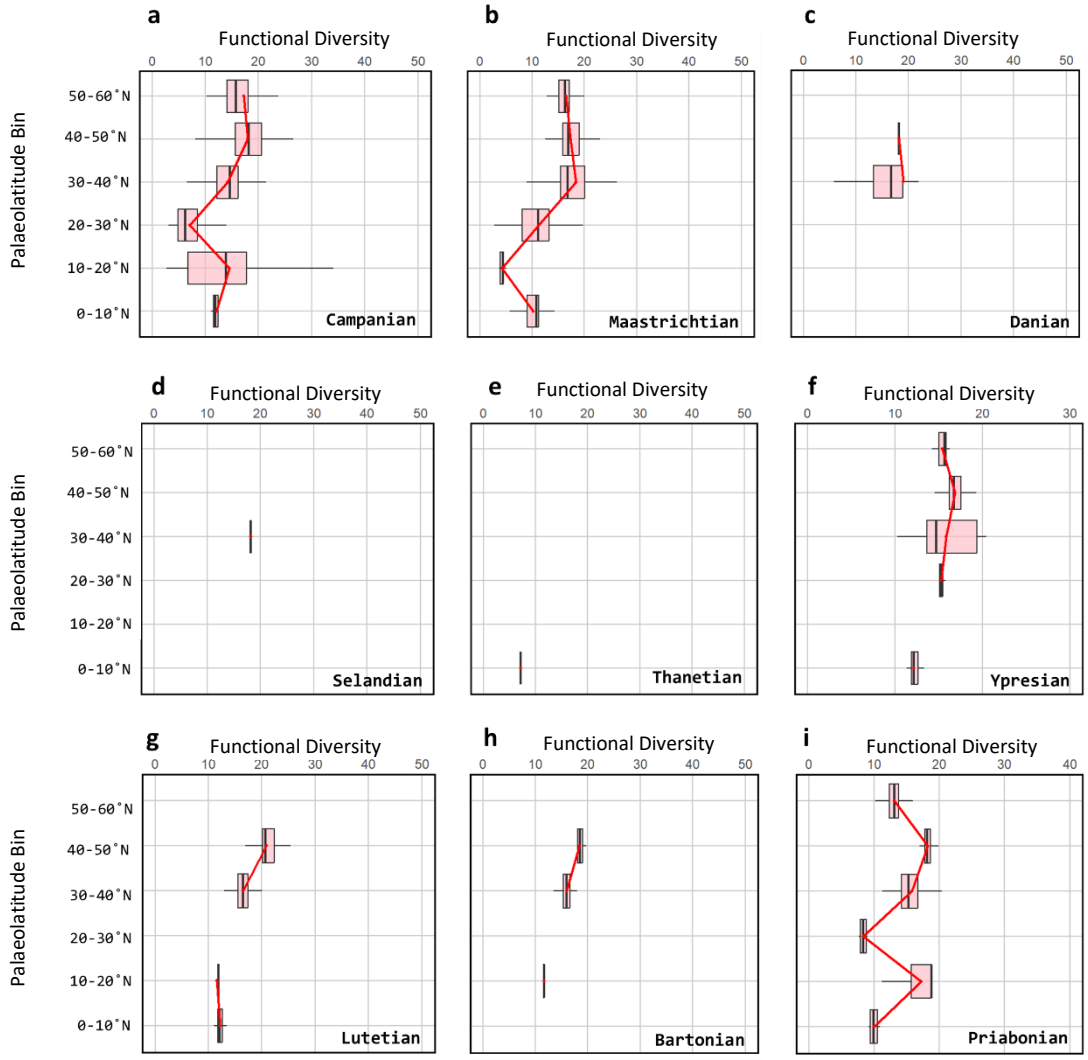

Figure 15. Nine panels, **a-i** of light red boxplots with Palaeolatitude Bin on the y-axis and SSFD (spatially-standardised functional diversity) on the x-axis (top). Each plot represents the latitudinal distribution of MoL diversity, in the Northern Hemisphere, across six palaeolatitude bins, from 0-10˚N to 50-60˚N, although there are gaps in most. A red line joins the mean SSFD value within each boxplot. Starting from the top left, each panel represents a stage in chronological order, from the Campanian in the Late Cretaceous to the Priabonian in the Late Eocene.

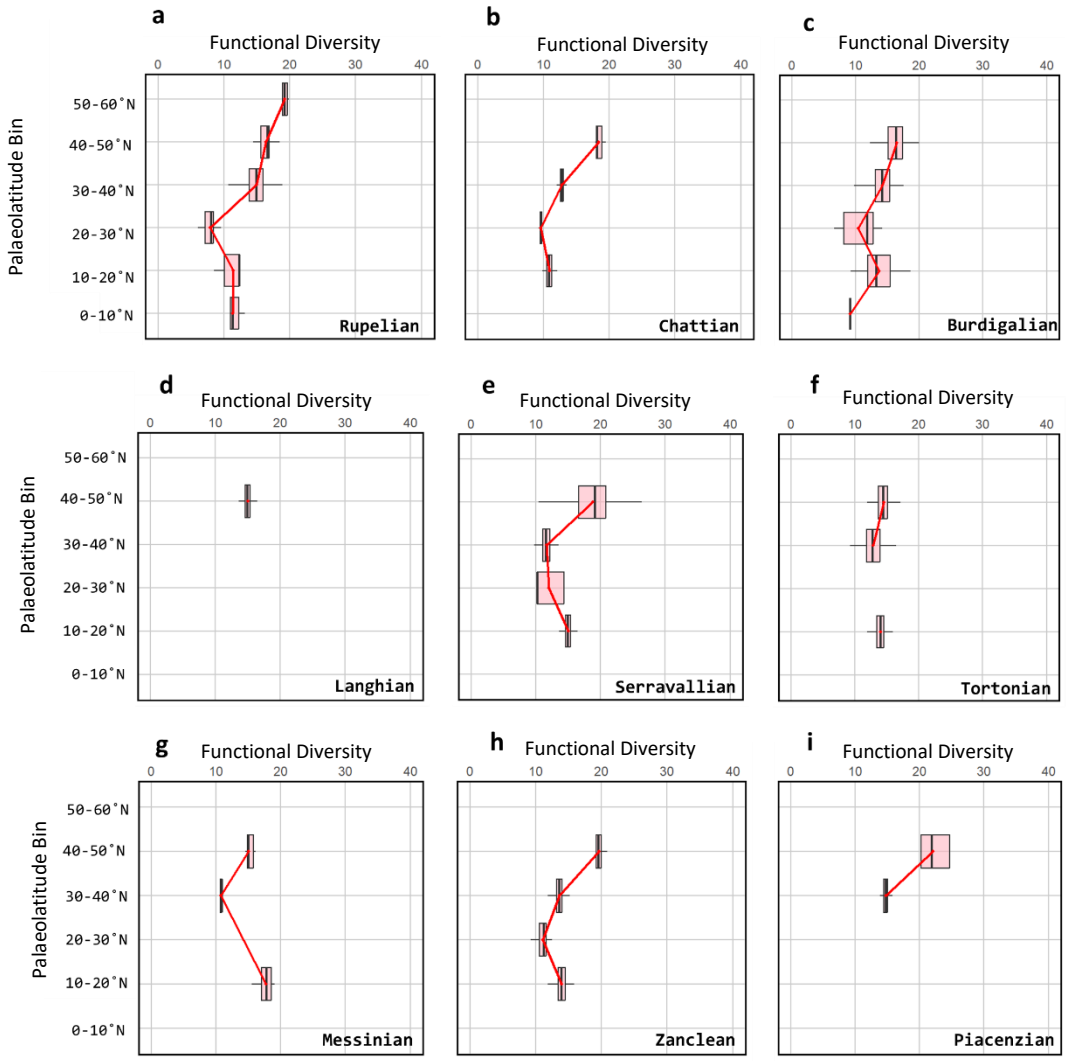

Figure 16. Nine panels, **a-i** of light red boxplots with Palaeolatitude Bin on the y-axis and SSFD (spatially-standardised functional diversity) on the x-axis (top). Each plot represents the latitudinal distribution of MoL diversity, in the Northern Hemisphere, across six palaeolatitude bins, from 0-10˚N to 50-60˚N, although there are gaps in most. A red line joins the mean SSFD within each box. from the top left, each panel represents a stage in chronological order, from the Rupelian in the Oligocene to the Piacenzian in the Late Pliocene.

3.3.6. Spatially-standardised diversity patterns across palaeolatitude at epoch level

At epoch scale, the larger sample size meant that spatial-subsampling could be run for some Southern Hemisphere palaeolatitude bins (Figs. 19a-f & 20a-f), although many gaps remain across the study interval. Firstly, Late Cretaceous mean SSFD sees the mid to high palaeolatitude plateau observed at Late Cretaceous stage level, from 30-40˚N through to 50-60˚N (Fig. 19a). However, this is not reported in analogous Southern Hemisphere palaeolatitude bins; instead, a slight decrease from 30-40˚S to 40-50˚S and then a sharp rise in 50-60˚S is seen (Fig. 19a). As observed

at stage level, the Northern Hemisphere low is at 20-30˚N, with a small peak at 10-20˚N, and a decline in SSFD through 0-10˚N to 0-10˚S, where gaps prevent further insight (Fig. 19a). The Paleocene has insufficient data to make many reliable observations, besides a peak at 30-40˚N and 0-10˚S, and a low at 0-10˚N (Fig. 19b). The Eocene shows the same Northern Hemisphere mean SSFD pattern as stage level, with a peak at 40-50˚N, with similar mean SSFD around 30-40˚N and 50-60˚N, and then a drop in 20-30˚N down to a low at 10-20˚N, with a smaller peak at 0-10˚N (Fig. 19c). The Southern Hemisphere Eocene mean SSFD has many gaps but also sees a peak at 40-50˚S, closely followed by 50-60˚S in the Eocene, similar to that reported in Northern Hemisphere, albeit with lower peak values in mean SSFD.

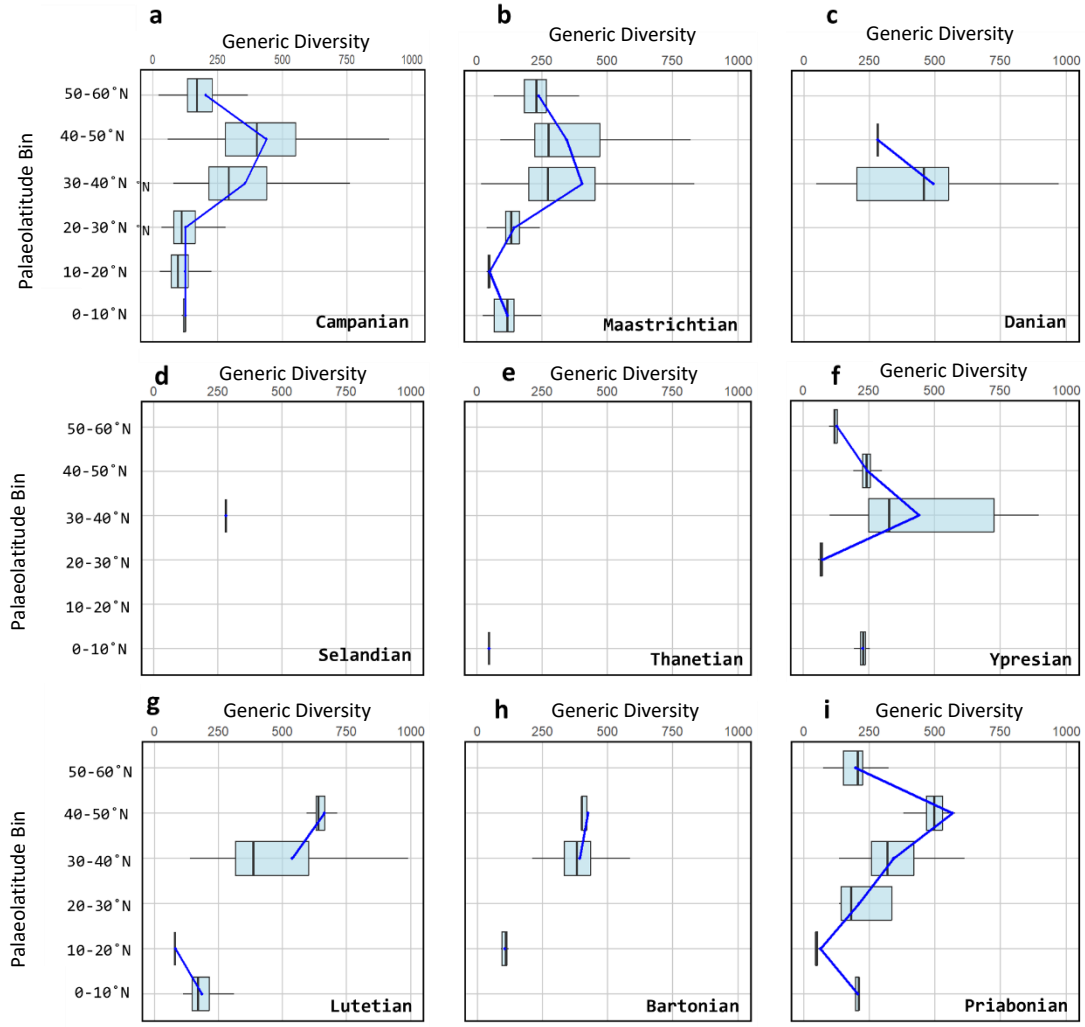

Figure 17. Nine panels **a-i** of light blue boxplots with Palaeolatitude Bin on the y-axis and SSGD, (spatially-standardised generic diversity) of marine invertebrates on the x-axis (top). Each plot represents the latitudinal distribution of generic diversity, in the Northern Hemisphere, across six palaeolatitude bins, from 0-10˚N to 50-60˚N, although there are gaps in most. A blue line joins the mean SSGD value within each boxplot. From the top left, each panel represents a stage in chronological order, from the Campanian in the Late Cretaceous to the Priabonian in the Late Eocene.

However, the same pattern cannot be confirmed for mean SSFD in the Oligocene, due to a lack of Southern Hemisphere data, except a single mean SSFD at 40-50˚S, of a lower value than the analogous 40-50˚N mean SSFD (Fig. 19d). However, the Oligocene witnesses the same peak at 40-50˚N and 50-60˚N as at stage level, along with a low at 20-30˚N and a smaller peak at 10-20˚N (Fig. 19d). Due to a very low 10-20˚S value, the Miocene latitudinal pattern appears flattened in the Northern Hemisphere compared to stage level, yet still shows a peak at 40-50˚N and a comparable value at the only available Southern Hemisphere bin, 30-40˚S (Fig. 19e). The Miocene also shows a steep drop off in mean SSFD at 50-60˚N. Finally, the Pliocene, retains a peak in mean SSFD at 40-50˚N, in the Northern Hemisphere, but sees its maximum value at 40-50˚S, along with a relatively higher mean SSFD around 0-10˚N than reported in older epochs, and again a steeper decline in SSFD between 40-50˚N and 50-60˚N than seen in pre-Miocene epochs (Fig. 19f).

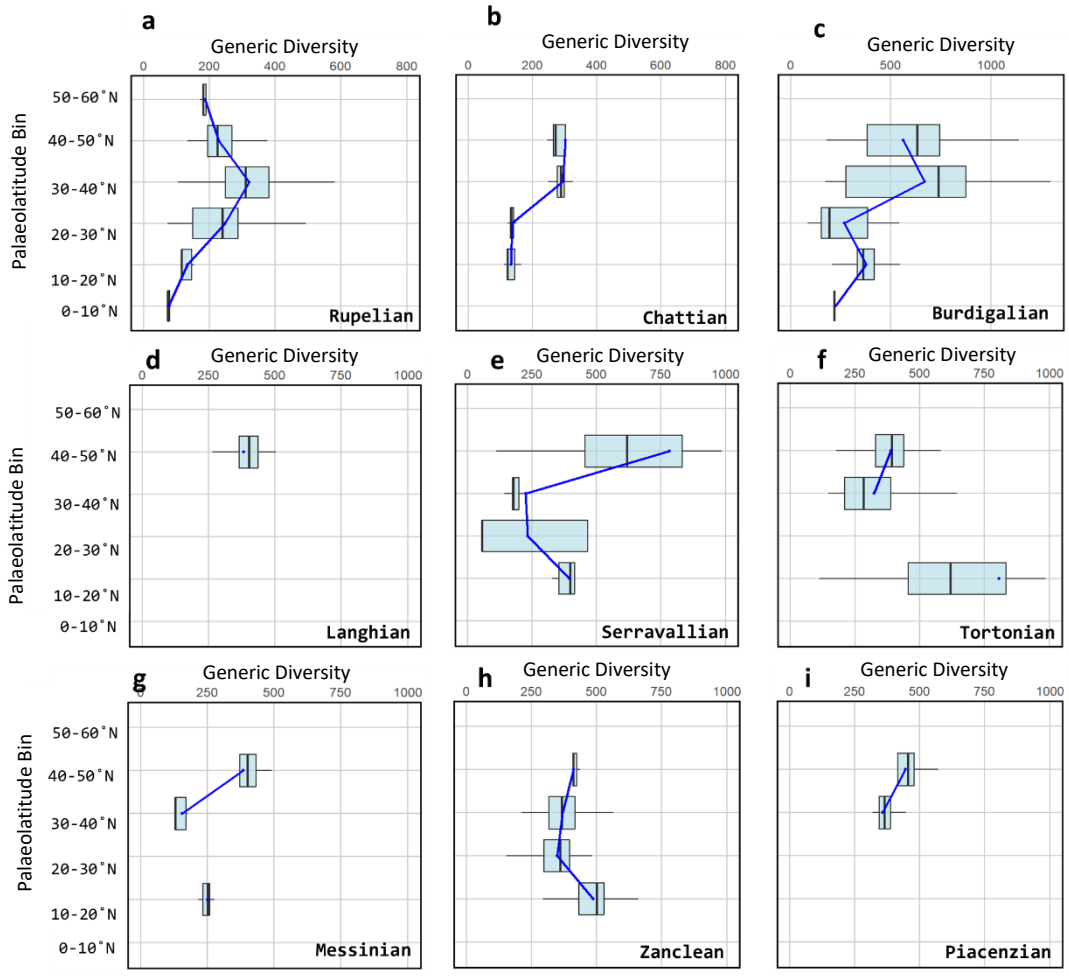

Figure 18. Nine panels **a-i** of light blue boxplots, with Palaeolatitude Bin on the y-axis and SSGD (spatially-standardised generic diversity) of marine invertebrates on the x-axis (top). Each plot represents the latitudinal distribution of generic diversity, in the Northern Hemisphere, across six palaeolatitude bins, from 0-10˚N to 50-60˚N, although there are gaps in most. A blue line joins the mean SSGD value within each plot. From top left, each panel represents a stage in chronological order, from the Rupelian (Oligocene) to the Piacenzian, (Late Pliocene).

Meanwhile, mean SSGD at epoch level shows a similar but not identical palaeolatitudinal pattern to mean SSFD over time (Fig. 20a-f). The Late Cretaceous sees a steep peak in mean SSGD in 30-40˚N, with no analogous peak in 30-40˚S, and no small peak around 10-20˚N or 0-10˚N (Fig. 20a) as observed in mean SSFD. There is also a decline in mean SSGD from 30-40˚N, through 40-50˚N and 50-60˚N (Fig. 20a), unlike the plateau in mean SSFD across the three highest latitude bins in the Late Cretaceous. Meanwhile, the Paleocene pattern in mean SSGD across palaeolatitude bins is like that of the mean SSFD, retaining many gaps, and an observed minimum at 20-30˚N instead of 0-10˚N (Fig. 20b). The Eocene SSGD shows a similar pattern to mean SSFD across palaeolatitude, with a Northern Hemisphere peak in mean SSGD centred on both 30-40˚N and 40-50˚N, and an analogous peak at 40-50˚S (Fig. 20c). The Oligocene, meanwhile, shows a prominent peak in mean SSGD at 30-40˚N, with a comparable mean at 40-50˚S as is seen at 40-50˚N (Fig. 20d). Furthermore, the Miocene shows relatively higher mean SSGD values (of ~400 genera) compared to earlier epochs (a mean of ~100-200 genera). Despite this, there remains a significant peak in mean SSGD at the temperate latitude (40-50˚N) and a steep drop into 50-60˚N (Fig. 20e). The Miocene also shows analogous 0-10˚S mean SSGD to 0-10˚N and a somewhat comparable 40-50˚S value to 40-50˚N, but very a low mean SSGD at both 10-20˚S and 30-40˚S (Fig. 20e). Finally, the Pliocene shows the peak in mean SSGD around 0-10˚N and 10-20˚N, unlike any other epoch, along with a smaller peak at 40-50˚N, and 40-50˚S (Fig. 20f).

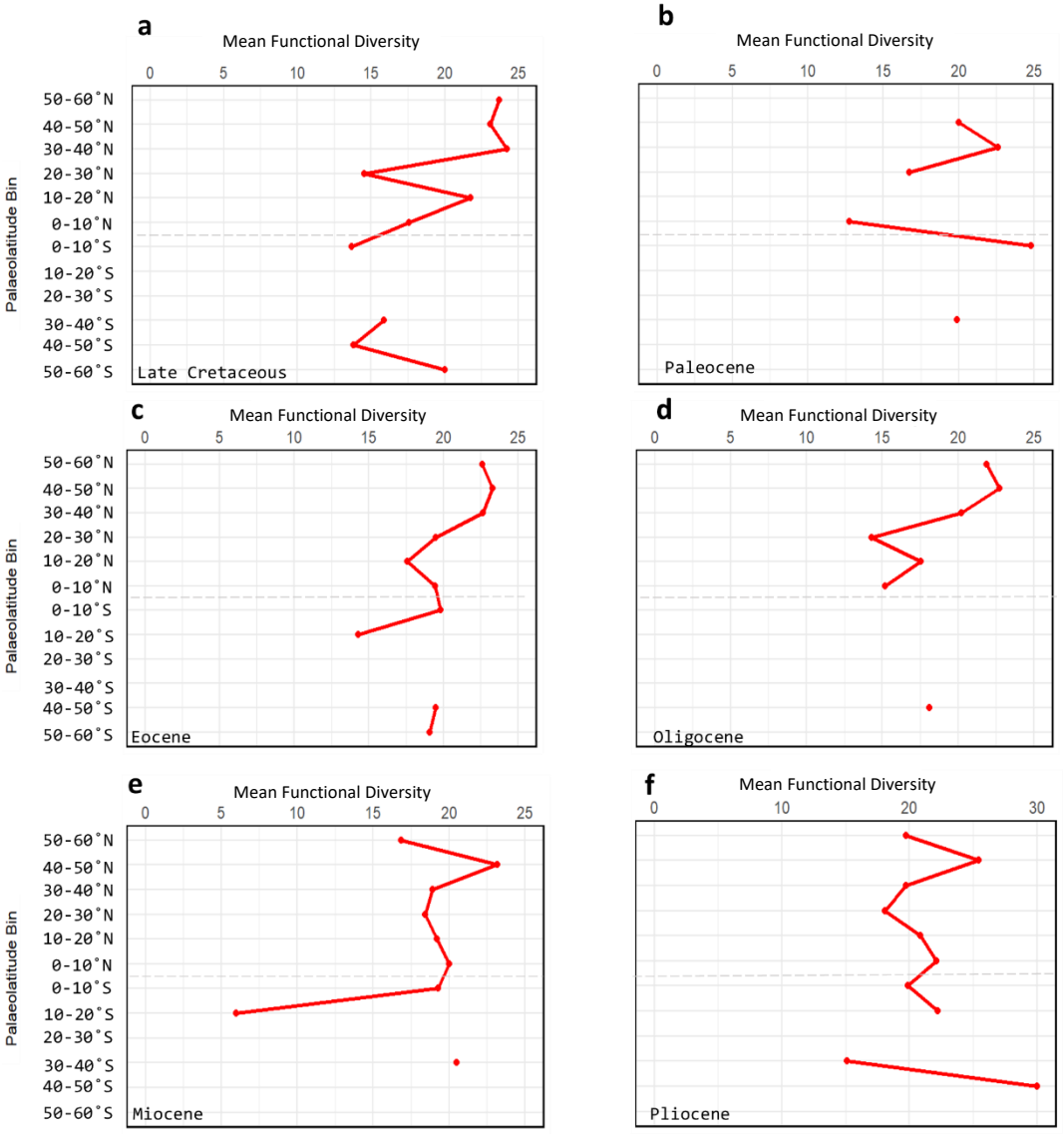

Figure 19. Panels a-f Mean spatially-standardised functional diversity (SSFD) of invertebrates (x-axis, top) across Palaeolatitude Bins (y-axis) for the epochs in this study interval. These include the Late Cretaceous (Campanian & Maastrichtian); the Palaeocene (Danian, Selandian and Thanetian); Eocene (Ypresian, Lutetian, Bartonian and Priabonian); Oligocene (Rupelian & Chattian); Miocene (Aquitanian, Burdigalian, Langhian, Serravallian, Tortonian, Messinian) and the Pliocene (Zanclean & Piacenzian).

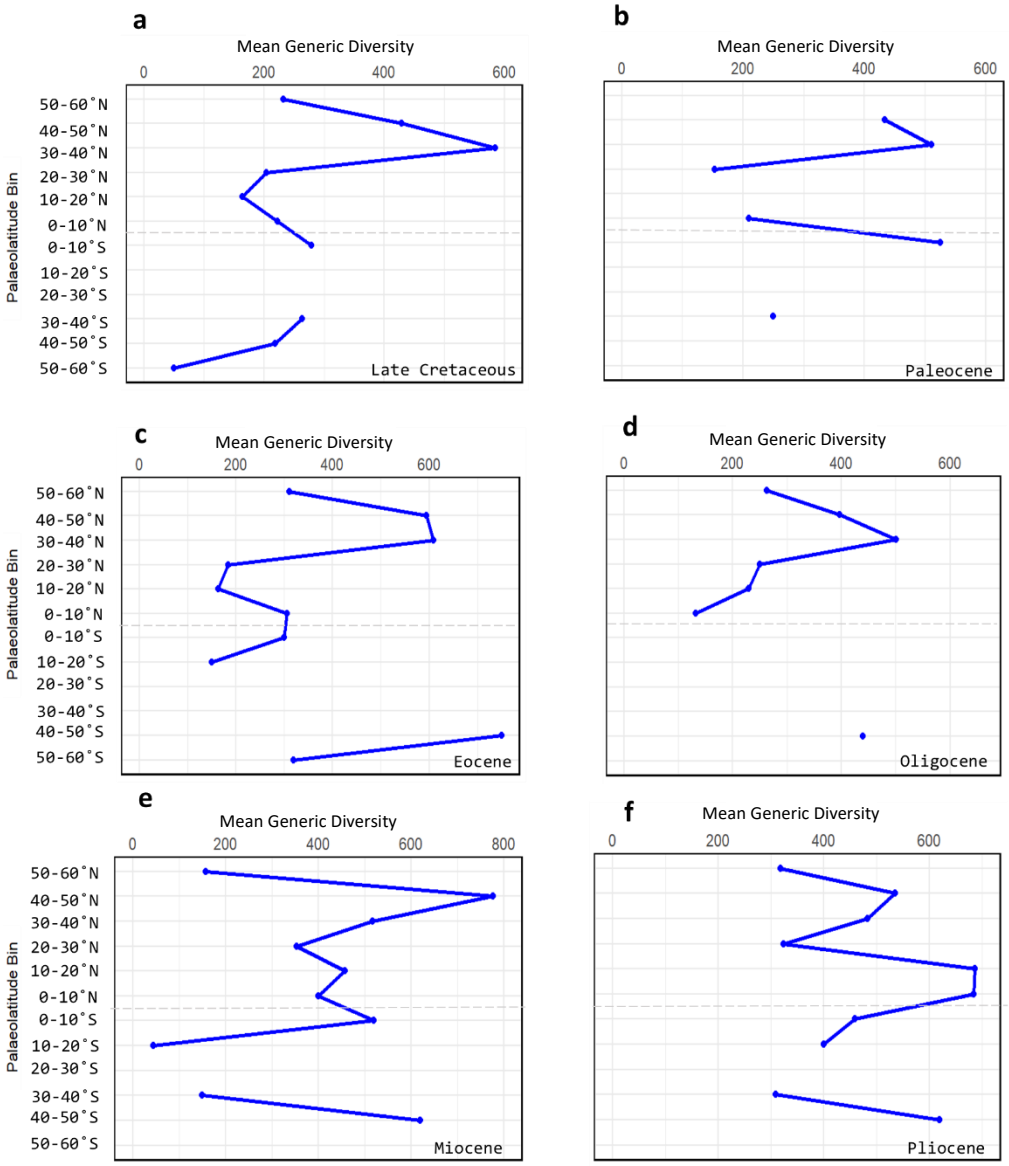

Figure 20 Panels a to f. Mean spatially-standardised generic diversity (SSGD) of invertebrates (x-axis, top) across Palaeolatitude Bins (y-axis) for the epochs in this study interval. These include the Late Cretaceous (Campanian & Maastrichtian); the Palaeocene (Danian, Selandian and Thanetian); Eocene (Ypresian, Lutetian, Bartonian and Priabonian); Oligocene (Rupelian & Chattian); Miocene (Aquitanian, Burdigalian, Langhian, Serravallian, Tortonian, Messinian) and the Pliocene (Zanclean & Piacenzian).

3.4. Discussion

3.4.1 Part A: Global Patterns of Functional Diversity

In the results presented, global raw, standardised, and spatially-standardised analyses display no obvious long-term trends in marine invertebrate functional diversity (FD) from the Campanian to the Piacenzian, ~83.6 - 2.58 Ma (Figs. 6, 7a & 8a). The lack of long-term FD trend opposes a previous suggestion of a continued rise in the number of modes of life (MoLs) occupied by marine fauna throughout the Phanerozoic (Bambach et al. 2007). Despite only comparing Ediacaran, Cambrian, Ordovician and Modern assemblages, Bambach et al. (2007) stated that, after a steep rise in MoL occupation during the GOBE (~497.05-467.33 Ma), MoL occupation continued to increase over the Phanerozoic, with the largest increases during the Paleozoic, a reorganisation during the Mesozoic Marine Revolution (MMR) and marginal expansion over the Cenozoic (Bambach et al. 2007; Buatois et al. 2016b). These results instead support diverging evidence whereby the number of MoLs filled by bivalves appears to plateau from the K-Pg onwards with no Cenozoic increase (Mondal & Harries 2016). Perhaps because Bambach et al. (2007) could only include teleost fishes, marine mammals, reptiles and chondrichthyans in their Modern assemblage, this produced a continued rise between the Ordovician and Modern, including across the Cenozoic, which is unseen in invertebrates here.

The results here also corroborate shows of stability in global marine FD across extreme climate perturbations in the fossil record (Foster & Twitchett 2014; Dunhill et al. 2018; Edie et al. 2018; Whittle et al. 2019). There is evidence for the global loss of only one functional group across the Permian-Triassic Mass Extinction (PTME), despite a loss of up to 74% of genera (Foster & Twitchett 2014); along with no net loss of functional groups across the Late Triassic Mass Extinction (LTME, Dunhill et al. 2018) or across the K-Pg mass extinction, in Antarctica (Whittle et al. 2019). It is thought that little change in FD despite losing most species is due to the skeleton crew hypothesis (Foster & Twitchett 2014; Dunhill et al. 2018), whereby high functional redundancy helps preserve functions during mass extinctions, since most MoLs retain taxa. With no major mass extinction in the Cenozoic Era, it is likely that FD remained stable across Cenozoic extreme climate events including the Paleocene-Eocene Thermal Maximum, the Eocene-Oligocene Transition and Mid Miocene Climate Transition. For example, stability in FD has been reported across the Pliocene-Pleistocene megafaunal extinction (Pimiento et al. 2017) which occurs after the end of the study interval. The results here find stability in FD over the long-term transition from the Late Cretaceous greenhouse climate to Pliocene icehouse conditions (Figs.

7-8a) (Westerhold et al. 2020), previously untested in marine macroinvertebrates. With that being said, there are between-stage variations in global FD that coincide with certain extreme Cenozoic climate events, including the Early Eocene hyperthermal events. The PETM, EECO and MECO occurred during the Early to Mid-Eocene and represent the highest temperatures recorded in the Cenozoic (Bohaty & Zachos 2003; Stokke et al. 2020)

Meanwhile, marine invertebrate generic diversity (GD) appears to display a slight long-term increasing trend in the raw (RGD) and standardised (SGD) analyses, despite stage-to-stage variation (Figs. 7 & 8b). This has previously been suggested as part of a sustained increase in invertebrate generic richness over the Phanerozoic, since the Cambrian Explosion (~539-535 Ma) to today due to continued origination and declining background extinction (Roopnarine 2006). A continued Cenozoic rise in marine generic diversity has also been reported after standardisation in Alroy (2010a). However, in this study, the apparent increasing trend disappears after spatial-standardisation was performed (Fig. 8b), supporting more-recent work (Close et al. 2020; Benson et al. 2025). The levelling effect of spatial-standardisation on the apparent positive trend in generic richness over the Cenozoic has recently been used as an argument in the case for using spatial-subsampling itself (Antell et al. 2024), in order to avoid potential false diversity peaks due to the ‘pull of the recent’ (Jablonski et al. 2003) and a seemingly increasing quality of the fossil record towards the present day (Benson et al. 2021).

However, within the described long-term stability, there are shorter-term variations in global FD between stages, common amongst the raw, standardised and spatially-standardised analyses. Firstly, there is little evidence of the K-Pg mass extinction in the global functional or generic diversity analyses (Figs. 5, 7 & 8). This was expected for functional diversity, given previous evidence of regional stability across the K-Pg itself (Whittle et al. 2019), and global stability in FD over the PTME (Foster & Twitchett 2014) and the LTME (Dunhill et al. 2018). There were also no permanent losses or gains in functional groups (MoLs) at any point over the study interval, including across the K-Pg boundary (*CH3_Supplementary_Material, S5*). This implies the K-Pg extinction did not represent global change in the ecospace occupation of marine invertebrates, supporting the results of Chapter 2 along with previous regional evidence from Whittle et al. (2019) and no net change in molluscan functional groups from Aberhan & Keissling (2015). However, the supported studies also observe a massive decline in taxonomic diversity across the K-Pg mass extinction, which is not reported here. This may be the culmination of both time-

averaging (Fürisch & Aberhan 1990) and a relatively rapid global recovery from the K-Pg (Birch et al. 2021). The estimated 0.1-1 Myr recovery period from the K-Pg, under varying definitions of ecosystem recovery (Alegret et al 2004; Lowery et al. 2018; Birch et al. 2021), would have taken 2.2 to 22% of the total duration of the Danian, which lasted ~4.4 Myr. Thus, occurrences from the remaining ~97-78% of the duration of the Danian likely masked the effect of the mass extinction when viewed at stage-level resolution. Time-averaging is less of an issue when examining mass extinctions with longer recovery periods, including the PTME where recovery likely spanned the majority or the entirety of post-extinction stages (Song et al. 2011; Chen & Benton 2012), and it is difficult to perform global analyses on finer temporal increments than stages (Kidwell 2013).

Between the Maastrichtian and Danian, the Bray-Curtis dissimilarity is the highest among raw values (0.750; Table 6) and the third highest when spatially subsampled (0.788; Table 7). This indicates a substantial generic turnover across the K-Pg boundary, more indicative of the ~50% estimated generic extinction (D'Hondt 2005). Additionally, the dissimilarity between the Maastrichtian generic composition and that of all subsequent stages increases incrementally from the Danian (Table 7), identifying the K-Pg as a turning-point from which global generic composition increasingly diverged from that of the Cretaceous. This has been previously reported on a regional scale in Antarctica, with a shift to modern invertebrate taxa across the boundary (Crame et al. 2014; Witts et al. 2016). In this respect, the K-Pg represents the origin of some elements of modern marine ecosystem structure; the identity and composition of taxa within global communities (Crame et al. 2014). However, a low functional dissimilarity between Maastrichtian-Danian implies the K-Pg did not cause a phase shift in community function, also supporting regional evidence (Aberhan & Kiessling 2015; Whittle et al. 2019). This result combined with the stability in trophic structure reported in the second chapter of this thesis, reiterates that modern marine community structure likely did not arise out of the K-Pg extinction.

The proportion of global genera within each MoL further exemplifies the taxonomic compositional shift across the K-Pg boundary, without change in the diversity of functional groups (Figs. 6 & 9). For example, the Campanian (Late Cretaceous) reported the largest proportion of global invertebrate genera in MoL 261; erect attached suspension-feeders, e.g. rudist bivalves, sponges and corals. Rudist reef-building bivalves became extinct at the K-Pg boundary (Jones et al. 1986), and the proportion of MoL 261 drops at this time, potentially linking to this extinction, along with the low diversity of Scleractinian corals during the Paleogene (Scheibner &

Speijer 2007). The proportion of MoL 115 (nektonic fast-moving predator) also sees a major drop across the K-Pg boundary - ammonites and belemnites became extinct and the MoL is thereafter only represented by Nautilus and soft-bodied cephalopods that do not preserve well (Krug 2009). Meanwhile, semi-infaunal and infaunal modes of life remain relatively stable over the entire interval including the K-Pg boundary (Fig. 9). This corroborates evidence found in burrowing ichnofossils, such as Zoophycos (Massalongo 1855), whose abundance remained unaffected by the K-Pg extinction perhaps because infaunality provides protection from environmental stress (Rodríguez-Tovar & Uchman 2006; Weist et al. 2016).

Gastropods are one of the most diverse clades of benthic marine invertebrates today (Sary & Pramod Kiran 2016). Gastropod-associated MoL, 325 (epifaunal slow-moving predator), becomes the largest component of global invertebrate genera from the Maastrichtian for the remainder of the entire study interval – at times encompassing over 25% of global invertebrate genera within stages (Fig. 9). Gastropod dominance is known to have occurred in the wake of the K-Pg extinction, whereby the predatory Neogastropoda proliferated in particular (Geiger 2006). Yet, the results here suggest predatory gastropods held the largest proportion of global genera in the preceding Maastrichtian (Fig. 9). However, the proportion of 325 increased further across the K-Pg boundary, into what was commonly seen across the remaining Cenozoic stages (Fig. 9). Nonetheless, this is perhaps evidence for emerging gastropod dominance prior to the K-Pg extinction, only increasing further post-extinction (Crame et al. 2014).

The relatively low values of functional and generic diversity in the Selandian and Thanetian (Middle-Late Paleocene) is more indicative of the extinction signal expected across the K-Pg boundary. However, the Selandian is by far the least-sampled stage in the study, with 121 collections compared to the mean of 1148 collections/stage in the interval (*LHW_CH3_Supplementary, S2 & S5*). Thus, the low raw and standardised Selandian functional and generic diversity measures are almost certainly artefacts of relatively poor sampling (Nanglu & Cullen 2023). Uneven spatial sampling effort is something that the divvy R package corrects for, (Antell et al. 2024), which could explain why mean SSFD does not report its lowest value in the Selandian, unlike RFD and SFD (Fig. 8a). As well as this, the Bray-Curtis Dissimilarity values indicate little change in invertebrate functional composition across the three stages of the Paleocene, with reasonable differences in generic composition (Table 7). This finds further support for a substantial K-Pg turnover in invertebrate genera, but little to no shift in community functional composition.

Furthermore, the Eocene epoch witnesses a sustained rise in global FD and GD, over the Ypresian, Lutetian, Bartonian and Priabonian stages (Figs. 5-8). The timing of this 'hump-like' rise coincides with the Early Eocene hyperthermal events, the Paleocene Eocene Thermal Maximum (PETM, ~55.8-55 Ma), the Early Eocene Climatic Optimum (EECO, ~53-51 Ma) and the Middle Eocene Climatic Optimum (MECO, ~40 Ma). These events represent the highest sustained temperatures identified within the Cenozoic Era (Kelly 2002; Stokke et al. 2020). Previously, the effects of these hyperthermals on macroinvertebrates have been poorly investigated. However, global-scale perturbation has been noted in microfossils; an extinction in deep-sea benthic foraminifera and poleward range shifts in planktic foraminifera, radiolaria and dinoflagellates during these events (Thomas & Shackleton 1996; Schneiber & Speijer 2005; Nwojiji et al. 2019; Foster et al. 2020; Li et al. 2020; Sarkar et al. 2022). By contrast, the positive global response in macroinvertebrate FD reported here is more similar to terrestrial cases of enhanced Eocene community function, such as sharply increased insect herbivory rates during the PETM (Currano et al. 2008). There is also Eocene evidence for the diversification of terrestrial and marine mammals, with at least 10 modern orders of Mammalia appearing during the Eocene (Rose 1984). This could be down to metabolic theory, which states that metabolic rates of organisms rise with increasing temperatures, in turn increasing evolutionary rates (Allen et al. 2006). Perhaps a similar diversification occurred in marine macroinvertebrates at this time, however the Bray-Curtis dissimilarity values do not imply a substantial generic turnover between stages of the Eocene, except slightly raised dissimilarity between Bartonian and Priabonian (Late Eocene, Table 7).

Alternatively, the Eocene increase in functional and generic diversity could also reflect an increase in habitat for marine macroinvertebrates across higher latitudes during the hyperthermals (Wing & Greenwood 1993; Willard et al. 2019). Sea-level rise occurred during the PETM (Sluijs et al. 2008) and it is thought Earth maintained largely ice-free conditions throughout the Early-Middle Eocene (Miller et al. 2020; Westerhold et al. 2020). A raised sea-level can increase continental shelf area (Rippeth et al. 2008), in turn increasing habitat size and complexity for invertebrates (Willard et al. 2019; de Juan et al. 2023). This, combined with an expanded tropical climate belt due to a shallower latitudinal temperature gradient in a greenhouse climate (Mittelbach 2007; Pross et al. 2012: Chaudhary et al. 2016), may have led to increased niche partitioning within a larger complex habitable area (Říha et al. 2025). Evidence of significantly amplified microfossil specialisation during the entire Eocene finds support for these results (Dominici & Zuschin 2016; Foster et al. 2020; Swain et al. 2024). Increased continental shelf area may not only drive

increased faunal diversity itself but also boost sedimentary rock deposition, known as the ‘common cause’ hypothesis (Peters 2006; He et al. 2020). This likely contributed to the observed increase in functional and generic richness, along with a genuine biological signal. Overall, these results find novel evidence for increased global macroinvertebrate functional and generic diversity coinciding with greenhouse world conditions that are punctuated with shorter periods of extreme hyperthermal conditions including the Early Eocene hyperthermal events.

However, the Eocene did not report positive effects for all marine invertebrates (Fig. 9). The proportion of global genera within the MoLs most-associated with reef-builders such as Scleractinian corals (i.e. 266, 261; erect attached other/suspension-feeder) were vastly reduced in the Bartonian (middle Eocene), together with an increase in proportion of gastropod-associated MoLs, 324 and 325 (epifaunal slow-moving grazers/predators, Fig. 9). This supports evidence for tropical coral reef collapse during the Eocene Epoch due to extreme heating and high temperatures, likely felt most-intensely in tropical climates (Weiss et al. 2025). Although, these results support evidence that global coral diversity recovered rapidly after the PETM (Weiss & Martindale 2019; Bosselini et al. 2025), and push coral reef collapse further into the Eocene than previously suggested, with less global disruption in reef-builder MoLs across the PETM and early Eocene than previous evidence suggests (Scheibner & Speijer 2008; Weiss et al. 2025).

The Bray-Curtis Dissimilarity values were at their lowest during the Eocene (Table 7), indicating the most consistent generic and functional compositions at any point in the study. This implies the PETM did not have significant negative impact on the global functional or generic composition of marine macroinvertebrates, supporting regional evidence in molluscs (Foster et al. 2020). Given that the PETM is compared to worst-case projected scenarios of warming under climate change (Meissner et al. 2014; Alley 2016), a lack of deleterious impact by this hyperthermal event on marine community function may be of significance. However, using the Ecospace Cube (Bambach et al. 2007) itself does not capture the full range of functional traits in certain taxa, particularly non-molluscan groups, and may mask functional changes. For example, Scleractinian corals almost exclusively fit into MoL 261 or 266 (erect attached suspension-feeder/other), but a recent study into coral life history strategies suggests hyperthermal Eocene reefs became dominated by stress-tolerant, slow-growing coral species adapted to marginal environments (Clay et al. 2025), effects masked using MoLs alone. However, the drop in MoLs most-associated with corals is noticeable particularly in the Mid-Eocene, Bartonian (Fig. 9).

Meanwhile, the Priabonian represents the beginning of a decline in functional and generic diversity from the Mid-Eocene high to a relatively lower global diversity across the Oligocene (Rupelian & Chattian). The Eocene-Oligocene Transition (EOT, ~34-33.6 Ma) represents the onset of long-term global cooling, probably due to a decline in atmospheric CO_2 (Hutchinson et al. 2021). Global scale cooling and onset of glaciation likely explain a major turnover in marine microfossils across the EOT, including extinction in planktic foraminifera, an increase in cold water taxa and a sharp decline in the abundance of larger-sized species (Prothero 1994; Coxall & Pearson 2007; Williams et al. 2007; Bordiga, 2015; Trejos et al. 2024). The Bray-Curtis Dissimilarity between the Priabonian and Rupelian, for generic composition (i.e. 0.691, Table 7) is evidence for a global turnover in macroinvertebrates during this time, not previously reported in literature. Meanwhile, a low dissimilarity for MoL composition (i.e. 0.220), finds stability in functional composition between the Eocene and Oligocene, despite taxonomic shifts.

As mentioned above, the Aquitanian (early Miocene) appears to be an anomalous result within the spatially-standardised data (Fig. 8). Aquitanian SSFD and SSGD are both very high, relative to the other stages in the interval, with no range in values. Meanwhile, Aquitanian RFD, RGD, SFD, and SGD are some of the lowest values recorded. With only 269 collections, as opposed to the mean of 1148.26 (2 d.p.) collections, the Aquitanian has the second lowest number of collections in the study. The parameters used for *divvy cookies()* spatial-subsampling function, i.e. nSite = 12, r = 2,000 km, could likely only subsample the same 12 sites repeatedly in the Aquitanian due to the geographical distribution of localities (*CH3_Supplementary, S2*), potentially also over-extrapolating these values (28.5 MoLs and 1728 genera), which would explain the anomalous result and the lack of range for this stage. As such, the Aquitanian SSFD and SSGD are disregarded from further interpretations because these intervals are too poorly sampled.

Excluding the Aquitanian, there appears to be a relatively small but sustained rise in functional diversity over the Langhian, Serravallian and Tortonian of the Miocene (Fig. 8c). The Miocene is characterised by continued global cooling, glaciation and sea-level fall (Halfar & Mutti 2005; von der Heydt & Dijkstra 2006). This sustained rise is not mirrored in generic diversity, besides a peak in the Serravallian, and this decoupling could be down to cold-water adapted taxa proliferating while warm-water taxa declined (Verducci et al. 2009). Sustained cooling likely decreased tropical habitat expanse, and simultaneous sea-level fall may have exposed shallow reefs (Halfar & Mutti 2005; von der Heydt & Dijkstra 2006), explaining the decrease

in proportion of global genera within reef-builder MoLs (261, 266) into the Serravallian, Tortonian and Messinian (Fig. 9). The Middle Miocene Climatic Transition (MMCT, ~14 Ma) was a particular cooling event that significantly increased polar ice-sheet volume (Pierce et al. 2017). Relatively high dissimilarity values for generic composition between each stage in the Miocene (0.666-0.875) indicate consistent turnover, perhaps linked with proliferations of cold-adapted taxa, as has been reported in microfossils (Verducci et al. 2009). However, once again it appears functional composition remained consistent despite taxonomic turnover, with dissimilarity values of between 0.145 and 0.437 between Miocene stages (Table 7).

Furthermore, the Messinian (latest Miocene) shows a relatively sharp decrease in functional and generic diversity, from the stages preceding (Tortonian) and succeeding it (Zanclean) (Fig. 7 & 8). Despite using global data, there is reason to believe the regional Messinian Salinity Crisis (MSC) influenced results (Roveri et al. 2008; 2014). The MSC took place in the Mediterranean, ~5.97-5.33 Ma (Agiadi et al. 2024a), whereby tectonic uplift of former gateways to the Atlantic disconnected the Mediterranean basin (Bulian et al. 2021; 2023). This caused strong salinity and temperature fluctuations, stratification of the Mediterranean water column and wide-scale salt deposition; over 1 million km^3 of gypsum was deposited during the MSC (Kontakiotis et al. 2022; Ebner et al. 2024). It has been postulated that the MSC, although a regional crisis, incited global declines in the species richness of molluscs (Monegatti & Raffi 2010) and marine mammals (Peredo & Uhen 2016). Not only this, but many Messinian PBDB invertebrate localities are distributed in and around the Mediterranean (*CH3_Supplementary_Material, S2*), perhaps an example of the 'bonanza' effect of sampling bias (Benton 2015), whereby locations and time intervals of particular interest are sampled more intensely than other localities. The Bray-Curtis Dissimilarity values point towards a particularly distinct assemblage of genera and MoLs within the Messinian, but a return to similar taxa and functional groups of the Tortonian by the Zanclean. Mediterranean species are believed to have extirpated to refugia in the Atlantic adjacent to the Mediterranean during the Messinian (Schwarzhans 2023; Aiello et al. 2024), only to return in the Zanclean with the 'Zanclean Flood' (Agiadi et al. 2024a; 2024b).

Finally, the Pliocene (Zanclean & Piacenzian) observes relative stability in both FD and GD in all measures (Figs. 5-8), despite Earth officially entering an 'icehouse' climate during this time. With a functional dissimilarity of 0.131, invertebrate functional composition remained almost unchanged across the Pliocene (Table 7). However, the Piacenzian increase in the proportion of gastropod-associated MoLs,

324 and 325, reflects the continued dominance of these modes of life in the later Cenozoic and modern benthic communities (Crame et al. 2014).

This study set out to investigate global patterns of marine invertebrate functional diversity (FD) from the Cretaceous to the Pliocene. The results indicate a remarkable long-term stability in FD between the Campanian and Piacenzian, with no directional trend through time. Some short-term variations persist after standardisation, most notably a sustained rise in the Eocene coinciding with Early Eocene hyperthermals, but these did not translate into long-term structural change. The minimal detectable effect of the K-Pg extinction on global functional or generic diversity reinforces the conclusion that this extinction, while transformative taxonomically, did not fundamentally reshape the functional structure of marine ecosystems. The absence of a long-term trend raises the question of whether marine invertebrate FD, as captured by modes of life (MoLs), may have reached a functional saturation point before the K-Pg boundary, as proposed by Mondal & Harries (2016), and contrary to suggestions of a continual Phanerozoic increase (Bambach et al. 2007). Alternatively, the apparent stability may reflect methodological limits: the Bambach Ecospace Cube, though effective for large-scale synthesis, may be too coarse to detect finer-grained functional shifts, particularly within diverse tropical assemblages.

3.4.2. Part B: Palaeolatitudinal Patterns of Functional Diversity

The most striking palaeolatitudinal diversity pattern is a consistent Northern Hemisphere mid-latitude peak (at 30-40˚N and/or 40-50˚N) in both the raw and spatially-standardised analyses, i.e. RFD, RGD, SSFD and SSGD (Figs. 10-20). This supports evidence of mid-latitude peaks in taxonomic diversity during greenhouse climates (Mannion et al. 2012; 2014) and provides novel evidence of the same for invertebrate MoL diversity as per Bambach et al. (2007). It is thought extreme greenhouse temperatures throughout Earth's history rendered equatorial zones less hospitable and instead subtropical/mid-latitude regions hosted the greatest diversity (Powell 2009; et al. 2012; Archibald 2010; Mannion et al. 2012; 2014). However, the results here also find a mid-latitude peak under both a warmhouse (Oligocene) and a coolhouse global climate in the Miocene (Westerhold et al. 2020), in both functional and generic diversity. Only true icehouse conditions have been associated with equatorial peaks in the literature to date (Mannion et al. 2014; Zhang et al. 2022), so perhaps a shallower coolhouse temperature gradient is less conducive to producing

a single equatorial peak in biodiversity than the steeper temperature gradient of a true icehouse regime.

Conversely, there is compelling evidence to suggest mid-latitude diversity peaks in the fossil record are mostly artefacts of sampling bias, driven by socio-economic inequality (Vilhena & Smith 2013; Close et al. 2020; Raja et al. 2022; Benson et al. 2025). For centuries, there has been more-intense sampling in Europe and North America than in other regions, skewing the spatial distribution of fossil taxa towards these zones (Raja et al. 2022). The distribution of fossil localities in Figs.10-14 indicate a strong European and North American influence on all stages. Benson et al. (2025), found that northern mid-latitude diversity peaks diminish after using a novel spatial-standardisation method that accounts for historic over-sampling, which provides evidence for the authors to strongly dismiss the existence of a true northern mid-latitude diversity peak in the fossil record.

Nevertheless, there also exists a 30-40˚S or 40-50˚S peak in functional and generic diversity in epoch level analyses and thus a mid-latitude peak is not only observed in the global north (Figs. 19 & 20). Evidence suggests the tropical climate belt during the Late Cretaceous and early Cenozoic was 40-50% larger than it is today, extending at times to palaeolatitudes of ~60°N/S (Morely et al. 2007; Pross et al. 2012; Crame 2020). Expansive tropics likely cultivated true mid-latitude peaks in functional and generic diversity, that is, if diversity distribution is indeed coupled with temperature and seasonality as is the current consensus (Roy et al. 2000; Jablonski et al. 2006; 2008; Mittelbach et al. 2007; Mannion et al. 2014; Saupe et al. 2019a; 2019b). Under a greenhouse climate, throughout the Late Permian to the Middle Triassic, terrestrial tetrapods display bimodal latitudinal diversity peaks (Mannion et al. 2012; Bernardi et al. 2018; Allen et al. 2020), and insects report a mid-latitude peak during the hothouse Eocene (Archibald 2010). The results here could be interpreted as tentative evidence for true mid-latitude peaks in the Southern and Northern Hemispheres, similar to the global bimodal diversity pattern in a greenhouse climate (Mannion et al. 2014). With that being said, the Southern Hemisphere often shows lower raw values than analogous Northern Hemisphere palaeolatitude bins (Figs. 10-14). As such, there was insufficient data to run spatial subsampling in any ˚S bins at stage level which ties to systematic sampling bias towards Europe and N. America (Close et al. 2020). Even at epoch level, most Southern Hemisphere localities appear in the latitude bins of 30-40˚S and 40-50˚S in Australia or South America (Figs. 10-14), often with gaps in the other palaeolatitudes – revealing potential cases of socio-economic inequality resulting in points of bias within the Southern Hemisphere.

It is difficult to investigate shifts in the palaeolatitudinal pattern of SSFD from the Campanian to the Piacenzian, due to the number of gaps in the stage level analyses (Figs. 15 & 16). However, the Cenozoic stages with SSFD values for at least five of the six palaeolatitude bins used (˚N), including the Ypresian (earliest Eocene), Priabonian (latest Eocene), Rupelian (Oligocene) and the Burdigalian (early Miocene), all report a pattern not too dissimilar from that observed in the Late Cretaceous. This pattern is a mid-latitude peak around 30-40˚N and/or 40-50˚N, a minimum value in 20-30˚N and a smaller peak around 10-20˚N and/or 0-10˚N (Figs. 15 & 16). The high values of SSFD in mid-latitude bins in these stages is further evidence for a mid-latitude peak in diversity during greenhouse (Eocene) climates (Powell et al. 2012) and, as mentioned, provides evidence for the same in a warmhouse (Oligocene) and a coolhouse (Miocene) climate. However, it is equally likely that these results instead reinforce the pervasive sampling bias at these latitudes, even after a cutting-edge spatial-standardisation method, i.e. *divvy* (Antell et al. 2024). This is a problem previously described by Jones et al. (2021), who state that while standardisation within latitude bands aids the reconstruction of latitudinal gradients, it cannot entirely account for absences introduced by geological and anthropogenic biases.

Spatially-standardised functional diversity (SSFD) retains the observed 40-50˚N mid-latitude peak, over the stages of the Eocene, despite gaps (Fig. 15). This coincides with the Paleocene-Eocene Thermal Maximum (PETM, ~55.8-55 Ma), the Early Eocene Climatic Optimum (EECO, ~53-51 Ma) and the Middle Eocene Climatic Optimum (MECO, ~40 Ma) (Kelly 2002; Stokke et al. 2020). These results find stability in functional diversity across latitude, over the hottest temperatures recorded in the Cenozoic Era (Stokke et al. 2020). The sustained rise in global FD observed over the Eocene (Part A, Fig. 8) does not appear to affect the latitudinal distribution of FD in the Northern Hemisphere. The potential influence of sampling bias on the latitudinal distribution of FD cannot be ignored here either. Meanwhile, the peak in SSGD shifts from 30-40˚N in the Ypresian to 40-50˚N in the remaining Eocene stages (Figs.17 & 18). This may indicate a poleward movement of macroinvertebrates due to extreme oceanic heating and high temperatures at this time, previously only reported in microfossils such as planktic foraminifera (Nwojiji et al. 2019; Foster et al. 2020; Li et al. 2020; Sarkar et al. 2022).

Meanwhile, the opposite occurs across the Eocene-Oligocene boundary (Priabonian to Rupelian): an equatorward shift in peak generic diversity, from 40-50˚N in the Priabonian to 30-40˚N in the Rupelian (Figs. 17 & 18). This may be indicative

of the global cooling occurring during and after the EOT (Westerhold et al. 2020), and perhaps an equatorward shift in both macroinvertebrate taxa and the 'cradle of life' itself, i.e. the zone of peak origination at the time (Jablonski et al. 2006). Unlike generic diversity, functional diversity maintains a mid-latitude peak across the EOT, and the highest Rupelian mean SSFD value is reported in the 50-60˚N bin, perhaps a result of polar functional groups expanding during later Cenozoic cooling (Crame 2023). The drop in SSGD in 0-10˚N between the Priabonian and the Rupelian (Figs. 17 & 18) finds support for microfossil evidence that the EOT was felt most-keenly at the lower latitudes where warm-water taxa suffered while their cold-water counterparts thrived (Oleinik & Marincovich 2003), although this again did not occur in SSFD. Invertebrate functional diversity once again exhibits stability over time and space, during a time that saw the taxonomic composition of marine communities dramatically shift, e.g. the divergence of pinnipeds from other mammals, archaeocetes replaced by modern whales (Uhen, 2010; Hull 2015), and the widescale radiation of diatoms (Rabosky & Sorhannus 2009).

The Aquitanian is missing from spatially-standardised analyses due to insufficient data. However, the following Burdigalian retains a mid-latitude (30-40˚N) functional diversity peak and a smaller peak at 10-20˚N, suggesting stability of the latitudinal distribution of FD into the Miocene despite global cooling and tectonic movement (Westerhold et al. 2020). The Langhian coincides with the Mid-Miocene Climate Transition (MMCT, ~14 Ma) a period of intense cooling and significant increase in polar ice-sheet volume (Mourik 2010; Pierce et al. 2017). The single Langhian [40-50˚N] bin shows comparable SSFD and SSGD values to those seen at 40-50˚N in other stages: ~15 MoLs and 250 genera, suggesting at least mid-latitude stability in FD in the Northern Hemisphere, despite a global cooling event that left its mark in other ways, one example being a shift in foraminiferal communities from warm-water to cold-adapted taxa at ~54˚S Kerguelen plateau (Verducci et al. 2009).

The Messinian Stage in the global analyses (Part A) shows a drop in functional and generic diversity relative to the stages preceding and following it (Fig. 8) along with a unique composition of genera and MoLs (Table 7). Given the Mediterranean distribution of many fossil localities, the Messinian Salinity Crisis (MSC) may have influenced global results. Across palaeolatitude, the Messinian shows maximum SSFD in, 10-20˚N, despite gaps, which is closer to the equator than other stages. Studies suggest the MSC led to an extirpation of Mediterranean marine fauna in the Atlantic, perhaps taking functional diversity from Mediterranean latitudes (i.e. 30-40˚N) with it (Agiadi et al. 2024a; 2024b). This would also explain the reduced SSGD

values at 30-40˚N in the Messinian (Figs. 8 &18). However, this lower latitude peak in SSFD does not last into the Pliocene, and both the Zanclean and Piacenzian return to peak SSFD at 40-50˚N. This could represent the return of Mediterranean taxa following the 'Zanclean flood' (Agiadi et al. 2024a) or is perhaps due to a less-Mediterranean distribution of fossil localities during this stage.

The existence of a modern Latitudinal Functional Diversity Gradient (LFDG) akin to the LDG, has not been previously reported. This is in part due to the subjective definition and scale of functional diversity (Laureto et al. 2015). Therefore, how and when a potential LFDG may have formed relative to the modern LDG also remains a mystery. Here, there is tentative evidence for a bimodal Northern Hemisphere pattern in functional diversity, with a substantial mid-latitude peak (around 40-50˚N and/or 30-40˚N) and smaller tropical peak (10-20˚N). This is seen in stages with sufficient data in the Late Cretaceous, Eocene, Oligocene and Miocene, i.e. consistent across deep time, major climate events and K-Pg mass extinction (Figs. 15 & 16). This bimodal pattern supports a pattern of similar shape reported in the FD of marine zooplankton in modern oceans (Tang et al. 2022; Ge et al. 2024), although based on different functional metrics. There is also regional evidence for what resembles a Miocene mid-latitude peak in gastropod functional richness ~45˚S (Grossman et al. 2022). Although, with no mention of standardisation (Grossman et al. 2022), the input of sampling bias cannot be ignored here.

However, Berke et al. (2014), Grossman et al. (2022) and Woodhouse et al. (2023), find an overall decrease in molluscan and foraminiferal functional richness with increasing latitude. An obvious decrease in FD with latitude is only reported here between 40-50˚N and 50-60˚N, observed in every stage from the Aquitanian (early Miocene) onwards. The early-Miocene is perhaps a turning-point in global cooling, whereby the global temperature gradient steepened to the extent that 50-60˚N became too cold to support a similar functional diversity to lower latitudes. Overall, there is little to no evidence here for an LFDG of the same shape as the modern Latitudinal [Species] Diversity Gradient (LDG) in marine macroinvertebrates, i.e. a single tropical peak in FD declining with latitude, as reported in modern bivalves and microfossils (Berke et al. 2014; Grossman et al. 2022; et al. 2023). Instead, there is evidence for a bimodal Northern Hemisphere LFDG as described, consistent in stages of the Late Cretaceous, Eocene, Oligocene and Miocene.

The exact nature and timing of the formation of the modern LDG remains debated (Mannion et al. 2014; Crame 2001; et al. 2014; 2020; Fenton et al. 2023). A post-K/Pg early Cenozoic radiation, most intense in the tropics, is cited as a

contributing factor to forming the LDG (Crame 2014; 2020). Consistent cooling from the EOT (~34 Ma) onwards is another possible driver, forcing warm-water species into lower latitudes, (Zachos et al. 2001; 2008; Mannion et al. 2014; Crame 2020), as well as shifting the latitude of the cradle of life (Jablonski et al. 2006). There is microfossil evidence that the modern LDG can be identified from the Langhian (~15 Ma) onwards (Fenton et al. 2023). By contrast, the results here find even later evidence for the origin of the modern LDG. By the Tortonian (~11.6-7.2 Ma), Zanclean (~5.33-3.6 Ma) and Piacenzian (~3.6-2.58 Ma), there is tentative evidence for a tropical peak equal-to or greater-than the mid-latitude peak in generic diversity, albeit in raw analyses only (Figs. 13 & 14). Meanwhile, spatially-standardised generic diversity at stage level, shifts equatorward by the Zanclean (Fig. 17) decoupling with functional diversity at this point. At epoch resolution this pattern is reinforced; Pliocene SSGD in 0-10˚N and 10-20˚N are larger peaks than 40-50˚N (Fig. 20). However, the same is not observed in the functional diversity of the Pliocene, which retains its largest value in 40-50˚S followed by 40-50˚N and a relatively small peak in 0-10˚N by comparison (Fig. 19). This is tentative evidence of a modern LDG forming by the Pliocene, not accompanied by an LFDG, at least of the same shape of a tropical peak in diversity. These results find a decoupling of functional and generic diversity across latitude over a period of extreme global cooling and steepening of the latitudinal temperature gradient, supporting modern instances where functional diversity does not follow the LDG, e.g. in new-world bats (Stevens et al. 2003) and as mentioned in zooplankton (Tang et al. 2022; Ge et al. 2024). These results reiterate that no macroinvertebrate LFDG had formed into the same pattern as the modern LDG by the Late Pliocene. This decoupling is evidence of a higher level of stability in functional diversity across latitude over deep time compared to taxonomic diversity. Functional stability has been noted globally across major biotic events including mass extinctions (Foster & Twitchett 2014; Dunhill et al. 2018) and the major Cenozoic climate and biotic events in Part A (Figs. 6-8).

These results provide evidence for long-term stability in marine invertebrate functional diversity across latitude and a tentative latitudinal functional diversity gradient (LFDG) in the Northern Hemisphere from the Late Cretaceous to the Late Pliocene. This LFDG pattern, characterised by a consistent mid-latitude peak in FD (around 30-40 or 40-50°N), a smaller tropical peak (10-20°N), and a relative low at 20-30°N, appears decoupled at times from taxonomic diversity (LDG). The persistence of this LFDG across major climatic and biotic transitions, including the K-Pg extinction, the Early Eocene hyperthermal events, and the long-term shift towards

an icehouse world following the EOT (Westerhold et al. 2020) suggests a remarkable functional stability in marine communities despite substantial taxonomic turnover.

However, these findings must be interpreted with caution. Sampling bias and inherent uncertainty in fossil interpretation make it difficult to disentangle genuine ecological patterns from artefacts of preservation and rock availability (Benton et al. 2011; Jones et al. 2021; Benson et al. 2025). Moreover, methodological limitations of Bambach et al. (2007) Ecospace Cube may underestimate tropical functional diversity. The cube's relatively coarse trait resolution, particularly for non-shelly taxa, risks underrepresenting groups that dominate low-latitude ecosystems, such as scleractinian corals and sponges, which exhibit high ecological and morphological diversity not easily captured by broad ecospace categories. This underestimation could artificially flatten tropical FD estimates, exaggerating the mid-latitude peak reported here. The 'latitude-niche breadth hypothesis' (Vázquez & Stevens 2004) predicts that decreased seasonality in the tropics leads to more stable populations, which in turn evolving smaller niches, therefore allowing more species to coexist in the tropics than at higher latitudes (Vázquez & Stevens 2004; Cirtwill et al. 2015). The Ecospace Cube tends to favour broader, more generalised modes of life common at higher latitudes where niches are perhaps more distinct (Bambach et al. 2007). Consequently, while the observed bimodal Northern Hemisphere LFDG may reflect a genuine ecological signal, it is also possible that methodological and preservational biases collectively obscure a stronger tropical FD peak. Despite these uncertainties, the overarching result remains clear: a palaeotemperate FD peak persisted throughout the entire interval at both stage and epoch resolution and this decoupled from that of GD by the end of the interval.

Chapter 4 – Discussion

4.1 The K-Pg is not the likely origin of modern marine ecosystem structure

The results presented in Chapters Two and Three demonstrate that the Cretaceous-Palaeogene (K-Pg) mass extinction did not permanently alter the trophic structure or functional diversity of marine communities, despite pronounced shifts in taxonomic composition and identity. This outcome, derived from reconstructed regional trophic meta-webs in the Antarctic (Fig. 3) and global analyses of macroinvertebrate functional diversity (FD, Fig. 8) challenges the idea that the K-Pg event marked the origin of the 'modern' marine community structure (Dunne et al. 2014). Instead, while taxonomic upheaval was substantial, the fundamental ecological architecture of

marine systems appears to have persisted across the boundary. The K-Pg extinction did, however, lead to the proliferation of the identity and composition of modern marine taxa, as seen occupying the trophic network nodes in Chapter Two and supported by previous studies (Uhen 2010; Crame et al. 2014; Hull et al. 2015; Whittle et al. 2019). The K-Pg also led to a shift in the proportion of taxa within each mode of life as seen in the global analyses in Chapter Three, with the gastropod-associated MoLs becoming the largest global proportion (Figs. 6 & 9). This is reflected by an increased Bray-Curtis dissimilarity in generic composition across the boundary (Bray & Curtis 1957). Yet, despite these taxonomic disruptions, trophic organisation remained strikingly stable, providing support for the conclusions of Yeakel and Dunne (2015), at least as early as the Late Cretaceous. Yeakel and Dunne (2015) stated that the core structural principles of marine food webs have potentially endured since the Cambrian, largely invariant to even the most catastrophic biotic crises.

The lack of change across the K-Pg in both Antarctic trophic structure and net global macroinvertebrate functional diversity finds further evidence of the skeleton crew hypothesis, coined by Foster & Twitchett (2014) and further supported by Dunhill et al. (2018). As explained earlier, the skeleton crew hypothesis posits that functional diversity remained stable across previous major extinctions in Earth's history due to a high level of functional redundancy which afforded the loss of most taxa without the loss of significant numbers of guilds or ecosystem function (Foster & Twitchett 2014; Dunhill et al 2018). Together, these results reinforce the view that marine ecosystem functioning is decoupled from taxonomic diversity during mass extinctions and suggest the persistence of key functional guilds enables rapid ecological recovery.

4.2 No directional trend in functional diversity between the Late Cretaceous and the Late Pliocene, but shorter-term variation between stages

The results in Part A of Chapter Three reveal long-term stability in global marine invertebrate FD from the Cretaceous–Palaeogene (K-Pg) boundary through to the Late Pliocene. Although some stage-to-stage fluctuations are evident, there is no evidence for a sustained directional trend in FD. This challenges previous interpretations of a continual, Phanerozoic-scale rise in ecological complexity and functional diversity since the Cambrian (Bambach et al. 2007; Bush et al. 2007).

Short-term deviations in FD correspond with key climatic perturbations. For example, the Early to Late Eocene shows a pronounced increase in FD, coinciding with the major hyperthermal events of the Palaeogene, the PETM, EECO, and MECO which represent the warmest intervals of the Cenozoic (Smith et al. 2010; Giorgioni

et al. 2019; Inglis et al. 2020). This pattern provides the first global evidence for a net rise in both functional and generic diversity across these events, extending beyond the previously reported stability of molluscan faunas in regional records (Foster et al. 2020). Importantly, these results suggest that, at the coarse resolution of the fossil record, marine ecosystems demonstrated functional resilience to rapid warming. Nevertheless, this apparent stability should not be conflated with modern trends: the current rate of anthropogenic CO_2 release is an order of magnitude greater than calculated during the PETM, compounded by habitat destruction, overfishing, and pollution (Zebre et al. 2016; Babila et al. 2018; Thomas & St John 2025).

While the marine macroinvertebrate fossil record represents the most comprehensive record for reconstructing community evolution, this study also underscores its limitations of uneven sampling, preservational biases, and time-averaging. Yet, the evidence indicates no evidence for a fundamental restructuring of global ecosystem function during the interval, despite clear taxonomic turnover towards more modern assemblages.

4.3 There may be a latitudinal functional diversity gradient (LFDG), however sampling bias remains a constant problem

The results presented in Part B of Chapter Three provide compelling evidence for a bimodal latitudinal functional diversity gradient (LFDG) in the Northern Hemisphere. This pattern is characterised by a consistent mid-latitude (30-40˚N/40-50˚N) peak, a pronounced lows at 20-30˚N and often 0-10˚N, with a smaller secondary peak in between (10-20˚N). This pattern persists from the Late Cretaceous to the Pliocene, remaining largely stable despite stage-to-stage fluctuations in global functional diversity and the occurrence of extreme hyperthermal events during this interval.

Importantly, this tentative LFDG is at times decoupled from generic diversity patterns, most notably during the Piacenzian, when a modern-style latitudinal diversity gradient (LDG) emerges, yet the LFDG retains its mid-latitude peak (Figs. 15 & 17). A similar decoupling is evident at the epoch scale in the Pliocene (Figs. 19 & 20), reinforcing this conclusion with a substantially larger dataset. Together, these results indicate that functional and taxonomic diversity were not necessarily aligned through deep time, suggesting that the ecological processes structuring marine communities may have evolved independently of taxonomic richness.

While the persistence of a mid-latitude functional diversity peak could reflect spatial sampling bias (Benson et al. 2025), the consistent decoupling from generic

diversity implies that this may instead represent a genuine ecological signal. It is possible that the Bambach Ecospace Cube's coarse resolution, particularly its underrepresentation of non-molluscan taxa, may accentuate a mid-latitude peak by underestimating tropical groups with finer niche partitioning, such as Scleractinia.

Modern LFDG studies remain limited and primarily focus on planktonic or microbial assemblages (e.g. Gilbert et al. 2010; Becker et al. 2021). Consequently, direct comparisons with fossil macroinvertebrate datasets are challenging. The findings presented here therefore represent one of the first palaeontological demonstrations of a tentative LFDG, providing a potential baseline for understanding how a functional diversity gradient evolved through geological time and how this may relate to the emergence of modern marine ecosystem structure.

4.4 Avenues for further research

Chapter Two in this study concludes the K-Pg mass extinction did not permanently alter the trophic structure and function of the Seymour Island marine community. Further research avenues include to assess this result in more locations, if there are sufficient fossil outcrops with a K-Pg record and minimal changes in preservation conditions across the boundary. As well as this, to search for the origin of modern marine trophic organisation or structure, research needs to examine the Phanerozoic prior to the Late Cretaceous. Trophic meta-web reconstructions across events such as the Great Ordovician Diversification Event (GOBE), the Permian-Triassic mass extinction (PTME) and the Mesozoic Marine Revolution (MMR) could represent potential origins of the modern range of structural network metrics observed in both modern webs and those across the K-Pg in this study.

Additionally, topological food web models, such as the PFIM (Shaw et al. 2023), are good for comparative studies of network structure and function using the metrics and motifs calculated. However, they do not incorporate interaction strengths, energy flows, and population dynamics. If possible, use of a dynamic trophic model for the same reconstructions across the K-Pg boundary, may identify nuanced differences in the marine community across the extinction. Dynamic webs represent networks as systems of differential equations describing biomass, abundance and energy flux (Blanchard et al. 2009; Gauzens et al. 2019). Using such a model would allow for more-detailed insights into changes to interaction strengths, abundance, extinction risks, and energy flow across the K-Pg boundary (Bellingeri and Bodini 2013; Nilsson & McCann 2016).

Furthermore, this study reiterates the constant influence of sampling bias on perceived fossil diversity patterns, despite using cutting-edge spatial standardisation methods (e.g. Antell et al. 2024). As well as this, using marine macroinvertebrates, i.e. potentially the best macrofossil record available, there remained gaps in palaeolatitude bins throughout the study interval, particularly in the Southern Hemisphere, as well as the Aquitanian - which lacked sufficient data to run spatial standardisation at all. Thus, it stands to recommend further research, sampling and existing collections and data to be uploaded to databases for under-studied locations. Focused study could shed light on whether there have existed true mid-latitude diversity peaks at times during Earth's history, most likely greenhouse climate regimes (Mannion et al. 2014). Alternatively, further exploration could instead resolve if the apparent peaks are solely down to sampling bias (Benson et al. 2025).

Finally, chapter three highlights both the benefits and caveats of the Bambach Ecospace Cube (Bambach et al. 2007), with its coarseness providing an ease of use on large datasets, albeit potentially grouping certain taxa into one mode of life and dampening their functional diversity. Perhaps it is too difficult to capture more functions of invertebrate clades all within one method such as in Bambach et al. (2007), but if done this could lead to an improved understanding of marine functional diversity across time and space in the fossil record.

4.5 Final Conclusions

Overall, the findings of this thesis demonstrate that the structure and function of marine communities have shown long-term stability across one of the most profound transitions in Earth's history, the Cretaceous–Palaeogene (K-Pg) mass extinction and the ensuing Cenozoic climate transition. Contrary to previous ideas suggesting that the K-Pg marked a turning point in marine ecosystem organisation, the results presented here reveal no permanent restructuring of trophic or functional networks and instead indicate that ecosystem function was resilient amid substantial taxonomic turnover, an example of the skeleton crew hypothesis (Foster & Twitchett 2014). Moreover, the persistence of a mid-latitude functional diversity peak throughout the Cenozoic, at times decoupled from patterns of taxonomic richness, suggests that FD may have been governed by environmental and ecological constraints distinct from those shaping species distributions.

The fossil record of marine macroinvertebrates remains arguably the most comprehensive archives of ecological and evolutionary changes available. Yet, as

this thesis highlights, even this record is riddled with gaps, biases, and uneven sampling, and as such reconstructions of ancient ecosystems remain uncertain. Despite these challenges, the analyses presented here demonstrate that meaningful ecological signals can still be extracted using functional approaches, providing new perspectives on stability across mass extinction and recovery intervals. These findings carry significant implications for understanding the origins of modern marine community structure and function, highlighting that structural and functional stability can persist despite major biodiversity crises and climatic perturbations. They also highlight the importance of incorporating functional and network-based approaches alongside traditional taxonomic metrics in deep-time studies to better capture ecological signals through extinction and recovery. In doing so, we can understand not only how modern marine ecosystems arose, but also how resilient they may be to the unprecedented environmental changes of the present and future oceans.

5. Bibliography

Aberhan, M. Weidemeyer, S. Kiessling, W. Scasso, R.A. and Medina, F.A. 2007. Faunal evidence for reduced productivity and uncoordinated recovery in Southern Hemisphere Cretaceous-Paleogene boundary sections. *Geology*, **35**(3), pp.227-230.

Aberhan, M. and Kiessling, W. 2015. Persistent ecolognanical shifts in marine molluscan assemblages across the end-Cretaceous mass extinction. *PNAS*, **112**(23), pp.7207–7212.

Agiadi, K. Hohmann, N. Gliozzi, E. Thivaiou, D. Bosellini, F.R. Taviani, M. Bianucci, G. Collareta, A. Londeix, L. Faranda, C. and Bulian, F. 2024a. The marine biodiversity impact of the Late Miocene Mediterranean salinity crisis. *Science*, **385**(6712), pp.986-991.

Agiadi, K. Hohmann, N. Gliozzi, E. Thivaiou, D. Bosellini, F.R. Taviani, M. Bianucci, G. Collareta, A. Londeix, L. Faranda, C. and Bulian, F. 2024b. Late Miocene transformation of Mediterranean Sea biodiversity. *Science Advances*, **10**(39), p.eadp1134.

Agustí, J. Cabrera, L. and Garcés, M. 2013. The Vallesian mammal turnover: A Late Miocene record of decoupled land-ocean evolution. *Geobios*, **46**(1-2), pp.151-157.

Aiello, G. R. Parisi, R. Barbieri, D. and Barra. 2024. Late Miocene palaeobiogeography of the Mediterranean–Atlantic Region: An analysis based on self ostracod assemblages of the Northwestern Morocco. *Palaeogeography. Palaeoclimatology. Palaeoecology*, **643** (1), 112155.

Alegret, L. Kaminski, M.A. and Molina, E. 2004. Paleoenvironmental recovery after the Cretaceous/Paleogene boundary crisis: evidence from the marine Bidart section (SW France). *Palaios*, **19**(6), pp.574-586.

Aller, R. C. 2001. Transport and reactions in the bioirrigated zone. *In The Benthic Boundary Layer: Transport Processes and Biogeochemistry*, pp. 269-301. Oxford University Press.

Allen, B.J. Oliveira, M.V.V. Stadler, T. Vaughan, T.G. and Warnock, R.C. 2024. Mechanistic phylodynamic models do not provide conclusive evidence that non-avian dinosaurs were in decline before their final extinction. *Cambridge Prisms: Extinction*, **2**, p.e6.

Allen, A. P. Gillooly, J. F. Savage, V. M. and Brown, J. H. 2006**.** "Kinetic effects of temperature on rates of genetic divergence and speciation." *Proceedings of the National Academy of Sciences*, **103**(24), pp.9130–9135.

Allesina, S. Alonso, D. and Pascual, M. 2008. A general model for food web structure. *Science*, **320**(5876), pp.658-661.

Allesina, S. and Levine, J.M. 2011. A competitive network theory of species diversity. *Proceedings of the National Academy of Sciences*, **108**(14), pp.5638-5642.

Alley, R.B. 2016. A heated mirror for future climate. *Science*, **352**(6282), pp.151-152.

Alroy, J. 2008. Dynamics of origination and extinction in the marine fossil record. *Proceedings of the National Academy of Sciences*, **105**(supplement_1), pp.11536-11542.

Alroy, J. Aberhan, M. Bottjer, D.J. Foote, M. and Harries, P.J. *et al*. 2008. Phanerozoic trends in the global diversity of marine invertebrates. *Science*, **321**, pp.97-100.

Alroy, J. 2010. Geographical, environmental and intrinsic biotic controls on Phanerozoic marine diversification. *Palaeontology*, **53**, pp.1211–1235.

Alvarez, L.W. Alvarez, W. Asaro, F. and Michel, H.V. 1980. Extraterrestrial cause for the Cretaceous-Tertiary extinction. *Science*, **208**(4448), pp.1095–1108.

Antell, G.T. Kiessling, W. Aberhan, M. and Saupe, E.E. 2020. Marine biodiversity and geographic distributions are independent on large scales. *Current Biology*, **30**(1), pp.115-121.

Antell, G.S. and Saupe, E.E. 2021. Bottom-up controls, ecological revolutions and diversification in the oceans through time. *Current Biology*, **31**(19), pp.1237-1251

Antell, G.T. Benson, R.B. and Saupe, E.E. 2024. Spatial standardization of taxon occurrence data—a call to action. *Paleobiology*, **50**(2), pp.177-193.

Archibald, S.B. 2010. Seasonality, the latitudinal gradient of diversity, and Eocene insects. *Paleobiology*, **36**, pp.374-398.

Arthur, M.A. Zachos, J.C. and Jones, D.S. 1987. Primary productivity and the Cretaceous/Tertiary boundary event in the oceans. *Cretaceous Research*, **8**(1), pp.43-54.

Araújo, M.S. and Costa-Pereira, R. 2013. Latitudinal gradients in intraspecific ecological diversity. *Biology Letters*, **9**(1), 20120778.

Babila, T.L. Penman, D.E. Standish, C.D. Doubrawa, M. Bralower, T.J. Robinson, M.M. Self-Trail, J.M. and Speijer, R.P. *et al*. 2022. Surface ocean warming and acidification driven by rapid carbon release precedes Paleocene-Eocene Thermal Maximum. *Science Advances*, **8**(11), p.eabg1025.

Bambach, R.K. Knoll, A.H. And Wang, S.C. 2004.Origination, extinction, and mass depletions of marine diversity. *Paleobiology*, **30**, pp.522–542

Bambach, R.K. 2006. Phanerozoic biodiversity mass extinctions. *Annual Review of Earth and Planetary Sciences*, **34**, pp.127-155.

Bambach, R.K. Bush, A.M. and Erwin, D.H. 2007. Autecology and the filling of ecospace: key metazoan radiations. *Paleontology,* **50**(1), pp.1-22.

Banker, R.M. Dineen, A.A. Sorman, M.G. Tyler, C.L. and Roopnarine, P.D. 2022. Beyond functional diversity: the importance of trophic position to understanding functional processes in community evolution. *Frontiers in Ecology and Evolution*, **10**, p.983374.

Bardet, N. 1994. Extinction events among Mesozoic marine reptiles. *Historical Biology*, **7**(4), pp.313-324.

Beck Eichler, P.P. and Barker, C.P. 2020. *Microfossil shells are carbon story tellers: microfossil communities: first responders to environmental impacts.* In Benthic Foraminiferal Ecology: Indicators of Environmental Impacts (pp. 49-70). Cham: Springer International Publishing.

Becker, C. Dias, C.O. Licandro, P. and Dias-Brito, D. 2021. Latitudinal gradient of copepod functional diversity in the South Atlantic Ocean. *Progress in Oceanography*, **190**, 102483.

Bellingeri, M. and Bodini, A. 2013. Threshold extinction in food webs. *Theoretical ecology*, **6**(2), pp.143-152.

Benson, R.B. Butler, R. Close, R.A. Saupe, E. and Rabosky, D.L. 2021. Biodiversity across space and time in the fossil record. *Current Biology*, **31**(19), pp.R1225-R1236.

Benson, R.B. Close, R.A. Antell, G.T. Whittaker, R.J. Valdes, P. Farnsworth, A. and Lunt, D.J. *et al*. 2025. Marine animal diversity across latitudinal and temperature gradients during the Phanerozoic. *Palaeontology*, **68**(3), p.e70006.

Benton, M.J. 1995. Diversification and extinction in the history of life. *Science*, **268**(5207), pp.52-58.

Benton, M.J. Dunhill, A.M. Lloyd, G.T. and Marx, F.G. 2011. Assessing the quality of the fossil record: insights from vertebrates.

Benton, M.J. 2018. Hyperthermal-driven mass extinctions: killing models during the Permian–Triassic mass extinction. *Philosophical Transactions of the Royal Society A: Mathematical, Physical and Engineering Sciences*, **376**(2130), p.20170076.

Benton, M.J. 2015. Palaeodiversity and formation counts: redundancy or bias? *Palaeontology*, **58**(6), pp.1003-1029.

Berke, S.K. Jablonski, D. Krug, A.Z. and Valentine, J.W. 2014. Origination and immigration drive latitudinal gradients in marine functional diversity. *PLoS One*, **9**(7), p.e101494.

Bernardi, M. Petti, F.M. and Benton, M.J. 2018. Tetrapod distribution and temperature rise during the Permian–Triassic mass extinction. *Proceedings of the Royal Society B: Biological Sciences*, **285**(1870), p.20172331.

Bersier, L.F. Banašek-Richter, C. and Cattin, M. F. 2002. Quantitative descriptors of food-web matrices. *Ecology,* **83**(9), pp.2394-2407.

Birch, H. Schmidt, D.N. Coxall, H.K. Kroon, D. and Ridgwell, A. 2021. Ecosystem function after the K/Pg extinction: decoupling of marine carbon pump and diversity. *Proceedings of the Royal Society B*, **288**(1953), p.20210863.

Blanchard, J.L. 2015. A rewired food web. *Nature,* **527**(7577), pp.173-174.

Blanchard, J.L. Jennings, S. Law, R. Castle, M.D. McCloghrie, P. Rochet, M.J. and Benoît, E. 2009. How does abundance scale with body size in coupled size-structured food webs?. *Journal of Animal Ecology*, **78**(1), pp.270-280.

Bohaty, S. M. and Zachos, J. C. 2003. Significant change in global climate and sea level during the late Paleocene, *Palaeogeography, Palaeoclimatology, Palaeoecology*, **195** (3-4), pp. 145-163.

Böhme, M. Ilg, A. and Winklhofer, M. 2008. Late Miocene "washhouse" climate in Europe. *Earth and Planetary Science Letters*, **275**(3-4), pp.393-401.

Bond, D.P. and Grasby, S.E. 2017. On the causes of mass extinctions. *Palaeogeography, Palaeoclimatology, Palaeoecology*, **478**, pp.3-29.

Bordiga, M. Henderiks, J. Tori, F., Monechi, S. Fenero, R. Legarda-Lisarri, A. and Thomas, E. 2015. Microfossil evidence for trophic changes during the Eocene–Oligocene transition in the South Atlantic (ODP Site 1263, Walvis Ridge). *Climate of the Past*, **11**(9), pp.1249-1270.

Bosellini, F.R. Benedetti, A. and Kiessling, W. 2025. Minor coral diversity loss but long-lasting coral reef crises in the early Paleogene hothouse. *Paleoceanography and Paleoclimatology*, **40**(3).

Bray, J.R. and Curtis, J.T. 1957. An ordination of upland forest communities of southern Wisconsin. *Ecological Monographs*, **27**(4), pp.325–349.

Brodie, J.F. and Mannion, P.D. 2023. The hierarchy of factors predicting the latitudinal diversity gradient. *Trends in Ecology & Evolution*, **38**(1), pp.15-23.

Brown, J.H. 2014. Why are there so many species in the tropics? *Journal of biogeography*, **41**(1), pp.8-22.

Buatois, L.A. Mángano, M.G. Olea, R.A. and Wilson, M.A. 2016a. Decoupled evolution of soft and hard substrate communities during the Cambrian Explosion and Great Ordovician Biodiversification Event. *Proceedings of the National Academy of Sciences*, **113**(25), pp.6945-6948.

Buatois, L.A. Carmona, N.B. Curran, H.A. Netto, R.G. Mángano, M.G. and Wetzel, A. 2016b. The Mesozoic Marine Revolution. *The Trace-Fossil Record of Major Evolutionary Events, Topics in Geobiology,* **40**. Springer, Dordrecht.

Bulian, F. Jiménez-Espejo, F.J. Andersen, N Larrasoaña, J.C. and Sierro, F.J. 2023. Mediterranean water in the Atlantic Iberian margin reveals early isolation events during the Messinian Salinity Crisis. *Global Planetary Change,* **231**, 104297.

Bulian, F. Sierro, F.J. Ledesma, S. Jiménez-Espejo, F.J. and Bassetti, M-A. 2021. Messinian West Alboran Sea record in the proximity of Gibraltar: Early signs of Atlantic-Mediterranean gateway restriction. *Marine Geology*, **434**, 106430 p.30.

Burgess, S.D. Muirhead, J.D. and Bowring, S.A. 2017. Initial pulse of Siberian Traps sills as the trigger of the end-Permian mass extinction. *Nature Communications*, **8**(1), p.164.

Bush, A.M. Bambach, R.K. and Daley, G.M. 2007. Changes in theoretical ecospace utilization in marine fossil assemblages between the mid-Paleozoic and late Cenozoic. *Paleobiology*, **33**(1), pp.76-97.

Carvalho, L.R.S. and Barros, F. 2017 Physical habitat structure in marine ecosystems: the meaning of complexity and heterogeneity. *Hydrobiologia,* **797**, pp.1–9.

Chao, A. and Jost, L. 2012. Coverage-based rarefaction and extrapolation: standardizing samples by completeness rather than size. *Ecolog*y, **93**, pp.2533-2547.

Chao, A. Gotelli, N.J. Hsieh, T.C. Sander, E.L. Ma, K.H. Colwell, R.K. and Ellison, A.M. 2014. Rarefaction and extrapolation with Hill numbers: a framework for sampling and estimation in species diversity studies. *Ecological monographs*, **84**(1), pp.45-67.

Chaudhary, C. Saeedi, H. and Costello, M.J. 2016. Bimodality of latitudinal gradients in marine species richness. *Trends in Ecology & Evolution*, **31**(9), pp.670-676.

Chen, Z.Q. and Benton, M.J. 2012. The timing and pattern of biotic recovery following the end-Permian mass extinction. *Nature Geoscience*, **5**(6), pp.375-383.

Chin, K. Bloch, J. Sweet, A. Tweet, J. Eberle, J. Cumbaa, S. Witkowski, J. and Harwood, D. 2008. Life in a temperate Polar Sea: a unique taphonomic window on the structure of a Late Cretaceous Arctic marine ecosystem. *Proceedings of the Royal Society B: Biological Sciences*, **275**(1652), pp.2675-2685.

Chiarenza, A.A. Farnsworth, A. Mannion, P.D. and Allison, P.A. 2020. Asteroid impact, not volcanism, caused the end-Cretaceous dinosaur extinction. *PNAS*, **117**(29), pp.17084-17093.

Cicimurri, D.J. Parris, D.C. and Everhart, M.J. 2008. Partial dentition of a chimaeroid fish (Chondrichthyes, Holocephali) from the Upper Cretaceous Niobrara Chalk of Kansas, USA. *Journal of Vertebrate Paleontology,* **28**(1), pp.34-40.

Cirtwill, A.R. Stouffer, D.B. and Romanuk, T.N. 2015. Latitudinal gradients in biotic niche breadth vary across ecosystem types. *Proceedings of the Royal Society B: Biological Sciences*, **282**(1819), p.20151589.

Clay, C.G. Dunhill, A.M. and Beger, M. 2025. Trait networks reveal turnover in Caribbean corals and changes in community resilience through the Cenozoic. *Paleobiology*, pp.1-20.

Close, R. A. Benson, R. B. J. Saupe, E. E. Clapham, M. E. and Butler, R. J. 2020. The spatial structure of Phanerozoic marine animal diversity. *Science*, **368**(6489), pp.420–424.

Cocozza, C.D. and Clarke, C.M. 2020. Type-Maastrichtian gastropod faunas show rapid ecosystem recovery following the Cretaceous–Palaeogene boundary catastrophe. *Palaeontology*, **63**(2), pp.349–367.

Convey, P. 2001. Antarctic ecosystems. *Encyclopaedia of biodiversity*, **1**, pp.171-184.

Conway Morris, S. 1993. The fossil record and the early evolution of the Metazoa. *Nature*, **361**(6410), pp.219–225.

Coxall, H. K. and Pearson, P.N. 2007.*The Eocene-Oligocene transition*. Deep-Time Perspectives on Climate Change: Marrying the Signal from Computer Models and Biological Proxies. Williams, M., Haywood, A. M., Gregory, F. J. & Schmidt, D. N. (eds) The Micropalaeontological Society, Special Publications. The Geological Society, London, pp.351-387.

Coxall, H.K. Pearson, P.N. Wilson, P.A. and Sexton, P.F. 2007. Iterative evolution of digitate planktonic foraminifera. *Paleobiology*, **33**(4), pp.495-516.

Crame, J.A. 2001. Taxonomic diversity gradients though time. *Diversity and Distributions*, **7**(4), pp.175-189.

Crame, J.A. Beu, A.G. Ineson, J.R. Francis, J.E. Whittle, R.J. and Bowman, V.C. 2014. The early origin of the Antarctic marine fauna and its evolutionary implications. *PLoS One*, **9(**22), pp. 10.1371/journal.pone.0114743.

Crame, J.A. 2020. Early Cenozoic evolution of the latitudinal diversity gradient. *Earth Science Reviews*, **202**, pp.1-10.

Crame, J.A. 2023. Late Cenozoic evolution of the latitudinal diversity gradient. *Journal of Biogeography*, **50**, pp.1213–1220.

Currano, E.D. Wilf, P. Wing, S.L. Labandeira, C.C. Lovelock, E.C. and Royer, D.L. 2008. Sharply increased insect herbivory during the Paleocene–Eocene Thermal Maximum. *Proceedings of the National Academy of Sciences*, **105**(6), pp.1960-1964.

Davies, J.H.F.L. Marzoli, A. Bertrand, H. Youbi, N. Ernesto, M. and Schaltegger, U. 2017. End-Triassic mass extinction started by intrusive CAMP activity. *Nature communications*, **8**(1), pp.1-8.

de Juan, S. Ospina-Alvarez, A. Hinz, H., Moranta, J. and Barberá, C. 2023 The continental shelf seascape: a network of species and habitats. *Biodiversity Conservtion,* **32**, pp.1271–1290.

D'Hondt, S. Donaghay, P. Zachos, J.C. Luttenberg, D. and Lindinger, M. 1998. Organic carbon fluxes and ecological recovery from the Cretaceous-Tertiary mass extinction. *Science*, **282**, pp.276–279.

D'Hondt, S. 2005. Consequences of the Cretaceous/Paleogene mass extinction for marine ecosystems. *Annual Review of Ecology, Evolution, and Systematics*, **36**, pp.295–317.

Diamond, J. and Roy, D. 2023. Patterns of functional diversity along latitudinal gradients of species richness in eleven fish families. *Global Ecology and Biogeography*, **32**(3), pp.450-465.

Dobson, A. Lodge, D. Alder, J. Cumming, G.S. Keymer, J. McGlade, J. Mooney, H. *et al*. 2006. Habitat loss, trophic collapse, and the decline of ecosystem services. *Ecology*, **87**(8), pp.1915-1924.

Dolbeth, M. Dolédec, S. and Pardal, M.Â. 2015. Relationship between functional diversity and benthic secondary production in a disturbed estuary. *Marine Ecology Progress Series*, **539**, pp.33-46.

Dominici, S. and Zuschin, M. 2016. Paleocommunities, diversity and sea-level change from middle Eocene shell beds of the Paris Basin. *Journal of the Geological Society*, **173**(6), pp.889-900.

Dunhill, A.M. Hannisdal, B. and Benton, M.J. 2014. Disentangling rock record bias and common-cause from redundancy in the British fossil record. *Nature communications*, **5**(1), p.4818.

Dunhill, A.M. Zarzyczny, K. Shaw, J.O. Atkinson, J.W. Little, C.T. and Beckerman, A.P. 2024. Extinction cascades, community collapse, and recovery across a Mesozoic hyperthermal event. *Nature Communications*, **15**(1), p.8599.

Dunhill, A.M. Foster, W.J. Sciberras, J. and Twitchett, R.J. 2018. Impact of the Late Triassic mass extinction on functional diversity and composition of marine ecosystems. *Palaeontology*, **61(**1), pp.133–148.

Dunne, J.A. Williams, R.J. and Martinez, N.D. 2004. Network structure and robustness of marine food webs. *Marine Ecology Progress Series*, **273**, pp.291-302.

Dunne, J.A. Williams, R.J. Martinez, N.D. Wood, R.A. and Erwin, D.H. 2008. Compilation and network analyses of Cambrian food webs. *PLoS biology*, **6**(4), p.e102.

Dunne, J.A. Labandeira, C.C. and Williams, R.J. 2014. Highly resolved early eocene food webs show development of modern trophic structure after the end-Cretaceous Extinction. *The Proceedings of the Royal Society Biological Sciences*, **281**(1782), p.20133280.

Dunne, J.A. Williams, R. and Martinez, N. 2002. Food web structure and network theory: the role of connectance and size. *PNAS Ecology*, **99**(20), pp.12917–12922.

Ebner, R.M. F. Bulian, F. J. Sierro, T. J. and Kouwenhoven, P. 2024. Th. Meijer, A tale of a changing basin - a transient 40 model of the 7.17 event leading to the Messinian Salinity Crisis. *Marine Geolology,* **470**.

Edie, S.M. Jablonski, D. and Valentine, J.W. 2018. Contrasting responses of functional diversity to major losses in taxonomic diversity. *Proceedings of the National Academy of Sciences*, **115**(4), pp. 732-737.

Erdős, L. Ho, K.V. Bátori, Z. Kröel-Dulay, G. Ónodi, G. Tölgyesi, C. Török, P. and Lengyel, A. 2023. Taxonomic, functional and phylogenetic diversity peaks do not coincide along a compositional gradient in forest-grassland mosaics. *Journal of Ecology*, **111**(1), pp.182-197.

Erwin, D.H. 2008. Macroevolution of ecosystem engineering, niche construction and diversity. *Trends in ecology & evolution*, **23**(6), pp.304-310.

Erwin, D.H. 1990. The end-Permian mass extinction. *Annual Review of Ecology and Systematics*, pp.69-91.

Fenton, I.S. Aze, T. Farnsworth, A. Valdes, P. and Saupe, E.E. 2023. Origination of the modern-style diversity gradient 15 million years ago. *Nature,* **614**(7949), pp.708-712.

Filgueira, R. and Castro, B.G. 2011. Study of the trophic web of San Simón Bay (Ría de Vigo) by using stable isotopes. *Continental Shelf Research*, **31(**5), pp.476-487.

FishBase, Froese, R. and D. Pauly. Editors. 2022. World Wide Web electronic publication. www.fishbase.org version (06/2022).

Foster, W.J. and Twitchett, R.J. 2014. Functional diversity of marine ecosystems after the Late Permian mass extinction event. *Nature Geoscience*, **7**, pp.233 – 239.

Foster, W.J. Garvie, C.L. Weiss, A.M. Muscente, A.D, Aberhan, M. Counts, J.W. and Martindale, R.C, 2020. Resilience of marine invertebrate communities during the early Cenozoic hyperthermals. *Scientific Shows*, **10**(1), p.2176.

Fürsich, F.T. and Aberhan, M. 1990. Significance of time-averaging for palaeocommunity analysis. *Lethaia*, **23**(2), pp.143-152.

Gabara, S.S. Konar, B.H. and Edwards, M.S. 2021. Biodiversity loss leads to reductions in community-wide trophic complexity. *Ecosphere*, **12**(2), p.e03361.

Gallagher, W. 2005. Recent mosasaur discoveries from New Jersey and Delaware, USA: Stratigraphy, taphonomy and implications for mosasaur extinction. *Netherlands Journal of Geosciences*, **84**(3), pp.241-245.

Gauzens, B. Barnes, A. Giling, D.P. Hines, J. Jochum, M. Lefcheck, J.S. Rosenbaum, B. *et al*. 2019. fluxweb: An R package to easily estimate energy fluxes in food webs. *Methods in Ecology and Evolution*, **10**(2), pp.270-279.

Ge, R. Chen, H. Chen, T. Zang, Y. Wang, W. Zhuang, Y. and Liu, G. 2024. Geographical patterns of mesozooplankton functional diversity in the northwestern Pacific. *Progress in Oceanography*, **221**, p.103195.

Geiger. A.O. 2006. Marine Gastropoda. The Mollusks: A guide to their study, collection, and preservation, p.295.

Gilbert, J.A. Field, D. Swift, P. Thomas, S. Cummings, D. Temperton, B. Weynberg, K. *et al*. 2010. The taxonomic and functional diversity of microbes at a temperate coastal site: a 'multi-omic'study of seasonal and diel temporal variation. *PloS one*, **5**(11), p.e15545.

Giorgioni, M. Jovane, L. Rego, E.S. Rodelli, D. Frontalini, F. Coccioni, R. Catanzariti, R. and Özcan, E. 2019. Carbon cycle instability and orbital forcing during the Middle Eocene Climatic Optimum. *Scientific Shows*, **9**(1), p.9357.

Glud, R. N. 2008. Oxygen dynamics of marine sediments. *Marine Biology Research*, **4**(4), pp.243-289.

Grossmann, M. Nielsen, S.N. Rivadeneira, M.M. and Valdivia, N. 2022. The latitudinal gradient of functional diversity of Miocene marine mollusks from Chile. *Ecography,* **2**, p.e06344.

Guinot, G. and Condamine, F.L. 2023. Global impact and selectivity of the Cretaceous-Paleogene mass extinction among sharks, skates, and rays. *Science,* **379**(6634), pp.802-806.

Gusmao, J.B. Brauko, K.M. Eriksson, B.K. and Lana, P.C. 2016. Functional diversity of macrobenthic assemblages decreases in response to sewage discharges. *Ecological Indicators*, **66**, pp.65-75.

Halfar, J. and Mutti, M. 2005. Global dominance of coralline red-algal facies: a response to Miocene oceanographic events. *Geology,* **33**(6), pp.481-484.

Hallam, A. 1996. Recovery of the marine fauna in Europe after the end-Triassic and early Toarcian mass extinctions. *Geological Society, London, Special Publications*, **102**(1), pp.231-236.

Hallam, A. and Wignall, P.B., 1997. *Mass extinctions and their aftermath*. Oxford University Press, UK.

Hansen, T. 1988. Early Tertiary radiation of marine mollusks and the long-term effects of the Cretaceous-Tertiary extinction. *Paleobiology,* **14**, pp.37–51.

Hempson, T.N. Graham, N.A. MacNeil, M.A. Hoey, A.S. and Wilson, S.K. 2018. Ecosystem regime shifts disrupt trophic structure. *Ecological Applications,* **28**(1), pp.191-200.

Henehan, M.J. Hull, P.M. Penman D.E. Rae, J.W. and Schmidt, D.N. 2016. Biogeochemical significance of pelagic ecosystem function: an end-Cretaceous case study. *Philosophical Transactions of the Royal Society B: Biological Sciences*, **371**(1694), p.20150510

Henehan, M.J. Ridgwell, A. Thomas, E. Zhang, S. Alegret, L. *et al.* 2019. Rapid ocean acidification and protracted Earth system recovery followed the end-Cretaceous Chicxulub impact. *Proceedings of the National Academy of Sciences*, **116**(45), pp. 22500-22504.

Hernández, J.O. 2011. Rudists. *Geology Today*, **27**(2), pp.74-77.

Hildebrand, A. R. Penfield, G. T. Kring, D. A. Pilkington, M. Camargo, Z. A. Jacobsen, S. B. and Boynton, W. V. 1991**.** Chicxulub Crater: A possible Cretaceous/Tertiary boundary impact crater on the Yucatan Peninsula, Mexico. *Geology*, **19**(9), pp.867–871.

Hillebrand, H. 2004. On the generality of the latitudinal diversity gradient. *The American Naturalist*, **163**(2), pp.192-211.

Holland, S.M. 2016. The non-uniformity of fossil preservation. *Philosophical Transactions of the Royal Society B: Biological Sciences*, **371**(1699), p.20150130.

Holt, R.D. and Bonsall, M.B. 2017. *Apparent Competition. Encyclopedia of Ecology (Second Edition)*. Elsevier. DOI: 10.1016/B978-0-12-409548-9.10427-0.

Hsieh, T.C. Ma, K. and Chao, A. 2016. iNEXT: an R package for rarefaction and extrapolation of species diversity (H ill numbers). *Methods in ecology and evolution*, **7**(12), pp.1451-1456.

Hull P. M. Norris, R.D. Bralower, T.J. and Schueth, J.D. 2011. A role for chance in marine recovery from the end-Cretaceous extinction. *Nature Geoscience*, **4**, pp.856–860.

Hull, P. Darroch, S. and Erwin, D. 2015. Rarity in mass extinctions and the future of ecosystems. *Nature,* **528**, pp.345–351.

Hull, P.M. and Darroch, S.A. 2013. Mass extinctions and the structure and function of ecosystems. *The Paleontological Society Papers*, **19**, pp.115-156.

Hull, P.M. 2015. Life in the aftermath of extinctions. *Current Biology*, **25**, pp.R941–R952.

Hull, P.M. 2017. Emergence of modern marine systems. *Current Biology,* **27**(11), pp.R466-R469.

Hull, P. M. Bornemann, A. Penman, D. E. Henehan, M. J. Norris, R. D. Röhl, U. and Bralower, T. J. 2020. On impact and volcanism across the Cretaceous-Paleogene boundary. *Science*, **367**(6475), pp.266–272.

Hutchinson, D. K. Coxall, H. K. Lunt, D. J. Steinthorsdottir, M. de Boer, A. M. Baatsen, M. *et al*. 2021. The Eocene–Oligocene transition: a review of marine and terrestrial proxy data, models and model–data comparisons, *Clim. Past*, **17**, pp. 269–315.

Ikejiri, T. Lu, Y. and Zhang, B. 2020. Two-step extinction of Late Cretaceous marine vertebrates in northern Gulf of Mexico prolonged biodiversity loss prior to the Chicxulub impact. *Scientific Shows*, **10**(1), p.4169.

Inglis, G.N. Bragg, F. Burls, N. Evans, D. Foster, G.L. Huber, M. Lunt, D.J. *et al*. 2020. Global mean surface temperature and climate sensitivity of the EECO, PETM and latest Paleocene. *Climate of the past Discussions, 2020*, pp.1-43.

Ivany, L.C. and Nesbitt, E.A. 2003. The marine Eocene-Oligocene transition: a synthesis:[chapter 30]. In *From greenhouse to icehouse: the marine Eocene-Oligocene transition*. p. 522.

Ivany, L.C. Pietsch, C. Handley, J.C. Lockwood, R. Allmon, W.D. and Sessa, J.A. 2018. Little lasting impact of the Paleocene-Eocene Thermal Maximum on shallow marine molluscan faunas. *Science Advances*, **4**(9), p.e5528.

Jablonski, D. 1994. Extinctions in the fossil record. *Philosophical Transactions of the Royal Society of London. Series B: Biological Sciences,* **344**(1307), pp.11–17.

Jablonski, D. Roy, K. and Valentine, J. W. 2006**.** Out of the tropics: evolutionary dynamics of the latitudinal diversity gradient. *Science*, **314**(5796), pp.102–106.

Jablonski, D. Roy, K. Valentine, J.W. Price, R.M. and Anderson, P.S. 2003. The impact of the pull of the recent on the history of marine diversity. *Science*, **300**(5622), pp.1133-1135.

Jamson, K.M. Moon, B.C. and Fraass, A.J. 2022. Diversity dynamics of microfossils from the Cretaceous to the Neogene show mixed responses to events. *Palaeontology*, **65**(4), p.e12615.

Jehle, S. Bornemann, A. Lägel, A.F. Deprez, A. and Speijer, R.P. 2019. Paleoceanographic changes across the Latest Danian Event in the South Atlantic Ocean and planktic foraminiferal response. *Palaeogeography, Palaeoclimatology, Palaeoecology*, **525**, pp.1-13.

Jiang, S. Bralower, T.J. Patzkowsky, M.E. Kump, L.R. And Schueth, J.D. 2010. Geographic controls on nannoplankton extinction across the Cretaceous/ Palaeogene boundary. *Nature Geoscience*, **3**, pp. 280–285.

Jørgensen, B.B. 1983**.** Processes at the sediment-water interface. *Biological Oceanography,* **4**(3), pp.77-128.

Jones, L.A. Gearty, W. Allen, B.J. Eichenseer, K. Dean, C.D. Galván S. and Kouvari, M. *et al*. 2023. palaeoverse: A community-driven R package to support palaeobiological analysis. *Methods in Ecology and Evolution,* **14**(09), pp.2205–2215.

Jones, L.A. Dean, C.D. Mannion, P.D. Farnsworth, A. and Allison, P.A. 2021. Spatial sampling heterogeneity limits the detectability of deep time latitudinal biodiversity gradients. *Proceedings of the Royal Society B: Biological Sciences*, **288**(1945), p.20202762.

Jones, D.S. and Nicol, D. 1986. Origination, survivorship, and extinction of rudist taxa. *Journal of paleontology*, **60**(1), pp.107-115.

Kaiho, K. Oshima, N. and Adachi, K. *et al.* 2016. Global climate change driven by soot at the K-Pg boundary as the cause of the mass extinction. *Scientific Shows,* **6**, p.28427.

Kidwell, S.M. and Holland, S.M. 2002. The quality of the fossil record: implications for evolutionary analyses. *Annual Review of Ecology and Systematics*, **33**(1), pp.561-588.

Kidwell, S.M. 2013. Time-averaging and fidelity of modern death assemblages: building a taphonomic foundation for conservation palaeobiology. *Palaeontology*, **56**(3), pp.487-522.

Kiessling, W. Simpson, C. Beck, B. Mewis, H.and Pandolfi, J.M. 2012. Equatorial decline of reef corals during the last Pleistocene interglacial. *Proceedings of the National Academy of Sciences*, **109**(52), pp.21378-21383.

Keller, G. Adatte, T. Gardin, S. Bartolini, A. and Bajpai, S. 2008. Main Deccan volcanism phase ends near the K-T boundary: Evidence from the Krishna-Godavari Basin, SE India. *Earth and Planetary Science Letters,* **268**(3/4), pp.293–311.

Keller, G. Sahni, A. and Bajpai, S. 2009. Deccan volcanism, the KT mass extinction and dinosaurs. J*ournal of biosciences,* **34**(5), pp.709-728.

Keller, G. Bhowmick, P. K. Upadhyay, H. Dave, A. and Reddy, A. N. *et al*. 2011. Deccan volcanism linked to the Cretaceous-Tertiary boundary mass extinction: New evidence from ONGC wells in the Krishna-Godavari Basin. *Journal of the Geological Society of India*, **78**(5), pp.399-428.

Kelly, D.C. 2002. Response of Antarctic (ODP Site 690) planktonic foraminifera to the Paleocene–Eocene thermal maximum: faunal evidence for ocean/climate change. *Paleoceanography*, **17**(4), pp.23-1.

Kennett, J. P. and Stott, L. D. 1991. Abrupt deep-sea warming, palaeoceanographic changes and benthic extinctions at the end of the Palaeocene. *Nature,* **353**(6341), pp.225-229.

Kidwell, S.M. and Holland, S.M. 2002. The quality of the fossil record: implications for evolutionary analyses. *Annual Review of Ecology and Systematics*, **33**(1), pp.561-588.

Klug, C. De Baets, K. Kröger, B. Bell, M.A. Korn, D. and Payne, J.L. 2015. Normal giants? Temporal and latitudinal shifts of Paleozoic marine invertebrate gigantism and global change. *Lethaia*, **48**(2), pp.267-288.

Knoll, A.H. and Follows, M.J. 2016. A bottom-up perspective on ecosystem change in Mesozoic oceans. *Proceedings of the Royal Society B: Biological Sciences*, **283**(1841), p.20161755.

Kontakiotis, G.G.A. Butiseacă, A. Antonarakou, K. Agiadi, S.D. and Zarkogiannis, D. *et al*. 2022. Hypersalinity accompanies tectonic restriction in the eastern Mediterranean prior to the Messinian Salinity Crisis. *Palaeogeography. Palaeoclimatology. Palaeoecology,* **592**, 110903.

Kortsch, S. Primicerio, R. Fossheim, M. Dolgov, A.V. and Aschan, M. 2015. Climate change alters the structure of Arctic marine food webs due to poleward shifts of boreal generalists. *Proceedings of the Royal Society B: Biological Sciences*, **282**(1814), p.20151546.

Kortsch, S. Primicerio, R. Aschan, M. Lind, S. Dolgov, A.V. and Planque, B. 2019. Food-web structure varies along environmental gradients in a high-latitude marine ecosystem. *Ecography*, **42**(2), pp.295-308.

Krijgsman, W. Hilgen, F.J. Raffi, I. Sierro, F.J. and Wilson, D.S. 1999. Chronology, causes and progression of the Messinian salinity crisis. *Nature*, **400**(6745), pp.652-655.

Krug, A. Z. Jablonski, D. and Valentine, J. W. 2009**.** Signature of the end-Cretaceous mass extinction in the modern biota. *Science*, **323**(5915), pp.767–771.

Krug A.Z. Jablonski, D. Roy, K. and Beu, A.G. 2010. Differential extinction and the contrasting structure of polar marine faunas. *PLoS ONE*, **5**(12): e15362.

Laliberté, E. and Legendre, P. 2010. A distance-based framework for measuring functional diversity from multiple traits. *Ecology,* **91**(1), pp.299-305.

Lamanna, C. Blonder, B. Violle, C. Kraft, N.J. Sandel, B. Šímová, I. and Donoghue, J.C. *et al*. 2014. Functional trait space and the latitudinal diversity gradient. *Proceedings of the National Academy of Sciences*, **111**(38), pp.13745-13750.

Laureto, L.M.O. Cianciaruso, M.V. and Samia, D.S.M. 2015. Functional diversity: an overview of its history and applicability. *Natureza & Conservação*, **13**(2), pp.112-116.

Leclerc, C. Reynaud, N. Danis, P.A. Moatar, F. and Daufresne, M. *et al*. 2023. Temperature, productivity, and habitat characteristics collectively drive lake food web structure. *Global Change Biology*, **29**(9), pp.2450-2465.

Leighton L.R. Webb A.E. and Sawyer, J.A. 2013. Ecological effects of the Paleozoic-Modern faunal transition: Comparing predation on Paleozoic brachiopods and molluscs. *Geology*, **41**, pp. 275–278.

Li, J. Hu, X. Zachos, J.C. Garzanti, E. and BouDagher-Fadel, M. 2020. Sea level, biotic and carbon-isotope response to the Paleocene–Eocene thermal maximum in Tibetan Himalayan platform carbonates. *Global and Planetary Change*, **194**, p.103316.

Lisiecki, L. E. and Raymo, M. E. 2005. A Pliocene-Pleistocene stack of 57 globally distributed benthic δ18O records. *Paleoceanography,* **20**(1).

Lowery C.M. Bralower T.J. Owens J.D. Rodríguez-Tovar F.J. and Jones H. *et al*. 2018. Rapid recovery of life at ground zero of the end-Cretaceous mass extinction. *Nature,* **558**(7709), pp.288-291.

Lowery, C.M. Bown, P.R. Fraass, A.J. and Hull, P.M. 2020. Ecological response of plankton to environmental change: thresholds for extinction. *Annual Review of Earth and Planetary Sciences*, **48,** pp.403-429.

Lopez-Rivas, J.D. and Cardenas, J.C. 2024. What is the economic value of coastal and marine ecosystem services? A systematic literature review. *Marine Policy*, **161**, p.106033.

MacLeod, N. Rawson, P.F. Forey, P.L. Banner, F.T. Boudagher-Fadel, M.K. Bown, P.R. and Burnett, J.A. *et al*. 1997. The Cretaceous-tertiary biotic transition. *Journal of the geological Society*, **154**(2), pp.265-292.

Mammola, S. Carmona, C.P. Guillerme, T. and Cardoso, P. 2021. Concepts and applications in functional diversity. *Functional Ecology*, **35**(9), pp.1869-1885.

Mannion, P.D. Benson, R.B. Upchurch, P. Butler, R.J. Carrano, M.T. and Barrett, P.M. 2012. A temperate palaeodiversity peak in Mesozoic dinosaurs and evidence for Late Cretaceous geographical partitioning. *Global Ecology and Biogeography*, **21**(9), pp.898-908.

Mannion, P. D. Upchurch, P. Benson, R. B. and Goswami, A. 2014**.** The latitudinal biodiversity gradient through deep time. *Trends in Ecology & Evolution*, **29**(1), pp.42–50.

Marenssi, S.A. Net, L.I. and Santillana, S.N. 2002. Provenance, environmental and paleogeographic controls on sandstone composition in an incised-valley system: the Eocene La Meseta Formation, Seymour Island, Antarctica. *Sedimentary Geology*, **150**(3-4), pp.301-321.

MarLIN. 2022. The Marine Life Information Network. https://www.marlin.ac.uk

Martin, J.E. Vincent, P. Tacail, T. Khaldoune, F. and Jourani, E. *et al*. 2017. Calcium Isotopic Evidence for Vulnerable Marine Ecosystem Structure Prior to the K/Pg Extinction. *Current Biology,* **27**(11), pp.1641-1644.

Massicotte, P. South, A. 2025. *rnaturalearth: World Map Data from Natural Earth*. R package version 1.1.0.9000, https://docs.ropensci.org/rnaturalearth/.

McGowan, A.J. and Smith, A.B. (eds) 2011. *Comparing the Geological and Fossil Records: Implications for Biodiversity Studies*. Geological Society, London, Special Publications, **358**, pp.63–94. The Geological Society of London 2011

McIntosh, R.P. 2004. *Ecology, the great integrator*. Fundamentals of Ecology. 5th ed. Eugene P. Odum and Gary W. Barrett. Brooks Cole, Belmont, CA, 2004. **624**.

McQuatters-Gollop, A. Mitchell, I. Vina-Herbon, C. Bedford, J. Addison, P.F. Lynam, C.P. and Geetha, P.N. *et al*. 2019. From science to evidence–how biodiversity indicators can be used for effective marine conservation policy and management. *Frontiers in Marine Science*, **6**, p.109.

Meissner, K.J. Bralower, T.J. Alexander, K. Jones, T.D. Sijp, W. and Ward, M. 2014. The Paleocene-Eocene thermal maximum: How much carbon is enough? *Paleoceanography*, **29**(10), pp.946-963.

Meredith, R.W. Janečka, J.E. Gatesy, J. Ryder, O.A. and Fisher, C.A. *et al*. 2011. Impacts of the Cretaceous terrestrial revolution and KPg extinction on mammal diversification. *Science*, **334**(6055), pp.521-524.

Mermillod-Blondin, F. Roy, J. Spehn, E. and van Peer, L. 2002. Species diversity, functional diversity, and ecosystem functioning. *Biodiversity and ecosystem functioning: synthesis and perspectives*, **17**, pp.195-208.

Mermillod-Blondin, F. 2011. The functional significance of bioturbation and biodeposition on biogeochemical processes at the water–sediment interface in freshwater and marine ecosystems. *Journal of the North American Benthological Society*, **30**(3), pp.770-778.

Miller, K. G. Browning, J. V. Schmelz, W. J. Kopp, R. E. Mountain, G. S. and Wright, J. D. 2020. Cenozoic sea-level and cryospheric evolution from deep-sea geochemical and continental margin records. *Science Advances,* **6**, eaaz1346.

Mindat.org. 2022. https://www.mindat.org

Mittelbach, G.G. Schemske, D.W. Cornell, H.V. Allen, A.P. Brown, J.M. Bush, M.B. and Harrison S.P. *et al*. 2007 Evolution and the latitudinal diversity gradient: speciation, extinction and biogeography. *Ecology letters*, **10**(4), pp.315-31.

Mondal, S. and Harries, P.J. 2016. Phanerozoic trends in ecospace utilization: the bivalve perspective. *Earth-Science Reviews*, **152**, pp.106-118.

Monegatti, P. and Raffi, S. 2010. The Messinian marine molluscs record and the dawn of the eastern Atlantic biogeography. *Palaeogeography, Palaeoclimatology, Palaeoecology*, **297**(1), pp.1-11.

Montes, S. Manuel, J. Beamud, E. Nozal, F. and Santillana, S. 2019. Late Maastrichtian-Paleocene chronostratigraphy from Seymour Island (James Ross Basin, Antarctic Peninsula). Eustatic controls of sedimentation. *Advances in Polar Science,* **30**, pp.303-327.

Mouillot, D. Graham, N.A. Villéger, S. Mason, N.W. and Bellwood, D.R. 2013. A functional approach reveals community responses to disturbances. *Trends in ecology & evolution*, **28**(3), pp.167-177.

Mourik, A.A. 2010. *Middle Miocene Climate Transition in the Central Mediterranean*. Utrecht University, Department of Earth Sciences.

Murray, J.W. 1995. Microfossil indicators of ocean water masses, circulation and climate. *Geological Society, London, Special Publications,* **83**(1), pp.245-264.

Nanglu, K. and Cullen, T.M. 2023. Across space and time: a review of sampling, preservational, analytical, and anthropogenic biases in fossil data across macroecological scales. *Earth-Science Reviews*, **244,** p.104537.

Navia, A.F. Cruz-Escalona, V.H. Giraldo, A. and Barausse, A. 2016. The structure of a marine tropical food web, and its implications for ecosystem-based fisheries management. *Ecological modelling*, **328**, pp.23-33.

Near, T.J. Eytan, R.I. Dornburg, A. Kuhn, K.L. Moore, J.A. Davis, M.P. Wainwright, P.C. Friedman, M. and Smith, W.L. 2012. Resolution of ray-finned fish phylogeny and timing of diversification. *Proceedings of the National Academy of Sciences*, **109**(34), pp.13698-13703.

Nilsson, K.A. and McCann, K.S. 2016. Interaction strength revisited—clarifying the role of energy flux for food web stability. *Theoretical Ecology*, **9**(1), pp.59-71.

Norris, R.D. Turner, S.K. Hull, P.M. and Ridgwell, A. 2013. Marine ecosystem responses to Cenozoic global change. *Science*, **341**(6145), pp.492-498.

Novack-Gottshall, P.M. 2007. Using a theoretical ecospace to quantify the ecological diversity of Paleozoic and modern marine biotas. *Paleobiology*, **33**(2), pp.273-294.

Nwojiji, C. and Marret-Davies, F. 2019. The impact of high palaeoproductivity on the ecological function and test of foraminifera in the equatorial Pacific Ocean during the PETM. *American Journal of Marine Science*.

Oksanen, J. Blanchet, F.G. Friendly, M. Kindt, R. Legendre, P. and McGlinn, D. *et al.* 2022. *vegan: Community Ecology Package. R package version 2.6-4.*

Oleinik, A.E. and Marincovich Jr, L. 2003. Biotic response to the Eocene–Oligocene transition: Gastropod assemblages in the high−latitude North Pacific. *From Greenhouse to Icehouse: The Marine Eocene–Oligocene Transition*, pp.36-56.

The Palaeobiology Database.org. 2025. https://paleobiodb.org/#/

Pascual, M. and Dunne, J. A. (Eds.). 2006. *Ecological Networks: Linking Structure to Dynamics in Food Webs*. Oxford University Press. ISBN: 9780198566199.

Peredo, C.M. and Uhen, M.D. 2016. Exploration of marine mammal paleogeography in the Northern Hemisphere over the Cenozoic using beta diversity. *Palaeogeography. Palaeoclimatology. Palaeoecology*, **449**, pp.227–235.

Petchey, O.L. Beckerman, A.P. Riede, J.O. and Warren, P.H. 2008. Size, foraging, and food web structure. *Proceedings of the National Academy of Sciences*, **105**(11), pp.4191-4196.

Petchey, O.L. and Gaston, K.J. 2006. Functional diversity: back to basics and looking forward. *Ecology letters*, **9**(6), pp.741-758.

Peters, S.E. and Heim, N.A. 2011. Macrostratigraphy and macroevolution in marine environments: testing the common-cause hypothesis. *Geological Society, London, Special Publications*. **358**, pp. 95–104.

Peters, S.E. and Heim, N.A. 2010. The geological completeness of paleontological sampling in North America. *Paleobiology,* **36**(1), pp.61-79.

Peters, S.E. 2006. Genus extinction, origination, and the durations of sedimentary hiatuses. *Paleobiology*, **32**(3), pp.387-407.

Pillar, S.C. Stuart, V. Barangé, M. and Gibbons, M.J. 1992. Community structure and trophic ecology of euphausiids in the Benguela ecosystem. *South African Journal of Marine Science*, **12**(1), pp.393-409.

Pielou, E.C. 1966. The measurement of diversity in different types of biological collections. *Journal of Theoretical Biology*, **13**(1), pp.131–144.

Pierce, E.L. van de Flierdt, T. Williams, T. Hemming, S.R. Cook, C.P. and Passchier, S. 2017. Evidence for a dynamic East Antarctic ice sheet during the mid-Miocene climate transition. *Earth and Planetary Science Letters*, **478**, pp.1-13.

Pimiento, C. Griffin, J.N. Clements, C.F. Silvestro, D. Varela, S. Uhen, M.D. and Jaramillo, C. 2017. The Pliocene marine megafauna extinction and its impact on functional diversity. *Nature ecology & evolution*, **1**(8), pp.1100-1106.

Pimiento, C. Leprieur, F. Silvestro, D. Lefcheck, J.S. Albouy, C. Rasher, D.B. Davis, M. Svenning, J.C. and Griffin, J.N. *et al*. 2020. Functional diversity of marine megafauna in the Anthropocene. *Science Advances*, **6**(16), p.eaay7650.

Pimm, S.L. 1979. The structure of food webs. *Theoretical Population Biology*, **16**, pp.144-158.

Powell, M.G. 2009. The latitudinal diversity gradient of brachiopods over the past 530 million years. *The Journal of Geology*, **117**(6), pp.585-594.

Powell, M.G. Beresford, V.P. and Colaianne, B.A. 2012. The latitudinal position of peak marine diversity in living and fossil biotas. *Journal of Biogeography*, **39**(9), pp.1687-1694.

Price, S.A. Schmitz, L. Oufiero, C.E. Eytan, R.I. and Dornburg, A. *et al*. 2014. Two waves of colonization straddling the K–Pg boundary formed the modern reef fish fauna. *Proceedings of the Royal Society B: Biological Sciences*, **281**(1783), p.20140321

Pross, J. Contreras, L. Bijl, P.K. Greenwood, D.R. Bohaty, S.M. Schouten, S., Bendle, J.A. and Huck, C.E. *et al.* 2012. Persistent near-tropical warmth on the Antarctic continent during the early Eocene epoch. *Nature*, **488**(7409), pp.73-77.

Prothero, D.R. 1994. The late eocene-oligocene extinctions. *Annual Review Of Earth And Planetary Sciences,* **22**, pp.145-165.

Opitz, S. 1996. *Trophic interactions in Caribbean coral reefs*. **1085**.

R Core Team. 2024. R: A Language Environment for Statistical Computing, Vienna, Austria. Available at: http://.R-project.org

Rabosky, D.L. and Sorhannus, U. 2009. Diversity dynamics of marine planktonic diatoms across the Cenozoic. *Nature*, **457**(7226), pp.183-186.

Raja, N.B. Dunne, E.M. Matiwane, A. Khan, T.M. Nätscher, P.S. Ghilardi, A.M. and Chattopadhyay, D. 2022. Colonial history and global economics distort our understanding of deep-time biodiversity. *Nature ecology & evolution*, **6**(2), pp.145-154.

Raup, D. M. 1986. Biological extinction in earth history. *Science,* **231**, pp.1528–1533.

Raup, D.M. and Sepkoski Jr, J.J. 1982. Mass extinctions in the marine fossil record. *Science*, **215**(4539), pp.1501-1503.

Raup, D.M. and Boyajian, G.E. 1988. Patterns of generic extinction in the fossil record. *Paleobiology*, **14**(2), pp.109-125.

Raymundo, L.J. Halford, A.R. Maypa, A.P. Kerr, A.M. 2009. Functionally diverse reef-fish communities ameliorate coral disease. *Proceedings of the National Academy of Sciences*, **106**(40), pp.17067-17070.

Reichow, M.K. Pringle, M.S. Al'Mukhamedov, A.I. Allen, M.B. Andreichev, V.L. Buslov, M.M. Davies, C.E. and Medvedev, A.Y. 2009. The timing and extent of the eruption of the Siberian Traps large igneous province: Implications for the end-Permian environmental crisis. *Earth and Planetary Science Letters*, **277**(1-2), pp.9-20.

Renne, P.R. Deino, A.L. Hilgen, F.J. Kuiper, K.F. Mark, D.F. Mitchell, W.S. and Morgan, L.E. 2013. Time scales of critical events around the Cretaceous-Paleogene boundary. *Science*, **339**(6120), pp.684–687.

Říha, M. Vejřík, L. Rabaneda-Bueno, R. *et al*. 2025. Ecosystem, spatial and trophic dimensions of niche partitioning among freshwater fish predators. *Mov Ecol,* **13**, p.36.

Rippeth, T.P. Scourse, J.D. Uehara, K. and McKeown, S. 2008. Impact of sea-level rise over the last deglacial transition on the strength of the continental shelf CO2 pump. *Geophysical Research Letters*, **35**(24).

Rincón-Díaz, M.P. Pittman, S.J. Arismendi, I. and Heppell, S.S. 2018. Functional diversity metrics detect spatio-temporal changes in the fish communities of a Caribbean marine protected area. *Ecosphere*, **9**(10), p.e02433.

Rodland, D.L. and Bottjer, D.J. 2001. Biotic recovery from the end-Permian mass extinction: behavior of the inarticulate brachiopod Lingula as a disaster taxon. *Palaios*, **16**(1), pp.95-101.

Rodríguez-Tovar, F.J. and Uchman, A. 2006. Ichnological analysis of the Cretaceous–Palaeogene boundary interval at the Caravaca section, SE Spain. *Palaeogeography, Palaeoclimatology, Palaeoecology*, **242**(3-4), pp.313-325.

Roopnarine, P.D. 2006. Extinction cascades and catastrophe in ancient food webs. *Paleobiology*, **32**(1), pp.1-19.

Roopnarine, P. 2010. Graphs, networks, extinction and paleocommunity food webs. *Nature Precedings*, pp.1-1.

Roopnarine, P.D. Angielczyk, K.D. Olroyd, S.L. Nesbitt, S.J. Botha-Brink, J. Peecook, B.R. Day, M.O. and Smith, R.M. 2017. Comparative ecological dynamics of Permian-Triassic communities from the Karoo, Luangwa, and Ruhuhu basins of southern Africa. *Journal of Vertebrate Paleontology*, **37**(1), pp.254-272.

Roopnarine, P.D. and Angielczyk, K.D. 2015. Community stability and selective extinction during the Permian-Triassic mass extinction. *Science*, **350**(6256), pp.90-93.

Roopnarine, P.D. and Hertog, R. 2013. Detailed food web networks of three Greater Antillean coral reef systems: the Cayman Islands, Cuba, and Jamaica. *Dataset Papers in Ecology*.

Rosenfeld, J.S. 2002. Functional redundancy in ecology and conservation. *Oikos*, **98**(1), pp.156-162.

Rose, K.D. 1984. Evolution and radiation of mammals in the Eocene, and the diversification of modern orders. *Series in Geology, Notes for Short Course*, **8,** pp.110-127.

Roveri, M. Lugli, S. Manzi, V. and Schreiber, B.C. 2008. The Messinian Sicilian stratigraphy revisited: new insights for the Messinian salinity crisis. *Terra Nova,* **20**(6), pp.483-488.

Roveri, M. Flecker, R. Krijgsman, W. Lofi, J. Lugli, S. Manzi, V. Sierro, F.J. and Govers, R. *et al.* 2014. The Messinian Salinity Crisis: Past and future of a great challenge for marine sciences. *Marine Geology*, **352**, pp.25-58.

Roy, K., Jablonski, D. and Valentine, J.W. 2000. Dissecting latitudinal diversity gradients: functional groups and clades of marine bivalves. *Proceedings of the Royal Society of London. Series B: Biological Sciences*, **267**(1440), pp.293-299.

Sadler, P.M. 1988. "*Geometry and stratification of uppermost Cretaceous and Paleogene units on Seymour Island, northern Antarctic Peninsula*", Geology and Paleontology of Seymour Island Antarctic Peninsula, R. M. Feldmann, M. O. Woodburne.

Sakamoto, M. Benton, M.J. Venditti, C. 2016. Dinosaurs in decline tens of millions of years before their final extinction. *Proceedings of the National Academy of Sciences*, **113**(18), pp.5036–5040.

Sarkar, S. Cotton, L.J. Valdes, P.J. and Schmidt, D.N. 2022. Shallow water records of the PETM: novel Insights from NE India (Eastern Tethys). *Paleoceanography and Paleoclimatology*, **37**(7), p.e2021PA004257

Sary, P.S. And Pramod Kiran, R.B. 2016. New distributional records of muricid snails (Mollusca: Gastropoda) from the Arabian Sea. *Journal Of Aquatic Biology & Fisheries.* **4**, Pp.166-168.

Saupe, E.E. 2023. Explanations for latitudinal diversity gradients must invoke rate variation. *Proceedings of the National Academy of Sciences,* **120**(33), p.e2306220120.

Saupe, E.E. Farnsworth, A. Lunt, D.J. Sagoo, N. Pham, K.V. and Field, D.J. 2019a. Climatic shifts drove major contractions in avian latitudinal distributions throughout the Cenozoic. *Proceedings of the National Academy of Sciences*, **116**(26), pp.12895-12900.

Saupe, E.E. Myers, C.E. Townsend Peterson, A. Soberón, J. Singarayer, J. Valdes, P. and Qiao, H. 2019b. Spatio-temporal climate change contributes to latitudinal diversity gradients. *Nature ecology & evolution*, **3**(10), pp.1419-1429.

Schafhauser, A. Götz, S. and Stinnesbeck, W. 2007. Rudist decline in the Maastrichtian Cardenas Formation (east-central Mexico). *Palaeogeography, Palaeoclimatology, Palaeoecology*, **251**(2), pp.210-221.

Scheibner, C. Speijer, R.P. and Marzouk, A.M. 2005. Turnover of larger foraminifera during the Paleocene-Eocene Thermal Maximum and paleoclimatic control on the evolution of platform ecosystems. *Geology*, **33**(6), pp.493-496.

Scheibner, C. and Speijer, R.P. 2007. Decline of coral reefs during late Paleocene to early Eocene global warming. *eEarth Discussions*, **2**(3), pp.133-150.

Scheibner, C. and Speijer, R.P. 2008. Late Paleocene–early Eocene Tethyan carbonate platform evolution- a response to long-and short-term paleoclimatic change. *Earth-science reviews*, **90**(3-4), pp.71-102.

Schoene, B. Eddy, M. P. Samperton, K. M. Keller, C. B. and Keller, G. *et al*. 2019. U-Pb constraints on pulsed eruption of the Deccan Traps across the end-Cretaceous mass extinction. *Science*, **363**, pp.862-866.

Schram, F.R. and Dixon, C.J. 2004. Decapod phylogeny: addition of fossil evidence to a robust morphological cladistic data set. *Bulletin of the Mizunami Fossil Museum*, **31**(1), p.19.

Schulte, P. Alegret, L. Arenillas, I. Arz, J. A. Barton, P. J. Bown, P. R. and Vajda, V. 2010. The Chicxulub asteroid impact and mass extinction at the Cretaceous-Paleogene boundary. *Science,* **327**(5970), pp.1214–1218.

Schumm, M. Edie, S.M. Collins, K.S. Gómez-Bahamón, V. Supriya, K. White, A.E. Price, T.D. and Jablonski, D. 2019. Common latitudinal gradients in functional richness and functional evenness across marine and terrestrial systems. *Proceedings of the Royal Society B*, **286**(1908), p.20190745.

Schwarzhans, W. 2023. Geology and stratigraphy of the Neogene section along the Oued Beth between Dar bel Hamri and El Kansera (Rharb Basin, northwestern Morocco) and its otolith-based fish fauna: a faunal inventory for the Early Pliocene remigration into the Mediterranean. *Swiss J. Palaeontol*. **124**, pp.3–85.

Sepkoski Jr, J.J. 1986. Phanerozoic overview of mass extinction. In *Patterns and Processes in the History of Life: Report of the Dahlem Workshop on Patterns and Processes in the History of Life Berlin 1985, June 16–21* (pp. 277-295). Berlin, Heidelberg: Springer Berlin Heidelberg.

Sepkoski, J.J. 1981. A factor analytic description of the Phanerozoic marine fossil record. *Paleobiology*, **7**(1), pp.36–53.

Sepkoski, J.J. 1984. A kinetic model of Phanerozoic taxonomic diversity. III. Post-Paleozoic families and mass extinctions. Paleobiology, **10**(2), pp.246–267.

Sepkoski, J.J. 1982. A compendium of fossil marine families. *Milwaukee Public Museum Contributions in Biology and Geology*. **51**, pp.1–125.

Sepkoski, J.J. and Sheehan, P.M. 1983. Diversification, faunal change, and community replacement during the Late Devonian. *Geological Society of America Special Paper*, **190**, PP.89–106.

Sepkoski, J.J. 1997. Biodiversity: Past, present, and future. *Journal of Paleontology*, **71**(4), pp.533–539.

Shaw, J.O. Dunhill, A.M. Beckerman, A. Dunne, J.A. and Hull, P.M. 2023. Constructing and comparing ancient food webs using functional diversity data. *Methods in Ecology and Evolution*, in review.

Shimada, K. 2008. The size of the extinct lamniform shark Cretalamna appendiculata from the Upper Cretaceous Niobrara Chalk of Kansas. *Journal of Vertebrate Paleontology*, **28**(3), pp.846-849.

Sikes, E.L. Keigwin, L.D. and Curry, W.B. 1991. Pliocene paleoceanography: circulation and oceanographic changes associated with the 2.4 Ma glacial event. *Paleoceanography*, **6**(2), pp.245-257.

Slater, B.J. and Bohlin, M.S. 2022. Animal origins: The record from organic microfossils. *Earth-Science Reviews*, **232**, p.104107.

Smith, R.Y. Greenwood, D.R. and Basinger, J.F. 2010. Estimating paleoatmospheric pCO2 during the early Eocene climatic optimum from stomatal frequency of ginkgo, Okanagan highlands, British Columbia, Canada. *Palaeogeography, Palaeoclimatology, Palaeoecology*, **293**(1-2), pp.120-131.

Smith, A.B. Lloyd, G.T. and McGowan, A.J. 2012. Phanerozoic marine diversity: rock record modelling provides an independent test of large-scale trends. *Proceedings of the Royal Society B: Biological Sciences,* **279**(1746), pp.4489-4495.

Song, H, Huang, S. Jia, E. Dai, X. Wignall, P.B. and Dunhill, A.M. 2020. Flat latitudinal diversity gradient caused by the Permian–Triassic mass extinction. *Proceedings of the National Academy of Sciences*, **117**(30), pp.17578-17583.

Song, H. Wignall, P.B. Chen, Z.Q. Tong, J. Bond, D.P. Lai, X. Zhao, X. Jiang, H. Yan, C. Niu, Z. and Chen, J. 2011. Recovery tempo and pattern of marine ecosystems after the end-Permian mass extinction. *Geology*, **39**(8), pp.739-742.

Speijer, R.P. Scheibner, C. Stassen, P. and Morsi, A.M.M. 2012. Response of marine ecosystems to deep-time global warming: a synthesis of biotic patterns across the Paleocene-Eocene thermal maximum (PETM). *Austrian Journal of Earth Sciences*, **105**(1), pp.6-16.

Steininger, F.F. 1999**.** Chronostratigraphy, geochronology and biochronology of the Miocene "European Land Mammal Mega-Zones" (ELMMZ) and the Miocene "Mammal-Zones (MN-Zones)". In *The Miocene Land Mammals of Europe*. pp. 9-24. Verlag Dr. Friedrich Pfeil.

Stelzenmüller, V. Maynou, F. Martín, P. 2009. Patterns of species and functional diversity around a coastal marine reserve: a fisheries perspective. *Aquatic Conservation: Marine and Freshwater Ecosystems*, **19**(5), pp.554-565.

Stevens, R.D. Cox, S.B. Strauss, R.E. and Willig, M.R. 2003. Patterns of functional diversity across an extensive environmental gradient: vertebrate consumers, hidden treatments and latitudinal trends. *Ecology letters*, **6**(12), pp.1099-1108.

Stokke, E.W. Jones, M.T. Riber, L. Haflidason, H. Midtkandal, I. Schultz, B.P. and Svensen, H.H. 2020. Rapid and sustained environmental responses to global warming: the Paleocene–Eocene Thermal Maximum in the eastern North Sea. *Climate of the Past Discussions*, pp.1-38.

Swain, A. Woodhouse, A. Fagan, W.F. Fraass, A.J. and Lowery, C.M. 2024. Biogeographic response of marine plankton to Cenozoic environmental changes. *Nature*, **629**(8012), pp. 616-623.

Tang, Q. Yang, J. and Sun, D. 2022. Functional diversity of copepod assemblages along a basin-scale latitudinal gradient in the North Pacific Ocean. *Ecological Indicators*, **141**, p.109112.

Thomas, E. and Shackleton, N.J. 1996. The Paleocene-Eocene benthic foraminiferal extinction and stable isotope anomalies. *Geological Society, London, Special Publications,* **101**, pp.401–441.

Thomas, D.J. Zachos, J.C. Bralower, T.J. Thomas, E. and Bohaty, S. 2002**.** Warming the fuel for the fire: Evidence for the thermal dissociation of methane hydrate during the Paleocene-Eocene thermal maximum. *Geology,* **30***(*12), pp. 1067-1070.

Thomas, E. 2007. Cenozoic mass extinctions in the deep sea: What perturbs the largest habitat on Earth? *The Geological Society of America*. *Special Paper* **424**, pp 1-23.

Thomas, D. and St. John, K. 2025. Abrupt climate change: The PETM. In *Climate Change: A Geoscience Perspective* (pp. 315-350). Cham: Springer Nature Switzerland.

Tierney, J.E. Poulsen, C.J. Montañez, I.P. Bhattacharya, T. Feng, R. Ford, H.L. Hönisch, B. and Tabor, C.R. 2020. Past climates inform our future. *Science*, **370**(6517), p.eaay3701.

Tilman, D. Reich, P.B. Knops, J. Wedin, D. Mielke, T. and Lehman, C. 2001. Diversity and productivity in a long-term grassland experiment. *Science*, **294**(5543), pp.843-845.

Tilman, D. Isbell, F. and Cowles, J. M. 2014**.** Biodiversity and ecosystem functioning. *Annual Review of Ecology, Evolution, and Systematics,* **45**, pp. 471-493.

Tracey, S. Todd, J.A. and Erwin, D.H. 1993. *Mollusca: Gastropoda*. In Benton, M.J. (Ed.). The Fossil Record 2. Chapman & Hall.

Tamayo, T.R. Garzón, D. Arias, V. Plata, A. Vallejo, F. Pardo, A. and Flores, J.A. 2024. *Microfossils provide evidence of environmental changes during the Eocene-Oligocene transition in northwestern South America*. EGU General Assembly 2024, Vienna, Austria, pp. 14–19, EGU24-1156.

Tyler, C.L. and Kowalewski, M. 2025. Fossil samples archive functional diversity in marine ecosystems: An empirical test from a present-day coastal environment. *Proceedings of the National Academy of Sciences,* **122**(31), p.e2405727122.

Uhen, M.D. 2010. The origin(s) of whales. *Annual Review of Earth and Planetary Sciences*, **38**(1), pp.189-219.

Valentine, J.W. Jablonski, D. Kidwell, S. and Roy, K. 2006. Assessing the fidelity of the fossil record by using marine bivalves. *Proceedings of the National Academy of Sciences*, **103**(17), pp.6599-6604.

Vasconcellos, M. Mackinson, S. Sloman, K. and Pauly, D. 1997. The stability of trophic mass-balance models of marine ecosystems: a comparative analysis. *Ecological modelling*, **100**(1-3), pp.125-134.

Vázquez, D.P. and Stevens, R.D. 2004 The latitudinal gradient in niche breadth: concepts and evidence. *Am. Nat*. **164**. (doi:10.1086/421445).

Vellekoop, J. van Tilborgh, K.H. van Knippenberg, P. Jagt, J.W., Stassen, P. Goolaerts, S. and Speijer, R.P. 2020. Type-Maastrichtian gastropod faunas show rapid ecosystem recovery following the Cretaceous–Palaeogene boundary catastrophe. *Palaeontology,* **63**(2), pp.349-367.

Verducci, M. Foresi, L.M. Scott, G.H. Sprovieri, M. Lirer, F. and Pelosi, N. 2009. The Middle Miocene climatic transition in the Southern Ocean: evidence of paleoclimatic and hydrographic changes at Kerguelen plateau from planktonic foraminifers and stable isotopes. *Palaeogeography, Palaeoclimatology, Palaeoecology*, **280**(3-4), pp.371-386.

Vermeij, G.J. 1977. *Evolution and Escalation: An Ecological History of Life*. Princeton University Press.

Vilhena, D.A. and Smith, A.B. 2013. Spatial bias in the marine fossil record. *PLoS One*, **8**(10), p.e74470.

Villamor, A. and Becerro, M.A. 2012. Species, trophic, and functional diversity in marine protected and non-protected areas. *Journal of Sea Research*, **73**, pp.109-116.

Villéger, S. Novack-Gottshall, P.M. and Mouillot, D. 2011. The multidimensionality of the niche reveals functional diversity changes in benthic marine biotas across geological time. *Ecology Letters*, **14**(6), pp.561-568.

von der Heydt, A. and Dijkstra, H.A. 2006. Effect of ocean gateways on the global ocean circulation in the late Oligocene and early Miocene. *Paleoceanography*, **21**(1).

Wagner, P.J. Kosknik, M.A. Lidgard, S. 2006. Abundance distributions imply elevated complexity of post-Paleozoic marine ecosystems. *Science*, **314**, pp.1289–1292.

Webby, B.D. Paris, F. Droser, M.L. and Percival, I.G. (Eds.). 2004. *The Great Ordovician Biodiversification Event*. Columbia University Press.

Weiss, A.M. and Martindale, R.C. 2019. Palaeobiological traits that determined scleractinian coral survival and proliferation during the late Paleocene and early Eocene hyperthermals. *Paleoceanography and Paleoclimatology*, **34**(2), pp.252-274.

Weiss, A.M. Foster, W.J. Kosir, A. Muscente, A.D. and Martindale, R.C. 2025. Shallow-marine, benthic ecosystems show compositional shifts in response to the Paleocene-Eocene thermal maximum (PETM) on the Adriatic carbonate platform. *Paleoceanography and Paleoclimatology,* **40**(4).

Wiest, L.A. Buynevich, I.V. Grandstaff, D.E. Terry Jr, D.O. Maza, Z.A. and Lacovara, K.J. 2016. Ichnological evidence for endobenthic response to the K–Pg event, New Jersey, USA. *Palaios*, **31**(5), pp.231-241.

Westerhold, T. Röhl, U. Laskar, J. Palike, H. Wilkens, R. H. Agnini, C. *et al.* and Zachos, J. C. 2020. An astronomically dated record of Earth's climate and its predictability over the last 66 million years. *Science,* **369**(6509), pp. 1383-1387.

Westlund, L. Charles, A. Garcia, S.M. and Sanders, J. 2017. Marine protected areas: Interactions with fishery livelihoods and food security. *FAO Fisheries and Aquaculture Technical Paper*, **603**, p.I.

Whittle, R.J. Witts, J.D. Bowman, V.C. Crame, J.A. Francis, J.E. and , J. 2019. Nature and timing of biotic recovery in Antarctic benthic marine ecosystems following the Cretaceous–Palaeogene mass extinction. *Palaeontology*, **62**(6), pp.919-934.

Wickham, H. 2016. *ggplot2: Elegant Graphics for Data Analysis*. Springer-Verlag New York. ISBN 978-3-319-24277-4, https://ggplot2.tidyverse.org.

Wignall, P.B. Twitchett, R.J. 1996. Ocean anoxia and the end Permian mass extinction. *Science*, **272**(5265), pp.1155-1158.

Williams, R.J. Berlow, E.L. Dunne, J.A. Barabási, A.L. Martinez, N.D. 2002. Two degrees of separation in complex food webs. *Proceedings of the National Academy of Sciences,* **99**(20), pp.12913-12916.

Williams, M. Haywood, A.M. Gregory, F.J. and Schmidt, D.N. (Eds) 2007. *Deep-Time Perspectives On Climate Change: Marrying The Signal From Computer Models And Biological Proxies*. The Micropalaeontological Society, Special Publications. The Geological Society, London, pp.351–387.

Williams, R.J. and Martinez, N.D. 2004. Limits to trophic levels and omnivory in complex food webs: theory and data. *The American Naturalist*, **163**(3), pp.458-468.

Wing, S.L. and Greenwood, D.R. 1993. Fossils and fossil climate: the case for equable continental interiors in the Eocene. *Philosophical transactions of the royal society of London. Series B: Biological Sciences*, **341**(1297), pp.243-252.

Witts, J.D. Newton, R.J. Mills, B.J. Wignall, P.B. and Bottrell, S.H., *et al*. 2018. The impact of the Cretaceous–Paleogene (K–Pg) mass extinction event on the global sulfur cycle: Evidence from Seymour Island, Antarctica. *Geochimica et Cosmochimica Acta*, **230**, pp.17-45.

Witts, J.D. Whittle, R.J. Wignall, P.B. Crame, J.A. and Francis, J.E*., et al*. 2016. Macrofossil evidence for a rapid and severe Cretaceous–Paleogene mass extinction in Antarctica. *Nature communications***,** **7**(1), pp.1-9.

Witts, J.D. Bowman, V.C. Wignall, P.B. Crame, J.A. Francis, J.E. and Newton, R.J. 2015. Evolution and extinction of Maastrichtian (Late Cretaceous) cephalopods from the López de Bertodano Formation, Seymour Island, Antarctica. *Palaeogeography, Palaeoclimatology, Palaeoecology*, **418**, pp.193-212.

Wood, S.A. Russell, R. Hanson, D. Williams, R.J. and Dunne, J.A. 2015. Effects of spatial scale of sampling on food web structure. *Ecology and evolution*, **5**(17), pp.3769-3782.

Woodhouse, A. Swain, A. Fagan, W.F. Fraass, A.J. and Lowery, C.M. 2023. Late Cenozoic cooling restructured global marine plankton communities. *Nature*, **614**, pp. 713–718.

Yeakel, J.D. and Dunne, J.A. 2015. Modern lessons from ancient food webs. *American Scientist*, **103**(3), pp.188-195.

Yodzis, P. 1998. Local trophodynamics and the interaction of marine mammals and fisheries in the Benguela ecosystem. *Journal of Animal Ecology*, **67**, pp.635-658.

Yu, J. Broecker, W.S. Elderfield, H. Jin, Z. McManus, J. and Zhang, F. 2010. Loss of carbon from the deep sea since the Last Glacial Maximum. *Science*, **330**(6007), pp.1084-1087.

Zachos, J.C. Pagani, M. Sloan, L. Thomas, E. and Billups, K. 2001**.** Trends, rhythms, and aberrations in global climate 65 Ma to present. *Science,* **292**(5517), pp.686-693.

Zachos, J.C. Dickens, G.R. and Zeebe, R.E. 2008**.** An early Cenozoic perspective on greenhouse warming and carbon-cycle dynamics. *Nature,* **451**(7176), pp.279-283.

Zachos, J.C. Wara, M.W. Bohaty, S. Delaney, M.L. Petrizzo, M.R. Brill, A. Bralower, T.J. and Premoli-Silva, I. 2003. A transient rise in tropical sea surface temperature during the Paleocene-Eocene thermal maximum. *Science*, **302**(5650), pp.1551-1554.

Zamagni, J. Mutti, M. Ballato, P. and Košir, A. 2012. The Paleocene–Eocene thermal maximum (PETM) in shallow-marine successions of the Adriatic carbonate platform (SW Slovenia). *Bulletin*, **124**(7-8), pp.1071-1086

Zeebe, R.E. Ridgwell, A. and Zachos, J.C. 2016. Anthropogenic carbon release rate unprecedented during the past 66 million years. *Nature Geoscience*, **9**(4), pp.325-329.

Zhang, S.H. Shen, S.Z. and Erwin, D.H. 2022. Latitudinal diversity gradient dynamics during Carboniferous to Triassic icehouse and greenhouse climates. *Geology*, **50**(10), pp.1166-1171.